Performance Evaluation of Semi-transparent CdTe Thin Film Photovoltaic for Building Façade Applications

Submitted by **Hameed Alrashidi** to the University of Exeter

as a thesis for the degree of

Doctor of Philosophy in Renewable Energy

In May 2019

I certify that all material in this thesis which is not my own work has been identified and that no material has previously been submitted and approved for the award of a degree by this or any other University.

Signature: …….

Abstract

In recent years, building integrated photovoltaic (BIPV) applications have gained a considerable interest. Different semi-transparent photovoltaic (STPV) glazing can be used in such applications. This thesis aims to investigate the thermal performance, energy performance and daylight performance of a CdTe thin-film based semi-transparent PV glazing of different transparencies.

Outdoor and indoor experimental setups were installed, in Penryn, UK, to investigate the performance of 35%, 25%, 19% and 0.5% CdTe thin-film based semi-transparent photovoltaic glazing in comparison to conventional clear glazing under realistic conditions. Data from the experimental setups were collected in different day conditions and different orientations that are South and South West. Overall heat transfer coefficient (U-value) and solar heat gain coefficient (SHGC) were calculated for thermal performance evaluation. Net energy performance was evaluated for energy performance assessment. Daylight glare index (DGI) and daylight factor (DF) were calculated for daylight performance evaluation.

Results showed that, CdTe STPV glazing are better thermal insulators than conventional single glazing, and CdTe STPV glazing with lower transparencies have better thermal insulation property than higher transparency ones. In addition, compared to conventional single glazing, the application CdTe STPV glazing can achieved a net energy saving up to 20%. Moreover, Using CdTe STPV as a glazing façade can control the daylight glare inside the enclosures to acceptable levels, it also permits for usable daylight to be transmitted into enclosures.

Papers Arising from This Thesis

The journal papers arising from this thesis are the following:

1. H. Alrashidi, A. Ghosh, W. Issa, N. Sellami, T. K. Mallick, and S. Sundaram, “Evaluation of solar factor using spectral analysis for CdTe photovoltaic glazing,” Materials Letters, vol. 237, pp. 332–335, Feb. 2019.
2. H. Alrashidi, A. Ghosh, W. Issa, N. Sellami, T. K. Mallick, and S. Sundaram, “Building Energy Evaluation Using Thermal Performance of CdTe Thin-Film Glazing”. Submit to Solar Energy Journal. (In preparation).
3. H. Alrashidi, A. Ghosh, W. Issa, N. Sellami, T. K. Mallick, and S. Sundaram, “Performance Assessment of Cadmium Telluride-based Semi-Transparent Glazing for Power Saving in Façade Buildings”. Submit to Energy and Buildings Journal. (In preparation).
4. H. Alrashidi, A. Ghosh, W. Issa, N. Sellami, T. K. Mallick, and S. Sundaram, “Daylighting performance and glare calculation of a CdTe thin-film based semi-transparent PV glazing”. Submit to Solar Energy Journal. (In preparation).

The research outcomes have been published in different conferences as follows:

1. H. Alrashidi, A. Ghosh, W. Issa, S. Sundaram and T. K. Mallick. Estimating Cooling Load Reduction Using 25% Transparency CdTe Thin Film PV glazing. SOLARIS Conference, July 2017. Brunel University.
2. H. Alrashidi, A. Ghosh, W. Issa, N. Sellami, T. Stuart, T. K. Mallick and S. Sundaram. Investigation of overall heat transfer coefficient of CdTe thin-film based PV glazing using indoor characterisation. 13th Photovoltaic Science Applications and Technology Conference (PVSAT-13). 5-7 April 2017. Bangor University, Wales.

Acknowledgement

First, I want to express my sincere gratitude to all my supervisors Dr. Senthilarasu Sundaram and Prof. Tapas Mallick, who have always supported my PhD research with their enthusiasm, knowledge and their guidance towards the achievement of my doctoral degree. Thanks for their endless support throughout the past four years. Many thanks to Prof. Stuart Townley, who served during my first year of my PhD as first supervisor, for his gradual instruction on how to perform efficiently my research. His wisdom and patience have taught me a lot. I remain grateful for Dr. Nazmi Sellami for his significant effort, guidance, technical and non- technical advices.

I record my profound gratitude to Dr. Walid Issa for his valuable ideas, keen interest, motivation and encouragement at various stages of my PhD study. Big thanks to Dr. Aritra Ghosh for his technical assistance.

Special thanks extended to Atif for his fruitful assistance and enthusiasm at all times of my PhD study. His insightful thoughts and suggestions have made my work more thorough. Thanks for making this trip enjoyable.

Most appreciated guidance and valuable work in Chapter-3 goes to Mr. James Yule at the University of Exeter for the assembly of the STPV enclosures and helping on the operations of the CdTe modules systems. This experimental work would not be achieved and feasible without his technical expertise.

I would like to calendar a special note of thanks to Saja Alghanim who was always very supportive at all stages of my study and keen to accomplish my PhD degree.

My appreciation goes to Cornwall Glass Co. Penryn branch for the assembly of the STPV modules into double glazing and providing the single glazing units.

Always I am thankful to all my colleagues at University of Exeter-Penryn campus “Renewable group” for the great discussions and useful disagreement we shared.

My heartfelt gratitude is given to my family, for their understanding, immense support and encouragement. I am also very grateful to my mom for her prays and unlimited support that have always been a light source of strength for me.

Finally, I would like to thank everyone who spends the time to understand the research of this thesis. I would be delighted to discuss its content with you. This work was funded by the Kuwait Fund development, high regards to them.

List of Abbreviations

BAPV	Building Attached Photovoltaic
BGI	British Glare Index
BIPV	Building Integrated Photovoltaic
CGI	(International Commission On Illumination) Glare Index
MPPT	Maximum Power Point Tracer
PV	Photovoltaic
STPV	Cdte Based Semitransparent Photovoltaic
UDI	Useful Daylight Illuminance
WWR	Window to Wall Ratio

List of Symbols

A	Area of glazing (m^2)
A_i	Anisotropic index
AST	Apparent solar time
A_w	Area of the polyisocyanurate insulation board (m^2)
C_{tc}	Heat capacity of air inside test cell (J/kg^oC)
DF	Daylight factor
DGI	Daylight glare index
E_d	Direct vertical illuminance (lux)
E_i	Indirect vertical illuminance (lux)
ET	Equation of time
$E_{v,adp}$	Adaptation vertical illuminance (lux)
$E_{v,neag}$	Near glazing vertical illuminance (lux)
$E_{v,win}$	Window vertical illuminance (lux)
h_i	Inside convection heat transfer coefficient (W/m^2K)
h_o	Outside convection heat transfer coefficient (W/m^2K)
$I_{hor,diff}$	Horizontal diffuse solar irradiance (W/m^2)
$I_{hor,dir}$	Horizontal direct solar irradiance (W/m^2)
I_o	Extra-terrestrial solar irradiance in (W/m^2)
I_{sc}	Solar constant irradiance (W/m^2)
$I_{ver,global}$	Global vertical solar irradiance (W/m^2)
K	Thermal conductivity of insulation board (W/mk)

Kg	Extinction coefficient
L	Thickness of insulation board (m)
L_{adp}	Adaptation luminance level (cd/m^2)
L_b	Background illuminance (foot-lamberts)
L_{ext}	External luminance level (cd/m^2)
L_i	Horizontal inside illuminance (lux)
L_o	Outside illuminance (lux)
L_s	Source illuminance (foot-lamberts)
LST	Local solar time
LSTM	Local longitude of standard time meridian
L_{win}	Window luminance level (cd/m^2)
M_{tc}	Mass of air inside test cell (kg)
Nd	Day number
Ng	Number of glass pane
P	Guth position index
Q_g	Heat transmitted through the glazing (W)
Q_{in}	Incident solar heat (W)
Q_{tc}	Heat stored nside the test enclosure (W)
Q_w	Heat transferred through test cell wall and inside and outisde convection (W)
R_b	Factor of beam radiation
R_g	Solar reflectance of glazing
SHGC	Solar Heat Gain Coefficient
t	Time

$T_{ambient}$	Ambient temperature (^oC)
T_g	Thickness of glazing (m)
T_{in}	Temperature of air inside test cell (C)
TSE	Transmitted solar energy (W/m^2)
U-value	Overall heat transfer coefficient (W/m^2K)
U_w	Combined overall heat transfer coefficient of wall with inside and ambient air (W/m^2K)
V_{tc}	Volume of air inside test cell (m^3)
V_{wind}	Wind speed (m/s)
α	Absorbance
β	Angle between the panel and horizontal surface
δ	Declination angle
τ	Transmittance
ρ	Density (kg/m^3)
ω'	Hour angle
ω_o	Solid angle of source (steradian)
ω_s	apparent area of source (steradians)
Φ	Azimuth angle
ϕ'	Configuration factor
Ω	modified solid angular subtense of the source
Ω_s	Angle subtended by light glare source
θ	Incident angle

Table of Contents

List of Tables

List of Figures

Chapter 1 Introduction

1.1 Research Background

Global awareness regarding energy generation from fossil fuels and its implications on pollution, global warming and climate changes has increased the need of reducing energy consumption and the use of green energy. Recent studies of International Energy Agency (IEA) [1] in 2018 showed that residential buildings are responsible for an average of 20% of energy consumption in Japan, Russia, India, US and China. Another study in Taiwan in 2013 [2] stated that the residential and commercial buildings are responsible for 40% of energy consumption. The major consumer of energy in this type of application is the cooling and heating loads. Other consumers are electric equipment and lighting. The excessive cooling and heating loads mainly result from the type of glazing used [3]. The glazing has to permit for heat transfer into the building during cold winter days and block heat transfer into the building during hot summer days. This makes the selection of the correct type of glazing of significant importance.

Building-integrated photovoltaics (BIPV) have come to be regarded as a promising technology that reduces the life-cycle costs of building construction and generates energy simultaneously [4] as shown in Figure 1.1 [5]. Apart from generating electricity, BIPV modules can be customized in a different dimension, thickness, shape, and colour to give a beautiful aesthetic view. BIPV products offer numerous advantages [6] such as to provide weather protection, thermal insulation, noise protection, and even structural strength, in addition to allowing the entry of daylight, providing a view to the outside, and generating electrical power.

In general, most building surfaces are available for the integration of PV modules. The integration can be implemented in different ways bringing four classes of integration:

a. PV facades (including glazing, curtains, etc),

b. PV roofs (including standing panels, tiles, etc),

c. PV windows (including semi-transparent PV, glass laminated, etc.) and

d. PV sunshades (including blinds, panels, etc.)

Figure 1.1 Building Integrated Photovoltaic

Different types of PV glazing systems are available to be used in BIPV applications [7]. Mainly, three different types of PVs such as Silicon-based PV, thin-film PV and organic solar cells are used in the production of BIPV. The selection of a semi-transparent photovoltaic (STPV) is achieved based on its cost, availability of raw materials, efficiency and environment in terms of energy saving and manufacturing process [4]. Thin-film and crystalline silicone-based PV dominate the market because they have proven their effectiveness in real applications [6]. However

thin-film PV modules have some advantages over crystalline silicone PV that can be summarized as follows:

1. Availability and affordability of raw materials.
2. The light weight of the PV
3. The availability in rigid and flexible forms.
4. The aesthetic appearance that encourages its usage in BIPV applications.
5. The different available transparency levels while keeping acceptable efficiencies.

Thin-film PVs are of different types depending on the material they are made of. Known materials include Cadmium sulfide (CdS), Copper indium diselinide (CIS) ($CuInSe_2$) and Cadmium telluride (CdTe). Previous studies have shown that CdS thin-film PV have low efficiency that reaches a maximum of 6%. This has resulted in less research to be oriented toward them [7]. CIS thin-film PV have high efficiency that can reach up to 20% for PV cells and 13% for large area modules [8]. However, they have a drawback regarding the shortage in indium [9]. According to First Solar Company, CdTe thin-film PV are the most suitable for large scale applications [10]. They have a cell efficiency reaching 20.4% and a large module efficiency of 16.7%. This makes the choice of CdTe thin-film PV to be the best among other thin-film types.

Recently, STPV-integrated window systems have become popular [11] . Onsite electricity generation capacity is the driving force behind the intense focus of research on STPV. However, like any other glazing system, the reflectivity, and transmissivity of STPV module change with the angle of incidence. The change in internal building daylight can be achieved by using different transparency STPV glazing. However, the high transparency of the glazing affects its power generation and permits for more heat to be transferred through it thus affecting its thermal properties. The excessive heat transfer through the glazing into the building results in an increase

in cooling load and a decrease in heating load. On the other hand, low transparency glazing leads to high power generation and decreases the heat transfer through them. Thus, decreasing the heating load and increasing the cooling load. However, this requires more lighting to be installed in the enclosures of the building in order to compensate for the lack of daylight which is unpleasant for human eyes as it makes them out of their comfort zone.

On the other hand, for a given geographical location, the sun position changes within days which resulted in variation of the incidence angle for a static surface. This difference leads to decrease in STPV energy generation compared to normal incidence. Therefore, the real practical implementation of this technology might give different results from the lab-based experiments. Orientation, place of installation and local climatic characteristics are the determining factors for this optical or angular loss of power generation. Variation in ambient temperature which changes from place to place and the existence of built-in cooling units are major factors which directly affects the cell temperature and thus the module efficiencies [12]. Weather conditions include solar irradiance, sky clearness, ambient temperatures and wind speed. These factors not only affect the power generation of an STPV glazing, but also affect its thermal performance that is characterized by the overall heat transfer coefficient (U-value) and the solar heat gain coefficient (SHGC). Therefore, besides analyzing the data provided by the manufacturer, performance assessment of STPV system in real operating condition are necessary to know the economic potential in that particular location. The performance analysis in a local climatic condition also establishes the suitability of a given STPV technology in that specific location and builds confidence among the designer and architecture to apply their energy assessment tools in the new smart buildings.

1.2 Research Motivations

Therefore, the scope of this research is set out because

- The glazing is a key factor to reduce the building energy, but more work is needed to be improve performance Thin Film-based STPV.
- Cooling loads are high in countries where high temperature is present and Façade with traditional glazing increases the electrical consumptions. Therefore, there is a need to investigate new glazing technology to reduce the cooling loads.
- Silicon PVs are opaque and suffer a lack of uniformity if spacing is made for daylight improvement. So, the study of semi-transparent photovoltaic (STPV) is crucial for better optical comfort of occupants and daylight performance of the building.
- Using STPV might reduce the cooling/heating loads in a building but it degrades the interior daylighting. Therefore, it is important to study the feasibility of using an STPV as a glazing through evaluating its daylight performance.
- CdTe-based STPV have high efficiencies and low cost, however few researches have been reported on using them for Façade energy improvement. So, more investigation must be done on the mentioned STPV.
- More research must be oriented towards the overall energy assessment including the Air-conditioning consumption, artificial lighting consumption and PV generation for office-based Façade because few researches have addressed them.
- Practical experimentation needs to be performed on STPV glazing to validate the outcomes of previous researches that are based on simulated scenarios.

- More work needs to be performed to assess the STPV glazing in outdoor conditions under different orientations, transparencies and sizes because very limited research is oriented towards them.

1.3 Research aim and objectives

The general aim of this research is to evaluate the energy performance and thermal performance of a various semi-transparent photovoltaic glazing in different climate conditions. The aim can be achieved through the following list of research objectives:

1. To design and implement an indoor and outdoor experimental setup with semi-transparent PV glazing be fitted on its wall and to develop the experimental methodology for a quantitative study that evaluates the glazing performance by calculating defined parameters.
2. To evaluate the thermal performance of different transparency semi-transparent PV characterized by overall heat transfer (U-value) and solar heat gain coefficient (SHGC) and compare it to clear single glazing.
3. To assess the net energy performance of an Air-conditioned office-based Façade integrating different transparency semi-transparent PVs and compare it to a clear glazing.
4. To evaluate the daylight performance of an Air-conditioned office-based Façade integrating different transparency semi-transparent PVs and investigate the comfort measures.

1.4 Methodologies and approaches

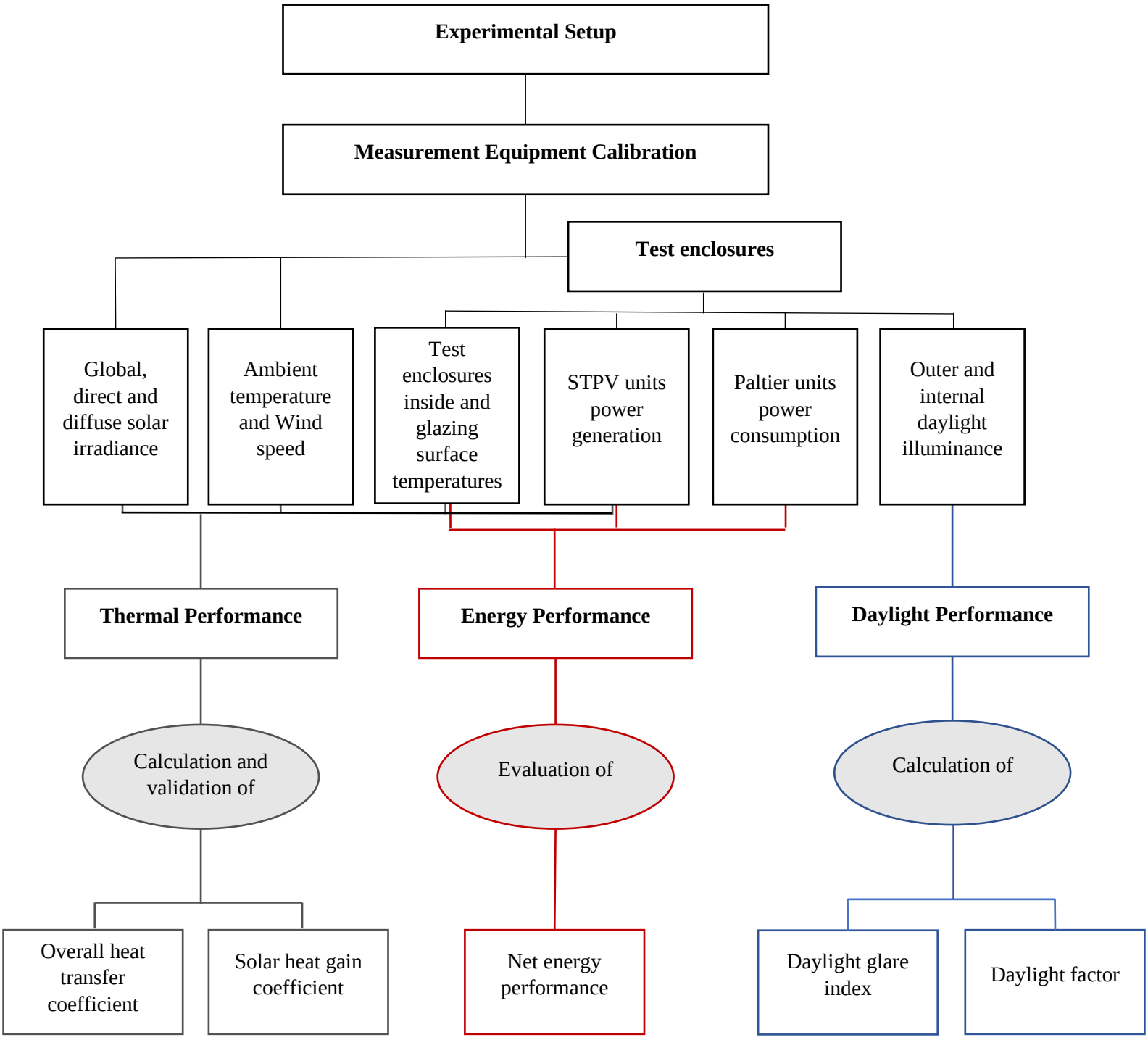

Figure 1.2 Thesis Approach and Methodology Structure

The research program involves the methodology of the experiments, field measurements and data analysis for performance evaluation. Experimental setups used by previous studies were reviewed to select the one that best fits the aim and objectives of the research. Three experimental setups were installed, two of them are outdoor test enclosures and one is an indoor test enclosure. The outdoor experimental setups were oriented to face South and South West. These two orientations were specifically selected because they provide PVs with maximum solar radiation collection making them economically optimal in terms of PV power generation in northern hemisphere areas [13][14]. Results from different experimental setups and different orientations are compared for results validation. The required measurement equipment were identified, selected and calibrated for precise data collection. Measured data include solar irradiance, weather conditions, temperatures, PV glazing's power generation, Paltier units' power consumption and internal and external daylight illuminances. The collected data were used to evaluate the thermal performance, energy performance and daylight performance of CdTe thin-film based semi-transparent photovoltaic glazing. STPV glazing performance was compared to that of conventional single glazing for better physical interpretation of the results. The thermal performance was assessed by calculating the overall heat transfer coefficient (U-value) and solar heat gain coefficient (SHGC) of glazing under study, using data collected from the three designed experiments. Energy performance was assessed by evaluating the net energy performance of the STPV glazing in outdoor experiments. Net energy evaluation involves STPV glazing power generation, Paltier units' power consumption and artificial lighting power demand. In addition, daylight performance of the glazing was assessed through calculating daylight glare index (DGI) and daylight factor (DF).

1.5 Research contribution

The contribution of the thesis can be summarized as:

- Unique provision of new outdoor performance data for CdTe glazing systems for climates similar to that of the UK.
- Thermal factors, represented by U-value and SHGC, assessment using different methods for different semi-transparent photovoltaic glazing transparencies have been determined.
- Net energy performance has been evaluated practically using small-scale outdoor setup, including the air-conditioning consumption, artificial lighting consumption and PV generation.
- Daylighting and glare assessment for a small office model setup, targeting semi-transparent photovoltaic glazing.

1.6 Arrangement of the Thesis

The thesis consists of 7 chapters starting from a general introduction of the subject passing through technical analysis and ending with conclusions and scope for future work. Brief description of the chapters is presented below.

Chapter 1 is an introductory chapter that presents the research background related to the photovoltaic (PV) systems in building and different BIPV technologies. Also, it provides the chapters outline in the thesis. The general aim and objectives are introduced in addition to the selected methodologies and approaches to achieve these objectives.

Chapter 2 narrates the history of the PV systems and related to BIPV. Different PV technologies are discussed but more attention to thin film is drawn. The state of the art is reviewed addressing the BIPV systems and energy performance assessment. The review included the technologies,

research methodologies, the simulation and practical results and conclusions. Therefore, the research gaps are identified in this chapter and ensures the novelty of the research outcomes.

Chapter 3 shows the design of the experimental apparatus and field measuring for the purpose of validating the theoretical calculation and drawing the conclusions. The discussion includes designing a test enclosure suitable for the thin film samples and equipping the required temperature sensors and other sensors (voltage, current, light) for data collection. The whole setup with the software is discussed. Initial tests are carried out indoor and outdoor to meet the safety and accuracy requirements.

Chapter 4 presents the thermal performance measures that need to be defined like the U-value, and solar heat gain. Formulas are provided, and different testing methods are carried out to assess the thermal performance for different semi-transparent PV (0.5%, 19%, 25%, 35%) on the rooftop of the ESI building in Penryn- Cornwall as well as the indoor experiment. The data is discussed, and some expectation are presented based on the test's outcomes.

Chapter 5 presents the use of thin film as BIPV system where it generates power and contributes to minimizing the air conditioning units power consumption. The study includes the power calculation of the STPV over selected days in different seasons as an example with the lighting requirements for a building. As a result, a net energy performance is discussed supported by all experimental data.

Chapter 6 discusses the effects of thin film PV on daylighting control and cooling load in Façade buildings. Some figures are defined like Daylight glare indexes (DGI) and daylight factor (DF). The STPV glazing has been evaluated using an outdoor south facing and south-west facing test cells for clear sunny, intermittent cloudy and overcast cloudy days. The study produces a feasibility

measures of using the STPV in Façades and in traditional building and its relation to the enclosure lighting for different STPV transparencies. This provides us with expectation about the comfortability of the enclosure.

Chapter 7 discusses the conclusions and reviews the achievement of the thesis aim. Finally, it provides some suggestions for future work based on the research outcomes and the expectations and presents some extended work for more investigation on other issues not addressed in this thesis.

Chapter 2 Literature Review

This chapter presents the basic information that builds a solid understanding of the topics and issues covered in other chapters. It highlights different technologies which have been considered in the literature and reviews previous studies which addressed issues relevant to this thesis and identifies the contributions of others toward investigating the various properties of glazing and improving the energy consumption figures.

2.1 Glazing and overall building energy performance

Glazing units are essential parts of a building's composition, whether they are used as windows or facades. Their primary role is to permit daylight transmission so that a contact between the inside and exterior environment is attained and as well as achieving optical comfort for the occupants. In addition, glazing provides an aesthetic architectural feature when used as facades. However, the use of glazing also permits heat gains and losses through glazed areas, leading to an increase in winter heating loads and summer cooling loads, which is a major issue when dealing with the overall energy performance of a building.

In 2018, the international energy agency (IEA) published a report stating that an average of 20% of generated energy was being used by residential buildings in Japan, Russia, India, the U.S.A and China [1]. However, further scenarios considered by the International Energy Agency (IEA) indicate that the domestic sector will lead the total energy consumption by 2035 [15]. The main fraction of a building's energy consumption is due to high cooling and heating loads that are mainly caused by low thermal insulation of glazing [3], as well as the use of artificial lighting, but in less proportion. Therefore, there is an urgent necessity to develop solutions that minimize heat transfer through building envelop to their surrounding areas while keeping the optical comfort and environmental contact within the acceptable ranges.

2.2 Factors affecting building energy consumption

Different factors affect the energy performance of a building, including the size, type and orientation of glazing. In 2017, El Jojo [16], through numerical modelling, showed that a reduction of 40% in energy consumption and 30% in CO_2 generation can be achieved by selecting the optimum position and type of glazing. Similarly, in a study in 2015 Pai and Siddhartha [17] showed that the energy performance of space cooling and lighting, measured in BTU, is affected by the orientation of glazing. In addition, Muhaisen and Dabbour [18] pointed out that, for optimal energy saving in the building, both the size of the glazing and glazing material have to be studied alongside the orientation of the glazing.

According to many studies, glazing window-to-wall ratio (WWR) is a main parameter in determining the amount of energy consumption, as a lower WWR leads to lower cooling and heating loads [19][20]. Saridar and El Kadi [21] studied the effect of different window-to-wall ratios at different orientations on the annual electricity consumption (in kilowatt-hours per m^2) in Lebanon. Their study revealed a significant effect of WWR on energy consumption. Their results are shown in Table 2.1 shown below.

Table 2.1 Effect of window-to-wall (WWR) on annual electricity consumption in Lebanon

WWR			**Annual Electricity Consumption (KWh/m^2)**
South Wall	**North Wall**	**East/West Wall**	
0.72	0.87	0.63	3.26
0.25	0.25	0.08	30.52
0.58	0.58	0.58	7.63
1	0	0.44	20.37

Shading devices are also effective factors in building energy performance, as reported in [22] and [23]. The presence of a shading device decreases the heat losses and heat gains through the glazing, resulting in a decrease of both heating and cooling loads. However, shading devices affect the transmission of daylight into the enclosure, leading to excessive usage of artificial lighting. Another effective factor is the building's location, which is characterized by solar irradiance and ambient temperature, which is a also a concern when analysing glazing performance, as discussed in [24].

In the light of these mentioned studies, it is clear that the energy performance of a building is strongly related to the thermal performance of the glazing, which that determines the summer cooling and winter heating loads, and the daylight performance of the glazing, which determines the need for usage of artificial lighting. This means that a full study of a building's glazing performance has to cover the three main types of performance: energy, thermal and daylight performance, as these are interrelated. An example of this interrelation is using a 35% transparency glazing instead of the 90% clear glazing. This leads to better thermal performance and energy saving but less interior daylight.

2.2.1 Thermal performance of a Building

The thermal performance of a building strongly affects energy consumption. The building material is generally well insulated, except for the glazed areas, whether they are used as façades or windows. Current conventional residential windows are responsible for around 47% of heat loss [25].

The main factors that describe the thermal performance of building glazing are the overall heat transfer coefficient (U-value) and the solar heat gain coefficient (SHGC). U-value is a coefficient

that measures how well a material transfers heat in (W/m^2K). High U-values mean a lower insulating effect of a material while lower U-values indicate a higher insulation effect of a material. For example, single glazing has a U-value of about 5.8 W/m^2K and air-filled double glazing has a U-value of about 3.7 W/m^2K, while a gas-filled double glazing (such as argon filled) has a U-value of only 1.9 W/m^2K, according to the Slimlite company in the U.K. [26]. The overall heat transfer coefficient measures the composite performance of an element, rather than describing the performance of its composing materials, and this gives an easier approach for comparison between different designs.

Solar heat gain coefficient (SHGC) describes the fraction of solar irradiance that enters the enclosure through the glazing. The solar irradiance can be directly transmitted through the glazing or stored and emitted again. The SHGC is unitless and has a value between 0 and 1. Low SHGC indicates less solar irradiance transmission through the glazing and vice versa. According to the Royal Institute of British Architects (RIBA), the SHGC of a whole window, with frames included, is less than 0.8 [27].

2.2.2 Building daylight performance

One basic reason for using windows and glazing facades is the daylight transmittance through them for the visual comfort of occupants. One way of determining the daylight performance is by measuring the glare index. Glare index measures the difficulty of seeing in a certain environment. Better daylight performance is, in many instances, associated with lower thermal performance of glazing, as in cases of semi-transparent glazing. In addition, lower daylight performance is sometimes associated with better thermal performance, such as the use of shading devices and the use of low window-to-wall ratios [28]. The importance of studying glazing daylight performance

is also an issue of concern for determining the overall energy performance of a building, as explained by Boyano et al.[29], who point out that lighting has a significant effect on building energy consumption.

In the light of the issues raised in this discussion, the search is in progress for the optimum glazing with good daylight transmission and low heat gains and losses, as well as low capital cost. This has made the use of constant transparency glazing the most popular type of glazing in recent years.

2.3 Constant Transparency Glazing

As mentioned in the above sections, glazing is used for windows and facades in building facilities to connect the occupants to the outer environment. However, glazing units induce high heat losses, leading to a higher heating load in cold areas and high heat gains, leading to high cooling loads in hot areas. In order to achieve an ideal glazing with good daylight transmission and low overall heat transfer, the glazing should have 100% transmission in the visible spectrum and 100% reflection in the infrared spectrum [30]. Different types of constant transparency glazing are available: the most used ones are discussed below.

2.4 Single Glazing

Single glazing is a common type of glazing used in windows and facades. It has the advantage of low initial and repair costs, compared to other types of glazing [31]. Moreover, clear single glazing has a transmittance percentage of 89% in the visible spectrum, which is a good property for daylight performance evaluation. However, the percentage of transmittance in the infrared spectrum is 84%. This is favourable in climates where heating is required, whereas it is not when cooling load is a concern, since it permits solar irradiance to pass though into the building [32]. Moreover, single glazing has a U-value of 5.8 W/m^2K [33], which indicates that it permits high

heat transfer from outside to inside on summer days and heat loss from the heated space to the outer cold environment on winter days. Therefore, the search for a glazing that maintains the high daylight transmittance with better thermal properties has been an important issue.

2.4.1 Double Glazing

In its early stages of development, double glazing consisted of two glass panes with an air gap in between, as shown in Figure 2.1 [34]. The idea was to take advantage of the low thermal conductivity of stagnant air, which is 0.026 W/mK [35]. The amount of heat transfer through the double glazing depends on the distance between the glass panes. As the air gap increases, thermal insulation increases, which means lower heat loss. However, an excessive increase in the air gap leads the convective heat transfer to dominate the conductive heat transfer, thus the heat loss through the double glazing increases again [36]. According to a numerical study in Turkey, the optimum air gap distance is 18 mm to 21 mm for areas where the temperature difference between inside and ambient is 19 ^{o}C, 15 mm to 18 mm for a temperature difference of 25 ^{o}C to 34 ^{o}C and 12 mm to 15 mm for a temperature difference of 49 ^{o}C [24].

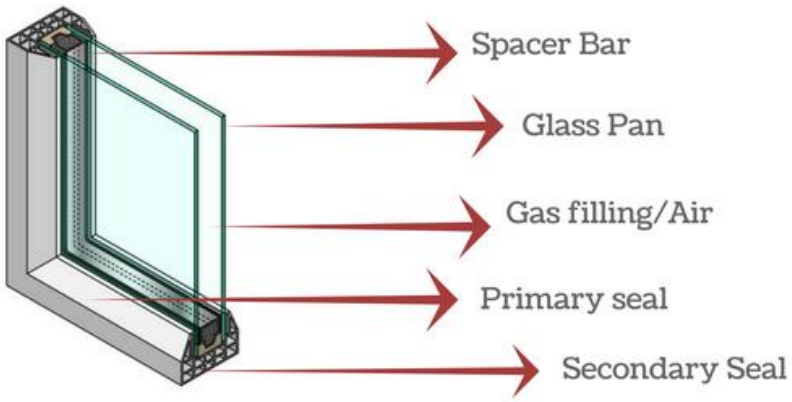

Figure 2.1 Components of double glazing

Researchers have sought to take maximum benefit of double-glazing systems. Gradually, the use of inert gases with lower thermal conductivities than air, such as Argon (0.016 W/mK), Krypton (0.0095 W/mK) and Xenon (0.005 W/mK), were introduced [32]. In addition, in order to reduce radiation heat transfer, infrared-absorbing gases were used [37] [38] [39]. Other glazing technologies have evolved from double glazing, such as evacuated glazing, which is similar to double glazing but with a vacuum gap between the glass panes [40]. This reduces the conduction and convection heat transfer dramatically, but a problem with radiation heat transfer arises. Thus, another glazing technology was developed in order to reduce radiation heat transfer in double glazing and evacuated glazing systems which is low e-coating glazing [32]. However, these modifications to double glazing have caused their initial cost to increase.

A report by the IEA has predicted that cooling loads, heating loads and lighting demands will increase to more than double by 2050 [1]. The current usage of single and double glazing will not limit the energy performance of buildings. This has made enclosure for a new concept of glazing to be introduced to reduce the energy consumption of buildings, which is building integrated photovoltaic (BIPV), which uses different PV technologies as glazing and other parts of the building.

2.4.2 Building Integrated Photovoltaic (BIPV) Glazing

During the last decade, with the use of PV applications and increased efficiency of PV materials, the photovoltaic industry has grown rapidly. One area where PV materials are generally used is in developing integrated PV systems. Buildings provide a substantial support to the global energy use balance, accounting for 20-30% of the entire main energy utilization of industrialized countries [41]. Previously, determinations of energy efficiency in building design were only related to thermal insulation or air circulation to combine human wellbeing with the least energy

consumption. However, due to the benefits of photovoltaic applications, engineers now think about adding a provision of photovoltaic systems when designing buildings, so that it helps the building to produce its own electricity. The use of photovoltaic systems in buildings may have two methodologies: Building Attached Photovoltaic (BAPV) applications and Building Integrated Photovoltaic (BIPV) applications [42]. A BAPV system denotes that the photovoltaic modules are connected to the structure of the building as an add-on, exclusive of changing any operational segment of the building, resulting in added capital cost. However, in BIPV applications, "photovoltaics are considered as a functional part of the building structure, or they are architecturally integrated into the building design" [42]. The BIPV methodology substitutes the standard building constituents such as roof tiles, windows and even facades with PV systems and [3][43].

Figure 2.2 [44] shows an illustration of BAPV and BIPV systems. The rack-mounted PV panel is the most well-recognized form of BAPV system.

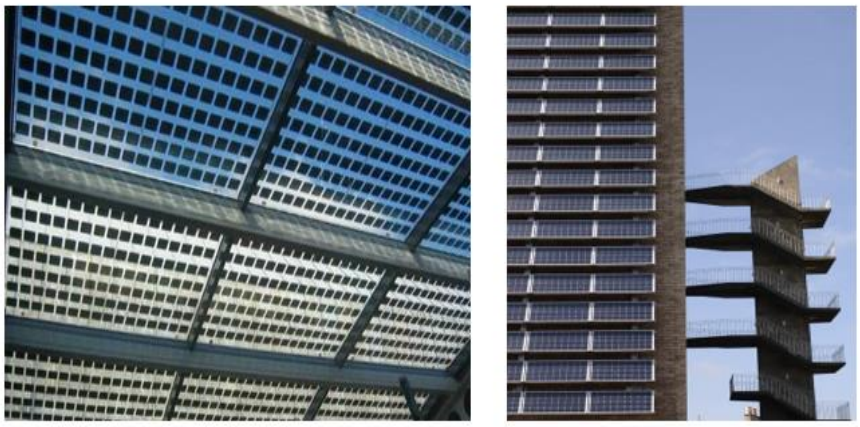

Figure 2.2 Example of (a) BIPV [45] and (b) BAVP systems on the roofs of buildings

In the recent past, the use of BIPV systems has attracted admiration from both economic and architectural perspectives whilst planning and building a new structure. BIPV systems produce power essential for household uses and the excess energy produced can be fed back into the grid, while such systems also substitute for the traditional building constituents as a weather protecting building envelope [46]. In addition, BIPV applications act as a substitute for using the land for energy production through PV module installations [47]. A BIPV system could be a very appropriate choice as a micro-power plant, particularly for urban and suburban locations. The benefits of BIPVs can be summarized as follows [41]:

1. No extra land is required for the installation of a PV system. As the building component itself is used for mounting the module. Heavily inhabited urban and sub-urban regions could seriously benefit from this.
2. It may avoid the extra infrastructure required for setting up PV modules.
3. Because of the on-site production of energy to be made use of in the buildings, the wastage of electricity during distribution and transmission can be reduced to a great extent.
4. It reduces electricity bills, as free electricity will be generated throughout the daylight hours, which is then used by the building.
5. The PV modules can replace the conventional building constituents and decrease the payback period of the installation.
6. It can develop the artistic look of a building with a cosmetic layer of PV modules in a state-of-the-art manner.
7. It may decrease the planning costs to a huge extent.

The facades and the roof are believed to be the most appropriate selections for BIPV installations. The PV modules can be set up over the entire roof and facades, as shown in Figure 2.3 [48], providing concentrated exposure to the solar radiation. In addition, BIPV modules can be utilized as features such as skylights, building exterior cladding panels, a semi-transparent roof or semi-transparent windows as well as being conventionally integrated into a roof or façade [43][49].

Figure 2.3 Architectural designs for BIPV elements in the roof and façade of a building

Various types of photovoltaic systems are available on the market and can be used as glazing. However, as stated earlier, the selection of the optimum glazing is related to different factors and the performance of the selected glazing has to be studied, as well. The next section describes the available PV glazing in the market.

2.5 PV Glazing Technology

Photovoltaic glazing technologies are available in different transparencies, giving them the ability to reduce the solar heat gain coefficient and allow for daylight control [14] [15] [16]. They also have an advantage over other types of glazing, which is power generation [17]. This triple benefit (daylight control, overall heat transfer reduction and power generation) has made PV glazing

favourable in different applications, such as building integrated photovoltaic (BIPV) applications [18] and roofs and facades [48].

The increasing demand for the use of photovoltaic (PV) applications has made enclosure for various technologies to enter the market. Photovoltaic technologies can be mainly be classified into silicone-based photovoltaic materials, thin-film based photovoltaic materials and organic solar cells. Among these types, thin-film PV and crystalline silicon PV materials are the most widely employed, because of their proven suitability in real applications. However, thin-film PV materials have some advantages over crystalline silicone, in terms of weight, form (rigid and elastic), aesthetic appearance and high transparency levels [6]. For a PV to be successfully commercialized, it has to be advantageous mainly in terms of cost, availability and environment. Fthenakis discussed the use of thin-film PV materials in the light of these three criteria and concluded that thin-film PVs are sustainable and can be enhanced with more research and development [30].

Thin-film PV modules are experiencing a revolution regarding their mass production since the millennium, occupying about 15 – 20% of the market share in 2011 [50]. Figure 2.4 [51] shows the increase in the annual production of thin film PVs in the U.S from 2013 to 2024.

Figure 2.4 Thin-film PV production size in MW from 2013 to predicted size in 2024

2.5.1 Silicon-Based PV

Crystalline silicon (c-Si) solar cells have the highest cell and module efficiency. Commercially available PV modules can reach up to 22% [and 25.6% in cell efficiency]. Nevertheless, despite their wide-ranging possibilities, the field of standard c-Si applications in the building envelope is limited by several technical constraints. One of these constraints is known to be the loss of performance as a consequence of high temperatures and of shading caused by the surrounding buildings, their chimneys, or other kinds of obstacles: even one single partly shaded c-Si module will thus lead to a significant loss of power, not only in that particular module, but in all the others connected in series within the same circuit [52]. Furthermore, they are opaque, which means that the light transmission through the modules can be achieved only by altering the spacing between the cells. For example, for mono-crystalline PV glazing to be made semi-transparent, the solar cells are laminated with a space between them to allow light transmission to the indoor space, as

shown in Figure 2.5 [53]. The light obtained through this kind of glazing has a changing pattern of shading and non-uniform daylighting and thermal performance.

Figure 2.5 Crystalline silicon semi-transparent solar cell

2.5.2 Amorphous-silicon Thin-Film

Amorphous silicon (a-Si) was one of the earliest thin-film PVs to be used. It was derived from the crystalline silicon photovoltaic technology [54]. a-Si can be integrated on glass with a layer of tin oxide (SnO_2) in between to increase its conductivity, and it reaches an efficiency of 12% [55] [56]. However, when these PVs, are subjected to sunlight, their efficiencies drop. This led researchers in the field to refer instead to their stabilized efficiencies that lie in the range of 4 to 6% [50]. The initial efficiency of laboratory a-Si solar cells was initially 2.4%, in 1976, but reached ~14–15% by 2016, as shown in Figure 2.6 [57].

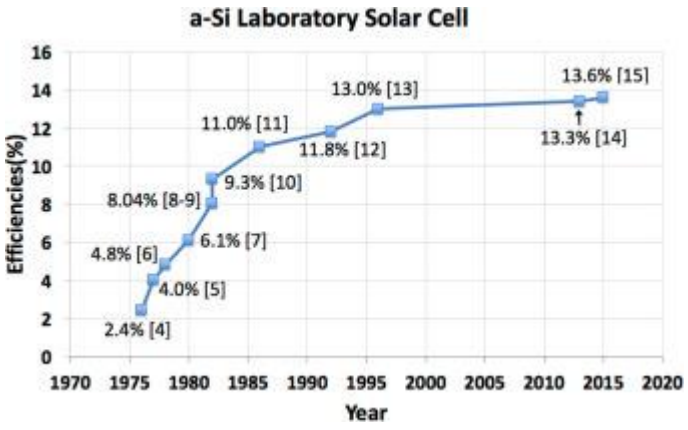

Figure 2.6 Best laboratory initial efficiencies for a-Si

2.5.3 Cadmium Sulphide (CdS) Thin-Film

Research and investigation on cadmium sulphide solar cells started in the 1950s. Their efficiency and environmental stability were low compared to silicon, as their best reachable efficiency was 6% [58] [7]. This led to little research being oriented toward them.

2.5.4 Cadmium Telluride (CdTe) Thin-Film

The efficiency of CdTe PVs is one of the highest among other thin-film PVs. Its efficiency has reached 20.4% [10] and the efficiency of a large module has reached 16.7% [46] [59]. According to First Solar, this type of thin-film PV is the most suitable for large scale production [10]. The first study of CdTe efficiency in the laboratory was by Bonnet and Rabnehors [60] , who reported a solar cell with 6% efficiency, however the efficiency had reached 22 % in 2016, as shown in Figure 2.7 [57].

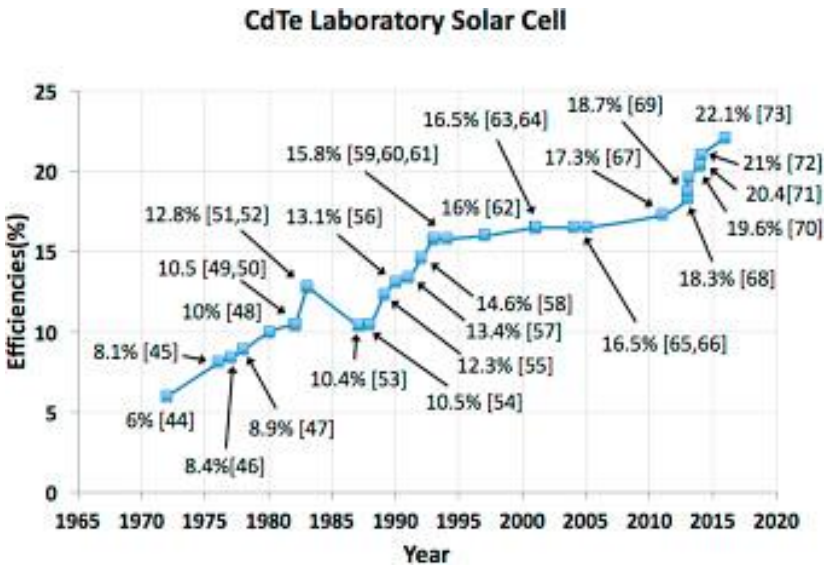

Figure 2.7 Best laboratory efficiencies for CdTe

2.5.5 Copper Indium Selenide (CIS) ($CuInSe_2$)

CIS thin-film technology has shown high efficiencies reaching, 20% in PV cells and 13% in large area modules [8][61]. This is due to the high optical absorption coefficient of its semi-conductor elements. However, some constraints are present that make it difficult to be affordable and commercialized. These constraints are the high production cost and the shortage of indium [9].

2.5.6 Emerging thin-film PV technologies

Recent years have seen the rise of new technologies, based on organic and dye-sensitized PV materials. These PV technologies have the advantages of low production cost [62] and simple manufacturing processes [63]. In addition, the dye-sensitized solar cells can be available in different colours and transparencies, which gives them the advantage of a pleasing aesthetic appearance [64]. These PV cells have relatively low efficiencies and more research is being carried out on these technologies in order to increase their efficiency [62].

2.6 Semi-Transparent Thin-Film-based PV glazing and its impact on building energy performance

The primary reason for using PV glazing in building integrated photovoltaic applications is the reduction of energy consumption, in addition to power generation. Optimized selection of semi-transparent PV glazing in a BIPV system offers less daylight transmission than using clear glazing. In other words, using semi-transparent PV units affects the heat transfer from solar source in form of radiation transmitted through the glazing of the building. This can lead to overall reduction in air-conditioning needs, thereby creating a system with less overall energy consumption [65].

Different types of PVs were investigated to establish their suitability to be used in BIPV applications. Silicon-based PVs, consisting of mono-crystalline and poly-crystalline silicon, were popular in research in the past. Studies in 2007 and 2008, in Brazil and Japan respectively, showed that using these types of photovoltaics as glazing could achieve an energy saving of 43% and 55%, compared to conventional single glazing [66][67]. However, recent studies, in 2018, have exposed some drawbacks in using mono-crystalline and poly-crystalline silicon PVs. Semba et al. [68] found that a degradation in power generated by crystalline silicon PV occurs at high temperatures and high pressures. Benghanem et al. [69] showed in their research that a loss in the maximum generated power can reach to 28% due to the dusting effect in desert countries. Quanesh and Adaramola [70] conducted a study on 29 mono- and poly-crystalline silicon PV modules in six different locations in Ghana. They found that a loss in power generation occurs in a range of 0.8% to 6.5% per year. They also reported that observable defects such as bubble formation, delamination and the appearance of a yellowish/brown colour were noticed for both types of PV materials. Bouraiou et al. [71] analysed and evaluated 608 PV modules in the Saharan region.

Among the promising types of photovoltaic materials are the semi-transparent thin-film based ones and this is mainly due to their high efficiency [72]. These PV materials were proven in research to

be superior to traditional single and double glazing. This is because they provide outdoor light transmittance for a building, together with power generation. Thus, adopting them in the façades of buildings is a promising solution, especially when the area of coverage is large, but several factors need to be considered for optimization of their use, such as orientation, place of installation, weather conditions, and PV transparency. In 2009, Li et al. [73] showed that the use of semi-transparent photovoltaic material with dimming control as a glazing in an office building in China could lead to a cooling load reduction of 450 kW and an overall electricity saving of 1203 MWh, through both energy saving and power generation. Moreover, CO_2, SO_2 and NO_x emissions could be reduced by 852 tons, 2.62 tons and 0.11 tons respectively. Another study found that the use of BIPV modules in multi-family dwellings in Brazil had the ability to supply more energy generation than was consumed for 30% of the year [74].

Miyazaki et al. [75] have shown, through simulation, that the use of a 40% transparent STPV material as a window in an office building led to an energy saving of 54% compared to the standard double glazing model. Poh et al. [56] studied the use of a semi-transparent photovoltaic material in BIPV applications in Singapore. They concluded that this technology can adopted in all orientations and can give better performance compared to single and double glazing. However, optimization of the window-to-wall ratio (WWR) has to be considered for having the best energy performance.

Olivieri et al. [76] conducted both numerical and experimental analysis, and showed that the use of an amorphous-silicon PV material could lead to an energy saving ranging from 5% to 59%, depending on the transparency of STPV material and the window-to-wall ratio. In a recent study, in 2016, Ghahremani and Fathy found that the efficiency of amorphous-silicon photovoltaic materials can be improved by 30% by using metallic nanoparticles inside their structure [77].

Emerging STPV technology such as CdTe has enormous potential, but the BIPV application has not received much attention in the available research work. Among thin-film photovoltaic materials, Cadmium Telluride (CdTe) thin-film PVs are the most suitable for large scale module production [78]. In 2018, Sorgato et al. [79] concluded in their study that the use of CdTe photovoltaic materials as facades and rooftops could meet all the energy demand of a four-story office in Brazil, making it a zero-energy building.

Some studies have provided a performance assessment of using STPVs for a specific location, but there is a crucial need for a generalized case as an energy assessment tool. Furthermore, the effects of the angle of incidence on power generation are subject to the place of installation, module orientation, and transparency. This factor has rarely been studied and reported in the energy calculation of the STPV windows [80]. Moreover, although PV material might reflect some heat and reduce the air conditioning (AC) units' energy consumption, it might also degrade the light intensity inside the building. Therefore, it is essential and meaningful to investigate the energy performance of an emerging STPV technology such as CdTe in applications as windows and facades.

2.7 Thermal Performance of Thin-film based Photovoltaic Materials

All external building elements should satisfy the thermal standards; this is generally described by an important property which is U-value. It is very important to know U-values to allow the designer to check the feasibility of projects and forecast the energy consumption and cooling/heating load required.

In a comparison of the performance of the three thin-film technologies, both Shen [81] and Aris et al. [82] found that amorphous-silicon semi-transparent PV glazing provides a better saving of the overall electricity consumption for cooling, compared to the mono-crystalline semi-transparent PV glazing. Shen found that a high photovoltaic coverage ratio >70% lead to the reduction of the air conditioning (AC) electricity consumption. There is a small penalty that comes with this, especially for countries having long cold winters with sunny days: more energy for heating will be required but there will not be much saving for the AC energy demand in summer. James et al. [83] compared different alternative shading solutions for the atrium at the University of Southampton. They studied the use of semi-transparent BIPV, the studied a-Si PV in their research has a U-value of 1.4 W/m^2 K, which is superior to standard double-glazed argon-filled units (~1.8 W/m^2 K).

A two-dimensional numerical analysis of a double-glazed window with an integrated semi-transparent thin film of a-Si photovoltaic (PV) cells was carried out [84]. It was found that a large quantity of heat transfer by radiation could be reduced, which was observed in the reduction of the U-value.

Didone and Wagner [85] showed that an 8% transparent a-Si PV has a U-value of 1.67 W/m^2K and a SHGC of 0.13, which is lower than conventional single glazing and double glazing, which have U-values of 5.82 W/m^2K and 2.73 W/m^2K respectively and SHGCs of 0.82 and 0.76 respectively. This led to a significant reduction in energy required for air conditioning in different cities in Brazil.

A study was carried out by Wang et al. [86] in 2017 to investigate the energy performance of two different a-Si semi-transparent PV materials. The calculated U-values and SHGC were 2.53 W/m^2K and 2.28 W/m^2K, and 0.152 and 0.238 respectively. These STPVs had lower thermal

characteristics and achieved a 30% energy reduction compared to the conventional glazing which was used.

Chae et al. [87] studied the effect of the transparency of a hydrogenated amorphous silicon (a-Si:H) semi-transparent PV material on its thermal characteristics and energy performance. They concluded that the STPVs with transparencies of 40%, 30% and 12% had U-values of 2.58 W/m^2K, 2.65 W/m^2K and 2.75 W/m^2K, respectively, and SHGCs of 0.277, 0.128 and 0.054 respectively. The authors also pointed out that the optical properties must always be investigated because the energy performance is sensitive to these properties.

It is clear from the literature that there is a lack of data regarding the thermal characteristics of the semi-transparent PV window, and a very few publications are available concerning CdTe thin-film PV materials. Thus, an experimental study is required to investigate the thermal performance of the different semi-transparent PV windows in order to generate the thermal characteristics of this type of window. Such data needs to be available for architects and civil engineers to adopt these types of BIPV units more widely in their designs and calculations.

2.8 Daylight Performance of Thin-film Based Photovoltaic Materials

There are different ways to integrate photovoltaic cells into glass facades and fenestration. These methods depend mainly on the type of the solar cell and the type of building structure for integration – roof, wall or window. These materials have different levels of transparency, and they are integrated into window glazing to change it to a source of electricity generation. The drawback of the semi-transparent PV windows is the blocking of the daylight from penetrating into the buildings. Daylight is always considered being the most energy efficient method to light the

interior of buildings and create visual comfort for the occupants, as lighting has a significant influence on a building's energy consumption. One of the main investigations of the daylighting efficiency of an office building was carried out by Boyano et al. [29], who concluded that the solution lies in controlling the daylight effectively by carrying out a careful design to avoid the negative effects, such as unbalanced indoor daylight and overheating.

Kapsis et al. used Daysim software to examine the daylight performance of three STPV facade configurations [88]. Both opaque spaced silicon solar cell modules and thin film technologies were investigated in this study. It was found that the use of the spaced silicon-based cells partially obstructs the view to the outdoors which not the case for the thin film technology. The Continuous Daylight Autonomy (CDA) and the Daylight Glare Probability (DGP) were used to evaluate the annual daylighting/lighting performance of different STPV modules. The authors found that STPV modules with 30 % transparency provided sufficient daylight inside the building enclosure. Other STPV modules with higher transparency were not recommended, because of the reduced annual generation of electricity and an increase in heat gain, resulting in an increase in the additional cooling load and, therefore, an increase in energy cost for cooling.

Ghosh et al. investigated experimentally the performance of a combined switchable suspended particle device and evacuated glazing [89] [90]. This type of glazing has the ability to perform at different visible light transparencies. The glazing studied in that work was found to achieve a dynamic transmission range from 2% (opaque state) to 38% (transparent state). The same authors published another study regarding the variation of the interior colour rendering of daylight transmitted through the same window technology. In another study by the same authors [35], it was found that the luminous transmittance varies from 0.02 to 0.55 in the opaque and transparent state respectively. The colour rendering index (CRI) was found less than 80, below 0.14

transmittance. This is a very good feature to modulate the transmittance of the total solar spectrum to control the daylight penetration. However, this technology consumes energy and requires power drivers, which is a disadvantage compared to the STPV windows that will generate electricity for the building and are less complex.

Aste et al. used a different parameter to characterise the quality of light in the indoor space [91]: they have used the correlated colour temperature (CCT). They found that the integration of the luminescent solar concentrator (LSC) glazing system in the building façades lowered the CCT in comparison with a clear glass solution. They demonstrated that visual comfort is related to the colour of the glass. The yellow LSC window produces more pleasant light environment with suitable CCT values for the occupants within the office space.

The colour rendering index (CRI) is a similar method to CCT, which was used by Lynn et al. to evaluate the colour rendering properties of STPV modules' light transmittance [92]. It was found that the coloured STPV modules tested in laboratory conditions had a CRI of less than 90, which is considered as visually uncomfortable.

Coloured a-Si:H transparent solar cells were designed and studied as a semi-transparent PV window [93]. This technology has a limited electrical efficiency of 6.36% at 23.5% average transmittance with a spectrum 500–800 nm. Thus, this technology requires an improvement in the conversion efficiency at the full range of the solar spectrum before it can be compared to the actual mature technologies of STPVs.

An experiment was carried out in Hong Kong to compare the energy performance of PV double skin façades (PV-IGU) and PV insulating glass units (PV-IGU) [86]. Using a light-meter, it was found that, on sunny days, the daylighting illuminance in the enclosures installed with PV-DSF

was equal to 350 lux. This performance is better than that of the enclosure installed with PV-DSF, which reached only 200 lux.

A numerical study investigated the potential energy benefits of STPV windows integrated into different orientations in a building [94]. The main finding of this study was that the east-facing window resulted in the largest annual lighting energy saving. These results are very important for the evaluation of the cost-effectiveness of STPV windows when they are installed in different building orientations; however, the results obtained need to be validated experimentally.

This research concerns the experimental investigation of applying different transparent CdTe thin films and their impact on the glare and daylighting performance. The study was conducted using outdoor test enclosures at different orientations. The findings will contribute to the dataset of CdTe thin film experiments. Scaling up the measure can be implemented in future, for any building.

2.9 Conclusion

In this chapter, previous studies and research in relation to the thesis topic have been discussed and important contributions have been acknowledged. The following conclusions can be drawn and summarized as follows:

1. Domestic buildings are the main consumers of energy, especially through glazing, which strongly affects cooling and heating loads and the use of artificial lighting.
2. For the selection of the optimum glazing, thermal performance, daylight performance and overall energy performance have to be evaluated. These types of performance are affected by different factors, such as the location, orientation, size and transparency of the glazing and also the ambient conditions.

3. Building integrated photovoltaic (BIPV) technology is in serious demand, and it has a promising future, because of its significant advantages in terms of efficiency, affordability of materials, weight and appearance.
4. Among the different available photovoltaic technologies, thin-film based PV materials are the most popular because of they are advantageous in terms of efficiency, affordability, availability and cost reliability. Thus, they have attracted researchers' attention.

In the light of the above discussion, it can be argued that a contribution to the topic of building integrated photovoltaic technology is essential. There is clearly a lack of in-depth research on the application of CdTe thin-film-based PV materials, so it is important to conduct a full study on this type of glazing. The research should include both theoretical investigation and practical validation, which will be provided by the current research.

Chapter 3 Experimental Setup and Field Measurement

This chapter demonstrates the use of the experimental setups selected by the 1st author for studying performance analysis in next chapters. Section 3.1 gives a background of experimental setups used by previous study and justifies the selection of the current setup. Sections 3.2 and 3.3 give detailed data on the setup and the measurement equipment. Section 3.4 provides useful results of field measurements.

3.1 Background of Experimental Setup

Useful investigation of PV glazing performance requires an experiment that emulates the real application. The performance of PV glazing is entirely dependent on its material construction and weather conditions. The relevant environmental conditions include sunlight intensity (irradiance), temperature, wind speed and humidity. Selecting and designing the experiment that measures all these conditions is vital for reliable results.

In this research, performance of semi-transparent thin-film PV glazing is investigated when it is used as a component in a building. Performances investigated are thermal, electrical and daylighting. The transparencies range from 0% to 35%. In order to choose the experimental arrangement that best fits the aims of the research, different types of experiments were reviewed. Familiar types of indoor and outdoor experiments are listed below.

3.1.1 Previous Constructions of Experimental Rooms or Enclosures

A. Guarded Hot Box

Guarded hot box is a type of indoor experimental setup used for measuring U-value. It consists of three parts; cold box, guard box and metering box. Figure 3.1 shows a guarded hot box used by Fang et al. [95]. The tested element is installed between the cold box and metering box. The cold box has a controlled low temperature achieved by using any type of cooling system. The guard

box is used to envelope the metering box while being kept at a desired high temperature in order to reduce heat losses from the metering box. The metering box contains a heater so that heat is transferred to the cold box through the tested element.

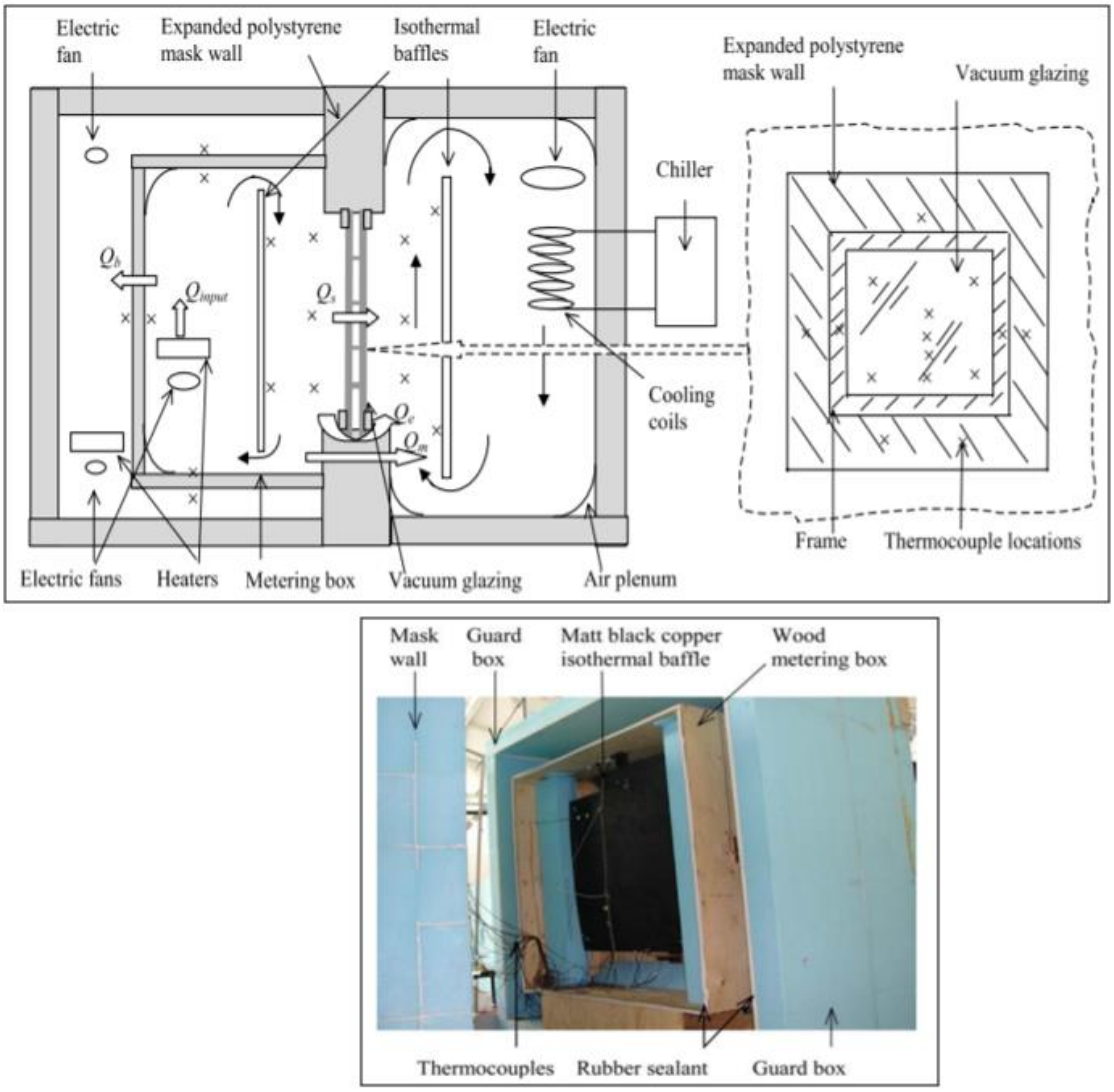

Figure 3.1 Guarded hot box used by Fang et al.

B. Mobile Window Thermal Test (MoWiTT)

This apparatus is designed to be mobile in order to permit location change. MoWiTT makes it possible to mimic the real environmental conditions for calculating U-value and/or G-value which

are the key parameters of the thermal performance of a glazing. Calorimeters and temperature sensors are required to measure the diurnal change of ambient temperatures and power consumption of the heat exchanger or the heat pump used for inside temperature control. Figure 3.2 shows a MoWiTT used by Robinson and Littler in 1993 [96].

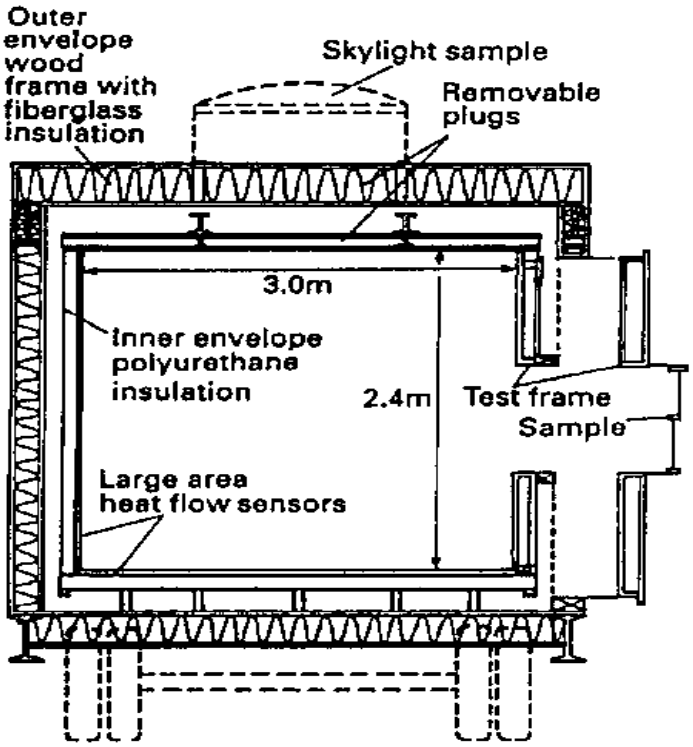

Figure 3.2 MoWiTT used by Robinson and Littler in 1993

C. Outdoor test enclosures

Test enclosures can be of different sizes to emulate the real performance of the installed glazing. They can be real size prototypes [97], or mini-scale prototypes [98][99], and both have shown reliable results. This facility permits the temperature inside the test enclosures to be controlled by

a warming/cooling system or fluctuate freely by environment changes. Parameters monitored are sun light intensity, temperature and wind speed. In order to measure the heat transfer in the enclosed air mass, two approaches can be applied. The first approach is the measurement of temperatures using thermocouples and to use heat transfer equations with the correct assumptions. The second approach is by using a heat flux sensor that measures the quantity of heat transferred through the glazing. It is to be noted that when using the heat flux, readings must be taken at night in order to eliminate the effect of solar radiation on the sensor's measurements [100]. Also, readings should be taken over a minimum of three nights for the heat transfer to be steady.

Of the available facilities, the 1st author decided to construct small-scale test enclosures. The reason behind this choice is that the aim of the research is to test different transparencies of PV cells simultaneously to compare their performance, so a real-scale prototype would not be feasible in terms of cost and space. However, the test enclosures are used in outdoor and indoor experiments. Some analogies are to be taken between the two experiments and are discussed throughout the chapters. Furthermore, the glazing samples available by the 1st author are small size and the indoor sun simulator test area is limited.

3.1.2 Technical Consideration on Insulated Enclosures and Measurements.

For the outdoor experiment, the designed test enclosures are implemented on the rooftop of a building at Exeter University – Penryn campus. To achieve accurate results of thermal, daylight and energy performances, some technical issues were considered and listed below:

1. Different test enclosures are to be designed and installed. This is because different PV glazing are to be tested simultaneously so that comparison is made possible.
2. The test enclosures are of small scale for the experimental setup to be cost effective while measuring different PV glazing at the same time.

3. Each test enclosure must be installed away from shading so that the tested element is exposed to whole quantity of irradiance uniformly.
4. In order to conduct full comparative study and validate the obtained data, the test enclosures are oriented to face South and South West.
5. The test enclosures have to be sufficiently separated from one another to avoid thermal or energy interference or any other effect.
6. Convenient sensors must be selected to take readings of temperatures, irradiance, wind speed, power generation, power consumption and other data.
7. Readings must be taken for sufficient periods so that full days and different weather conditions are covered.
8. Data acquisition of measurements should be obtained using reliable equipment.
9. Test enclosures' walls should be made of insulating material so that one dimensional heat transfer can be assumed in analysis and calculation.

Regarding the indoor experiment, the solar irradiance is replaced by a solar simulator that gives a reliable consistent radiation with time. The experiment should be set over a sufficient period so that a steady state heat transfer condition can be achieved. The consistent irradiance of solar simulator makes it possible to set up one experiment at a time instead of simultaneous experiments, yet the size of the test enclosures should be considered to fit the size of the simulator and to be comparative with the cells used in the outdoor experiment.

3.2 Description of Experimental Setup

Eight identical test enclosures were designed and implemented at ESI building, Exeter University, Penryn, UK, where latitude and longitude coordinates are 50.169174 and -5.107088 respectively. The test enclosures were equipped with thermo-electric coolers (Peltier unit) in order to permit temperature control of the air enclosed by the insulated cell. Another two test enclosures of a larger size were used to fit the larger size glazing. These test enclosures are made of a well-insulated cooler/warmer unit with glazing fitted to one of its walls. An indicative drawing is shown in Figure 3.3.

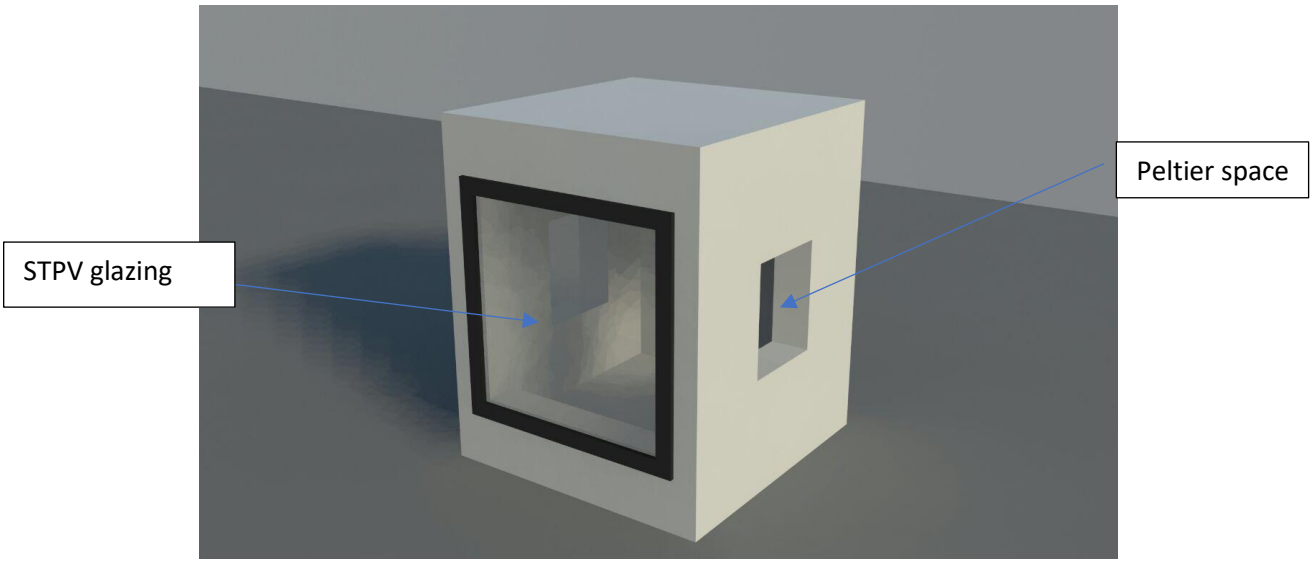

Figure 3.3 3D design of one of the eight test enclosures

3.2.1 Layout of the test enclosures

Each test enclosure size is 0.22 m x 0.2 m x 0.18 m, made of polyisocyanurate (PIR) foam panel (thickness 2.5cm) laminated with aluminium foil sheets to provide good insulation so that any

thermal disturbances can be neglected. Each test enclosure was installed in a box that protects it from rain, dust ingress and bad weather conditions. Each box was laminated with reflective mirror foil to reduce the effect of solar radiation on the sides of each box. Details of the test enclosures are presented in Table 3.1. Four test enclosures were oriented to face South and the other four test enclosures were oriented to face South West. This permits the study of four different glazing simultaneously in two different orientations. Details, layout and photographs of the test enclosures are shown in Figure 3.4 and Figure 3.5.

Table 3.1 Test enclosure details

Dimensions of the test enclosures	0.22 m x 0.2 m x 0.18 m
Dimensions of glazing	0.15 m x 0.15 m
Glazing area	0.0225 m^2
Wall material	Polyisocyanurate laminated with aluminium foil
Wall thickness	0.025 m
Temperature control	Thermo-electric cooler (Peltier unit)

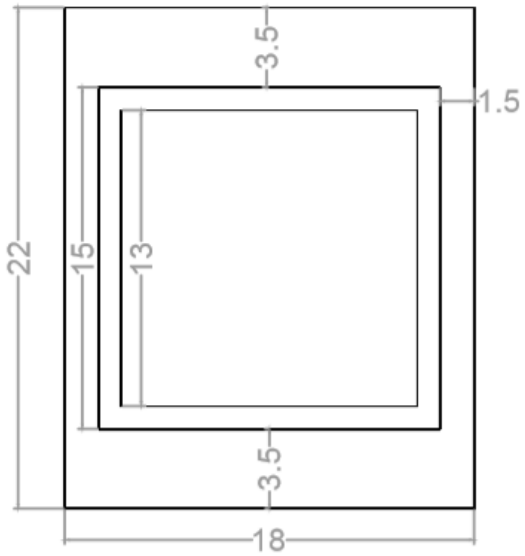

Figure 3.4 Layout of single test enclosure (Dimensions in cm)

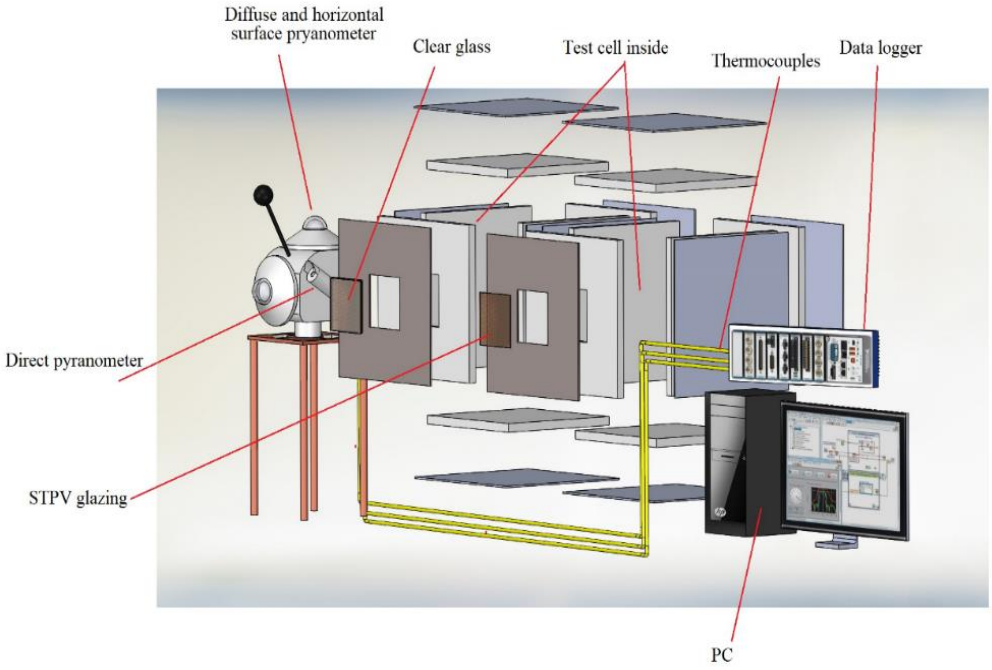

Figure 3.5 Exploded view of two test enclosures side by side – oriented as if in box (omitted)

The same test enclosures were then set for indoor experiment where an AAA+ type solar simulator was used to simulate solar irradiance and a constant speed fan was used to emulate the effect of

wind speed in the outdoor experiment. A photograph of the indoor experiment is shown in Figure 3.6

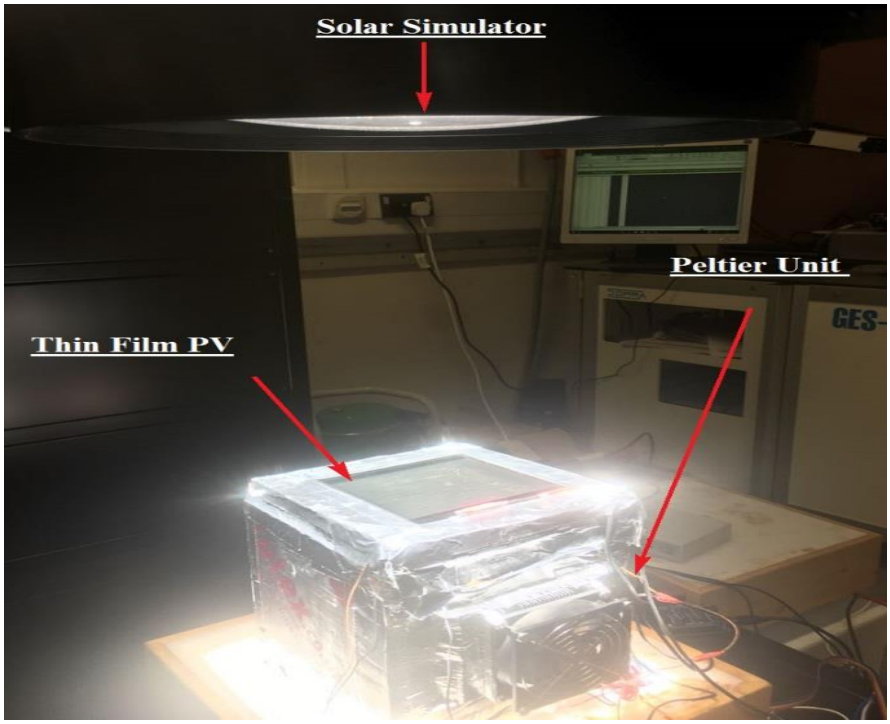

Figure 3.6 Photograph of the indoor experiment

Another test enclosure which can warm and cool the enclosed air volume was used for glazing with larger dimensions. Details and photograph of the cooler/warmer unit test enclosure are shown in Table 3.2 and Figure 3.8 to Figure 3.9

Table 3.2 Cooler/Warmer dimensions

Dimensions	0.49 m x 0.35 m x 0.34 m
Dimensions of glazing	0.3 m x 0.3 m
Glazing area	0.09 m^2
Wall material	Polypropylene, Acrylonitrile butadiene styrene (ABS), Polystyrene
Insulation	Polyurethane foam – PIR laminated with aluminium foil

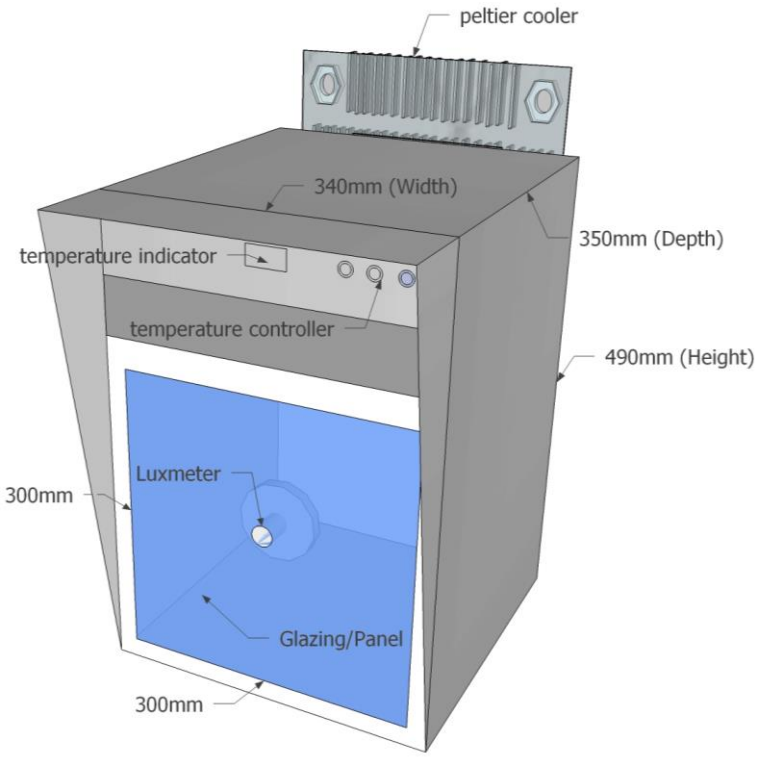

Figure 3.7 Sketch of warmer/cooler unit test enclosures with 30 x 30 cm^2 clear single glazing

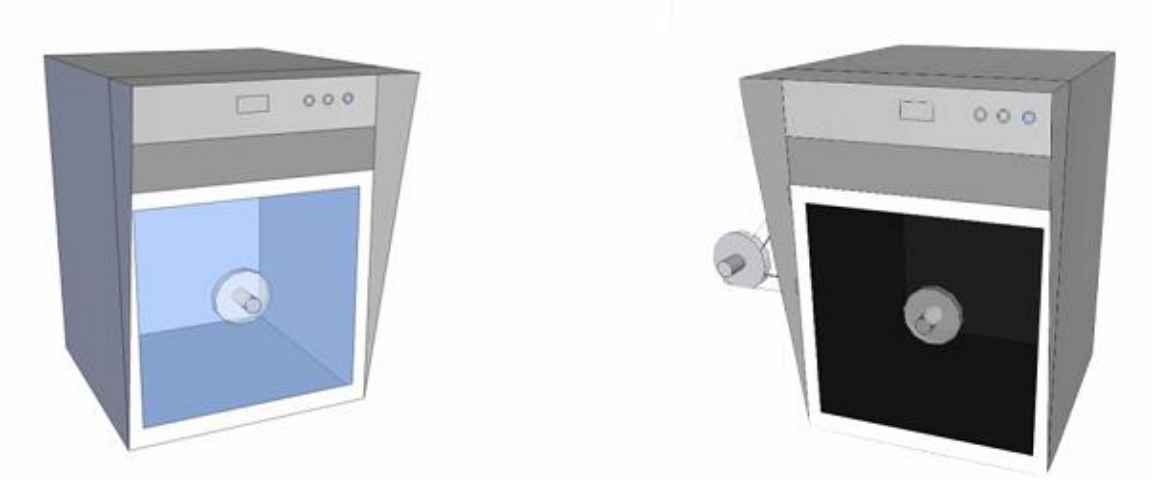

Figure 3.8 Design of the two units test enclosures with a clear single glazing and STPV glazing

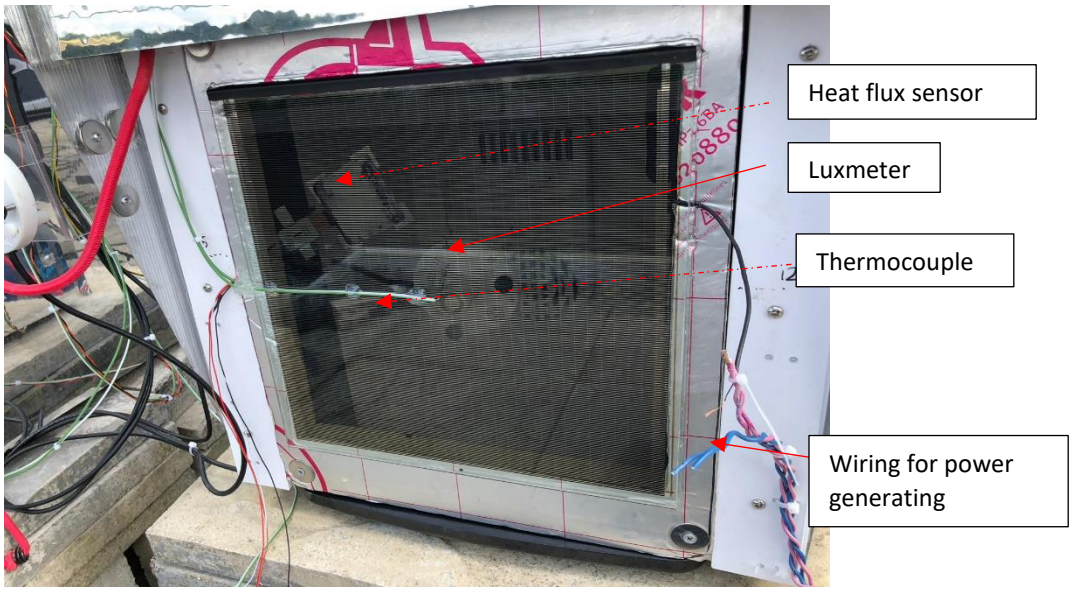

Figure 3.9 Photograph of the test enclosures

3.2.2 Properties of PV glazing

Semi-transparent thin-film PV glazing manufactured to four different transparencies are used in this research and they are referred to as S1, S2, S3 and S5. Details of the PV glazing are presented in Table 3.3. The main difference in the selected STPV glazing is their transparencies. According to Miyazaki et al. [75], the optimum transparency for a South West oriented STPV glazing is in the range of 30% to 40% in order to achieve lowest power consumption of a building, higher transparencies would result in lower power generation. Nevertheless, according to Barman et al. [80], South oriented STPV glazing favour lower transparency for better net energy saving. Therefore the selected transparencies of STPV glazing are 25%, 19%, 0.5% and 35% for S1, S2, S3 and S5 glazing respectively.

Table 3.3 PV glazing specification

PV Glazing	**S0**	**S1**	**S2**	**S3**
Type	Clear Glazing	CdTe Thin-film based PV glazing	CdTe Thin-film based PV glazing	CdTe Thin-film based PV glazing
Transparency	90%	25%	19%	0.5%
Dimensions	15 cm x 15 cm	15 cm x 15 cm	15 cm x 15 cm	15 cm x 15 cm
Thickness	6 mm	6 mm	6 mm	6 mm
Composition	Single Glazing	3 mm tempered glass – thin film – 3 mm tempered glass	3 mm tempered glass – thin film – 3 mm tempered glass	3 mm tempered glass – thin film – 3 mm tempered glass

Solar cell Dimensions	Ø	11 cm x 11 cm	11 cm x 11 cm	11 cm x 11 cm
Solar cell area	Ø	0.0121 m^2	0.0121 m^2	0.0121 m^2
Solar cell ratio	Ø	72.4 %	79.2 %	99.48 %
Output power	Ø	0.815 W	0.996 W	1.414 W
Operating voltage	Ø	7.05 V	7.57 V	8.647 V
Operating current	Ø	0.115 A	0.131 A	0.163 A
Open-circuit voltage	Ø	9.734 V	10.39 V	11.14 V
Short-circuit current	Ø	0.14 A	0.161 A	0.21 A
Weight	0.75 Kg	0.9 Kg	0.9 Kg	0.9 Kg
PV Glazing	**S4**		**S5**	
Type	Single Glazing		CdTe Thin-film based PV glazing	
Transparency	90%		35%	
Dimensions	30 cm x 30 cm		30 cm x 30 cm	
Thickness	6 mm		6 mm	
Composition	3 mm tempered glass – thin film – 3 mm tempered glass		3 mm tempered glass – thin film – 3 mm tempered glass	
Solar cell Dimensions	Ø		26 cm x 26 cm	

Solar cell area	Ø	0.0676 m^2
Solar cell ratio	Ø	61%
Output power	Ø	4.5 W
Operating voltage	Ø	16 V
Operating current	Ø	0.28
Open-circuit voltage	Ø	22 V
Short-circuit current	Ø	0.35 A
Weight	1.5 Kg	1.8 Kg

3.2.3 Thermo-Electric Cooler

As mentioned in the above sections, a thermo-electric cooler (Peltier unit) is fitted to each test enclosure in order to enable the control of the inside temperature of the enclosed air and to measure its absorbed power for energy performance evaluation. Three identical thermo-electric coolers are fitted to each test enclosure to enable cooling the enclosures to a setpoint temperature. The specifications of the thermo-electric cooler are presented in Table 3.4. Photographs of the thermoelectric cooler with its installation and wiring are shown in Figure 3.10 and Figure 3.11

Table 3.4 Thermo-electric cooler specifications

Item	Thermo-electric Peltier cooler
Size	20 cm x 15 cm x 15 cm
Weight	0.44 kg
Material	Aluminium
Voltage	12 V DC
Current	6 A (2 A per unit)

Figure 3.10 Photograph of a single thermo-electric cooler

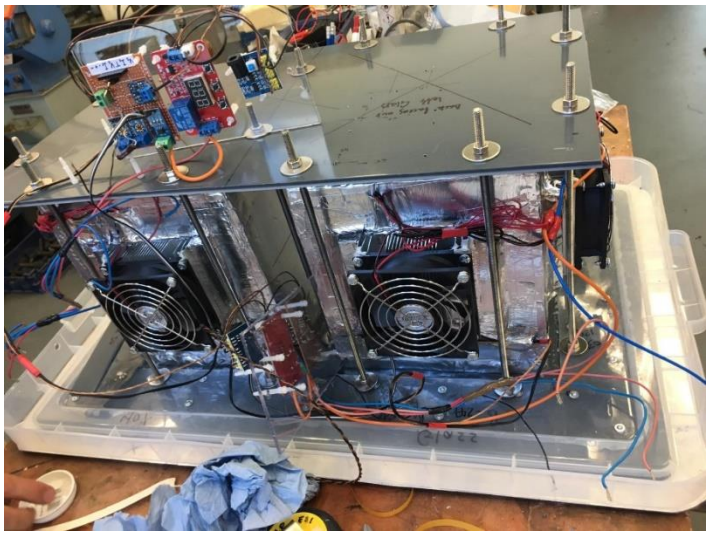

Figure 3.11 Photograph of installed thermo-electric cooler wiring – Two test enclosures are shown

3.3 Measurement Equipment

3.3.1 Field Measurement

Before setting the semi-transparent PV cells for experiment, a spectrometer was used to investigate their optical properties especially transmittance. Thereafter, the field experiment was conducted 24 hours a day from September 2017 to September 2018. The equipment used includes I-V tracer, pyranometer, thermocouples, luxmeter, and a weather station. Real time readings were recorded using a data logger with an interval of 5 seconds during the period of the experiment. Details of the used equipment are presented in Table 3.5.

Table 3.5 Sensors and measurement equipment used in the experiments

Device	Specification and Manufacturer	Measurements
Spectrometer	Perkin Elmer Lambda 1050, USA	Spectral components of light
Pyranometer	Kipp & Zonen, CMP-6, Netherlands	Global and diffuse solar irradiance
Pyrheliometer	Kipp & Zonen CMP1	Direct solar irradiance
I-V Tracer	EKO instruments, MP-160, Japan	PV glazing current and voltage
Thermocouple	K-type, UK	Ambient temperature, temperature of air inside test enclosure, temperature of glazing inner and outer surface temperatures
Heat flux sensor	FHF02 Hukseflux, Netherlands	Heat flux
Luxmeter	MESA Systemtechnik GmbH, D-78467 Konstanz, Germany	Outdoor and inside test enclosure luminance
Data Logger	NI cDAQ-9131, U.S.A Omega RDXL12SD, UK Campbell Scientific CR1000, USA	Data logging
Weather Station	Gill instruments MetPak weather station, UK	Atmospheric pressure, ambient temperature, wind velocity

3.3.2 Temperature Measurement

A total of 30 K-type thermocouples were used to measure the temperature inside the test enclosures and the inside surface and the outside surface of the different PV glazing and single glazing and the ambient temperature. All thermocouples were connected to two data acquisition apparatus, one of them is made by National Instruments and the other is made by Omega. Thermocouples that are fitted on test enclosures with the same orientation were connected to the same data acquisition system so that simultaneous real time reading is ensured. The simultaneous temperature data were

captured once per five seconds and were sent to a PC through a network cable. The thermocouples were calibrated by placing them together in a boiling tube holding glycerine. This was in turn placed in a flask containing a saturated ice bath. Each thermocouple tested was within ±0.5 ^{o}C of 0 ^{o}C. The glycerine tube was placed in a beaker of boiling water and after a stabilization period, each thermocouple was within ±0.5 ^{o}C of 100 ^{o}C. This is satisfactory for test requirements. To avoid the unnecessary solar heat gain from solar radiation on the thermocouple of the outer surface a piece of aluminium foil is needed to avoid direct solar radiation and minimize heating up the thermocouple. The thermocouples' calibration and fixation are shown in figures Figure 3.12 and Figure 3.13 respectively.

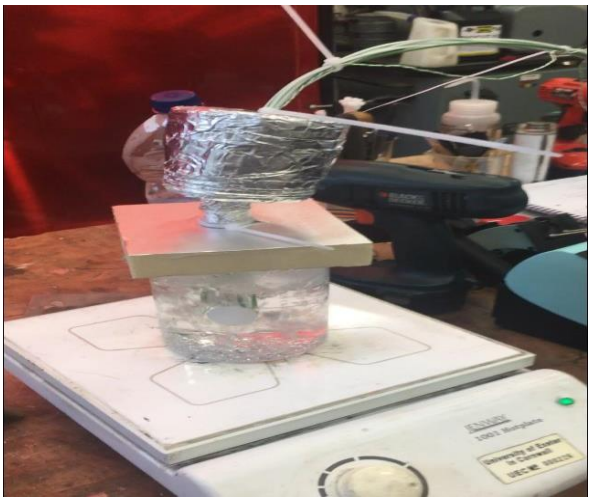

Figure 3.12 Thermocouple calibration

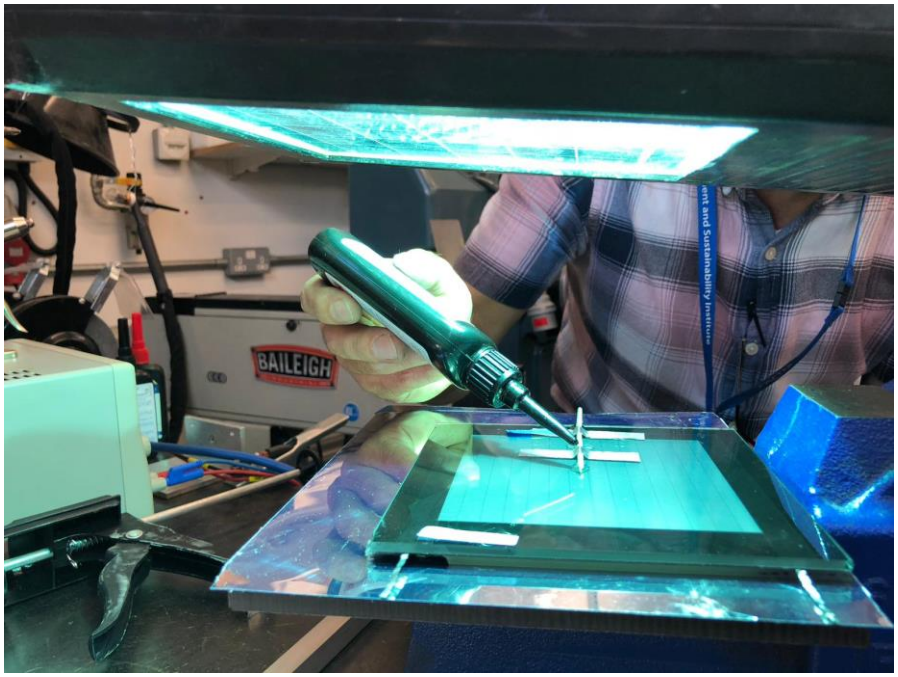

Figure 3.13 UV curing adhesive used to fix thermocouple to STPV glazing on inner and outer surface

3.3.3 Heat flux measurement

A 5cm x 5cm heat flux sensor was used to measure the heat per unit area passing through clear glazing and STPV glazing. The sensor is equipped with integrated T-type thermocouples with a temperature measurement range of -40 ^{o}C to 150 ^{o}C. Table 3.6 shows the specifications of the heat flux sensor. Figure 3.14 shows the heat flux sensor fitted to the surface of a STPV glazing.

Table 3.6 Heat flux sensor specifications

Specifications	**FHF02 Heat Flux Sensor**
Measurement Range	(-10 to +10) x 10^3 W/m^2
Nominal Sensitivity	5.5 x 10^{-6} V/(W/m^2)
Sensing Area	9 x 10^{-4} m^2
Uncertainty of Calibration	± 5 %

Figure 3.14 Fitting heat flux sensor to internal surface of STPV glazing

3.3.4 Solar Irradiance Measurement

Three pyranometers were installed on the roof of the building as a group. One pyranometer was used to measure the global solar irradiance on the horizontal plane. Another pyranometer, fitted with a shadow ring to block the direct sun, was used to measure the diffuse solar irradiance on the horizontal plane. The ring has a polar axis design that requires adjustment for solar declination periodically every few days. The third is a pyrheliometer that measures direct solar irradiation. The maximum solar irradiance range of the pyranometers is up to 2000 W/m^2. A photograph of the pyranometers and pyrheliometer is shown in Figure 3.15. Properties of the pyrometers and pyrheliometers are shown in Table 3.7.

The pyranometers were connected to a National Instrument data acquisition system in order to transfer solar irradiation data each five seconds for computer storage. It is to be noted that the

output of the pyranometers is voltage and the sensitivity of each pyranometer is used to calculate the exact solar irradiance. A LabView VI was built to collect the data from the data acquisition system.

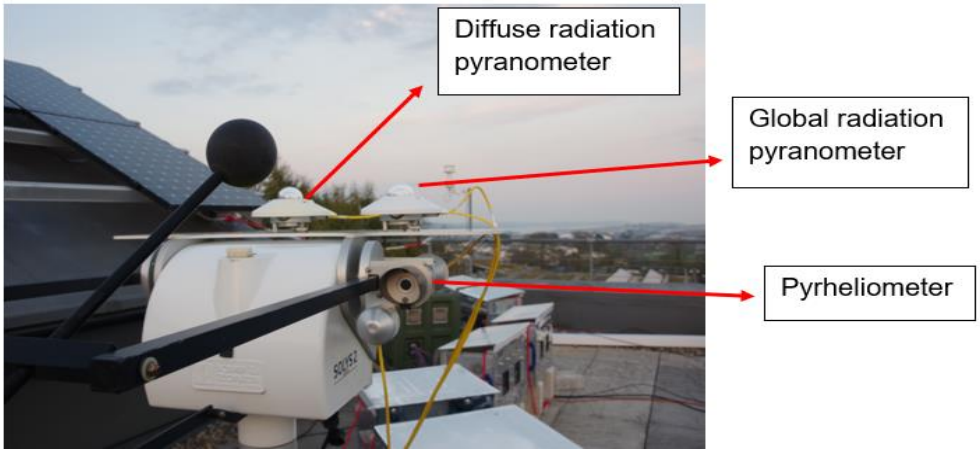

Figure 3.15 Photograph of pyranometer and pyrheliometer

Table 3.7 Pyranometer and Pyrheliometer specifications

Specification	**Pyranometer**
Sensitivity	7 to 14 µV/W/m²
Wavelength	285 to 2800 nm
Range	0-2000 W/m²
Operating Temperature Range	40 °C to +80 °C
Directional response (up to 80° with 1000 W/m² beam)	< 10 w/m^2
Response Time	< 5 s

3.3.5 Output Power Measurement of PV Glazing

In the outdoor experiment, the solar irradiance changes with time. As solar irradiance changes, the maximum power output of a photovoltaic glazing changes. The maximum power output is defined by the optimum voltage point multiplied by its corresponding current. So, a high accuracy maximum power point tracer (MPPT) system was used to trace the maximum power. And an I-V tracer was used to measure the voltage and current of each PV glazing at thirty seconds intervals throughout the experiment so the power can be calculated. Details of the used IV tracer are tabulated in Table 3.8.

Table 3.8 I-V Tracer specifications

Specifications	**IV Tracer**
Voltage Measurement Range	0.05 – 300 V
Current Measurement Range	0.005 – 10 A
Power Measurement Range	0 – 300 W
Accuracy	0.5%
Weight	9 kg
Operating Temperature Range	0 – 40 ^{o}C
Input Channels	1 channel

3.3.6 Daylight Luminance Measurement

GmbH, D-78467 luxmeters, shown in Figure 3.16, were used to measure the luminance outside and inside the test enclosures. The luxmeters are manufactured and calibrated by MESA Systemtechnik. Three luxmeters were used during the experiment. One was placed outside close

to the test enclosure at a height of 0.25 m to measure the daylight luminance before entering the test enclosures. The other two luxmeters were fixed inside at the front and back of the test enclosures. Measurements were taken for three days when the luxmeter was 2 mm away from the front of the glazing and another measurement had taken place during same period with the sensor fitted at the back (180 mm away from the glazing), to record the luminance after passing the glazing. These measurements were taken with the test enclosures facing two orientations namely South and South West.

The three luxmeters were connected to a computer directly through CR1000 data logger. The luminance data by luxmeter were recorded once per minute. The specifications of the luxmeter are presented in Table 3.9.

Figure 3.16 Photograph of MESA SystemtechnikLuxmeter

Table 3.9 Luxmeter specifications

Specifications	Luxmeter
Range	0..10klux (indoor) 0..160klux (outdoor)
Accuracy	< 4% at 100klux @22°C
Response Time	< 1 sec
Operating Temperature	-40 ^{o}C to 60 ^{o}C
Temperature Drift	< 0.1%/K
Weight	150 gram

3.3.7 Completed Setup Overview

Figure 3.17 depicts an indoor test for one test enclosure under the sun simulator which provides various uniform irradiance per request over 20 * 20 cm^2, thus, one enclosure per time is tested. All sensors are attached to the setup and data from them was collected by a computer.

As shown in Figure 3.18, a simplified sketch illustrates the eight test enclosures. The first four enclosures are oriented to the South and the second four to the South West. Each has different glazing transparency as explained before, denoted as S1, S2, S3 and S4. All enclosures are equipped with various sensors and cooling units and send the data to a computer.

Figure 3.19 shows the completed setup installed on the roof of the building with all parts mentioned above. Each enclosure has been combined in one box but is still thermally insulated. Figure 3.20 shows the outdoor experimental setup to test a bigger sample. The cooler/warmer test enclosures presented in Figure 3.20 are fitted with 30 x 30 cm^2 double clear glazing and double STPV glazing.

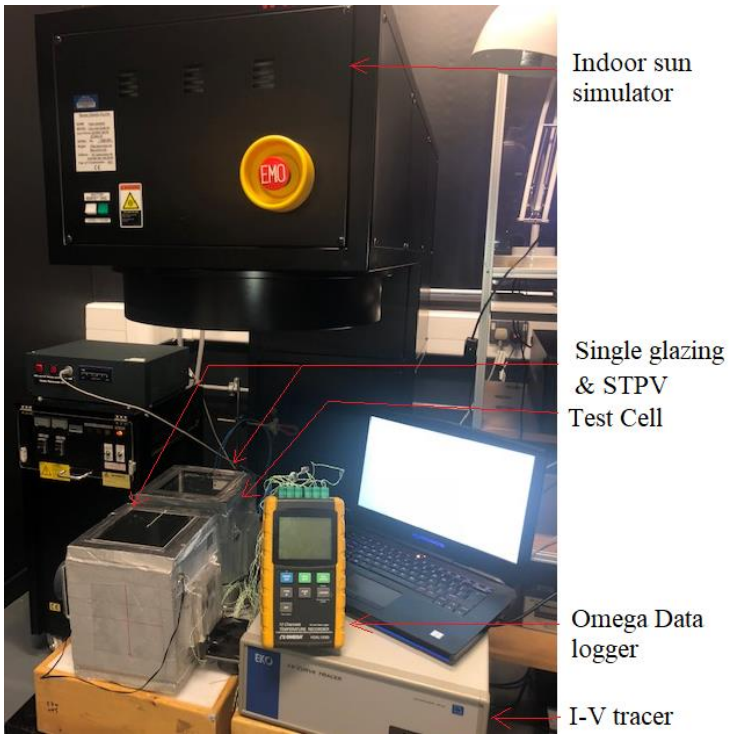

Figure 3.17 Photograph of the indoor experiment

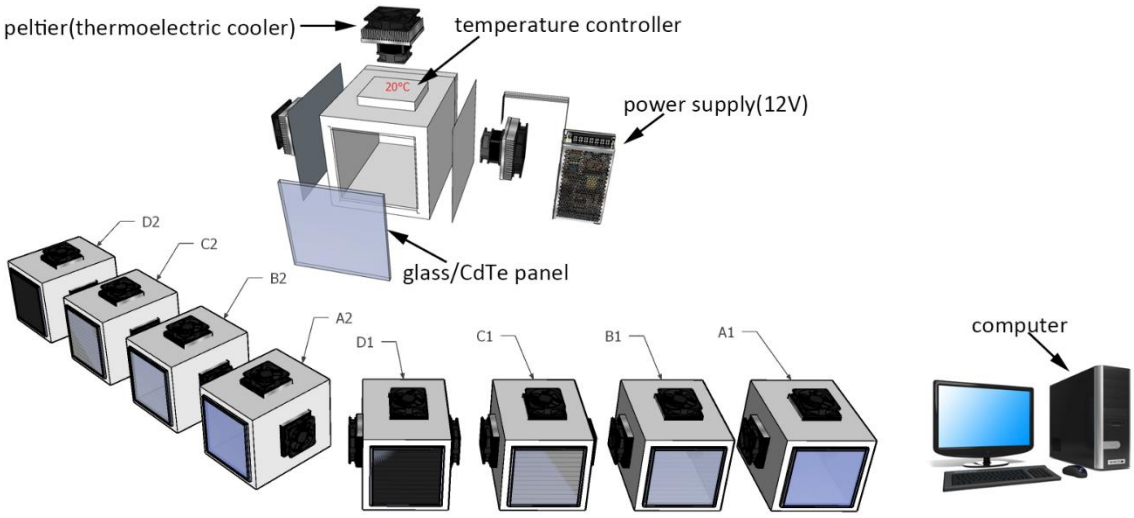

Figure 3.18 Sketch of the outdoor experimental setup showing the eight test enclosures – The outer shield box was omitted for clarity

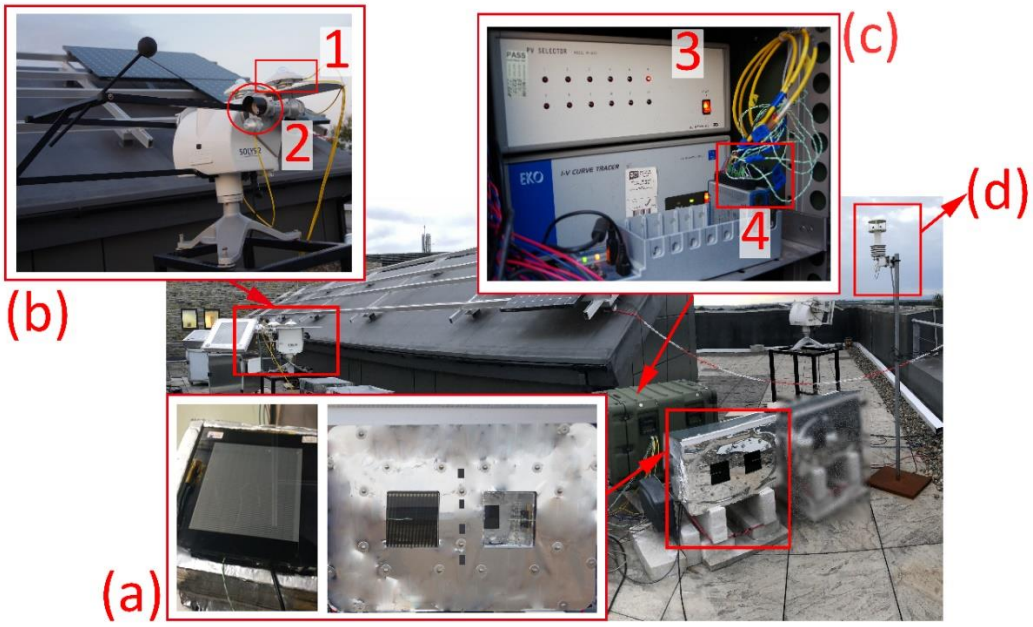

Figure 3.19 Completed view of the whole setup (a) test cell (b) solar tracker (1) global and diffuse radiation (2) the direct radiation (c) data logger (3) IV-tracer (4) thermocouple data logger (d) weather station

Figure 3.20 Photograph of the full outdoor experimental setup with warmer/cooler units test enclosures are fitted with 30 x 30 cm^2 double clear glazing and double STPV glazing

3.4 General Measurements in the Field Experiment

The outdoor experiment was conducted for one year from August 2017 to August 2018. Semi-transparent photovoltaic glazing of different transparencies were tested throughout this period in two different orientations, namely South and South West. The semi-transparent photovoltaic (STPV) glazing were meant to experience different weather conditions in different seasons including both sunny and cloudy days. Main measurements included the reading of solar irradiance, temperatures and daylight luminance.

3.4.1 Solar Irradiance Measurements

Direct, diffuse and global horizontal and vertical irradiances were recorded throughout the time of the experiment for both South and South West orientations. Four different days were selected to be representative of the weather conditions in Penryn, UK to justify the selection of which performance analysis was carried out. Figure 3.21 to Figure 3.24 show the horizontal, vertical South and vertical South West irradiances for each selected day.

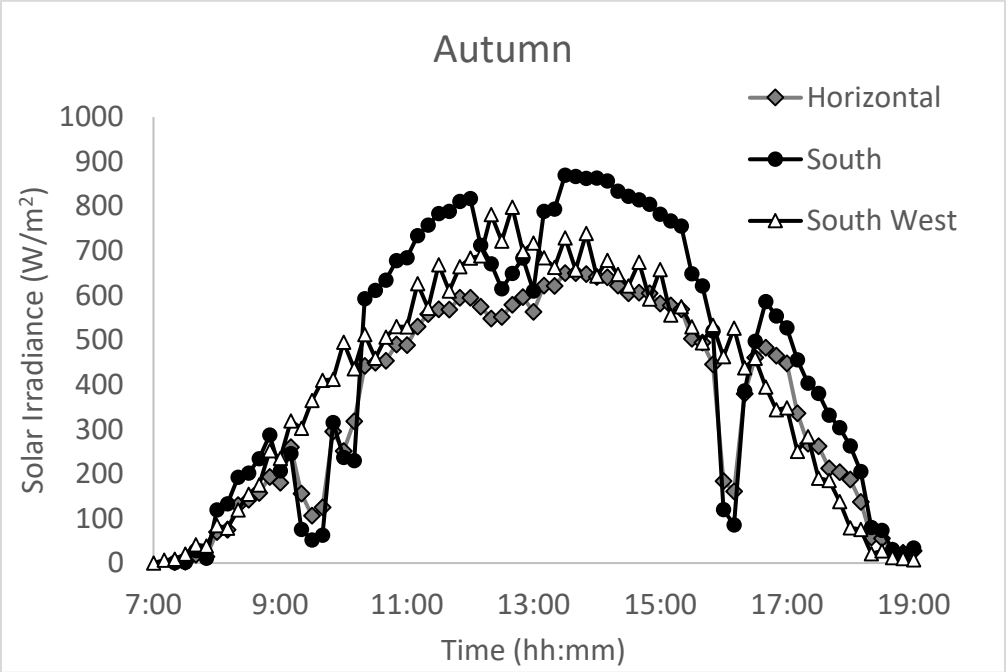

Figure 3.21 Vertical South, vertical South West and horizontal solar irradiances in Autumn season, September, 25th, 2017

Starting with autumn season, September 25th, 2017, as shown in Figure 3.21 the horizontal solar irradiance shows a maximum of 650 W/m^2 which is lower than vertical solar irradiance in both South and South West orientations that reach 870 W/m^2 and 800 W/m^2 respectively.

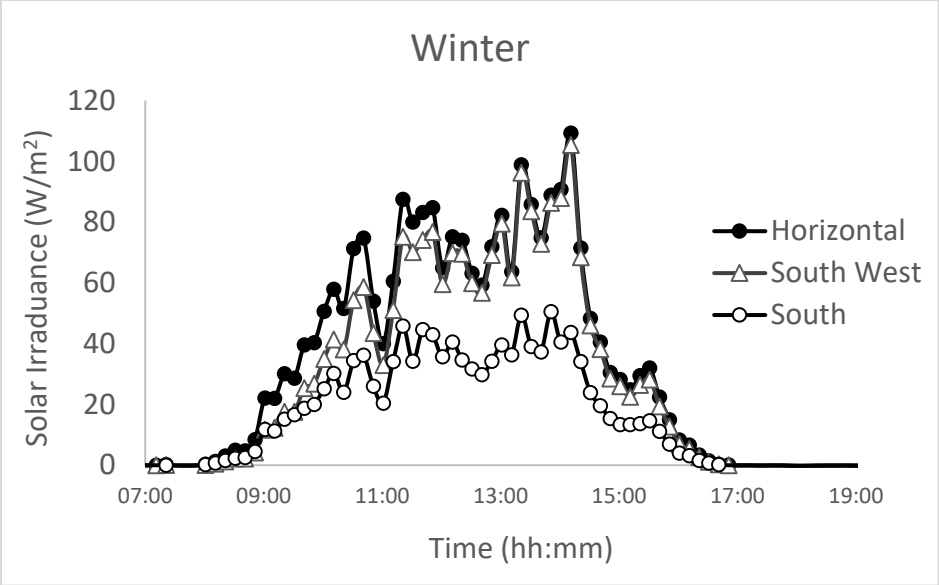

Figure 3.22 Vertical South, vertical South West and horizontal solar irradiances in Winter season, January 23rd, 2017

Winter season, January 23rd, 2017, Figure 3.22 had the minimum solar irradiance among other seasons. The maximum horizontal irradiance was 109 W/m^2, South West vertical irradiance showed very close values to horizontal irradiance especially at the mid-day time and the maximum irradiance reached 105 W/m^2. However vertical irradiance at South was almost half these values reaching 50 W/m^2.

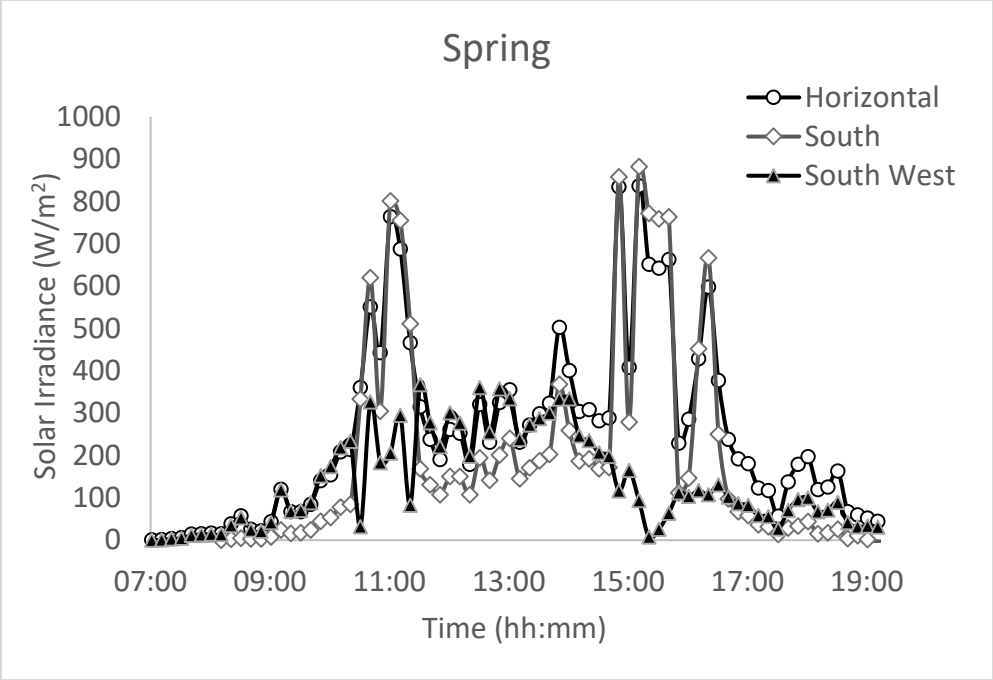

Figure 3.23 Vertical South, vertical South West and horizontal solar irradiances in Spring season, March 27th, 2017

In Spring season, March 27th, 2017, Figure 3.23 horizontal and vertical South irradiances were very close with the maximum value of horizontal irradiance being slightly less than that of vertical South as they both reached 840 W/m^2 and 880 W/m^2 respectively. However, the South West orientation showed the lowest irradiance in this season reaching a maximum of 370 W/m^2.

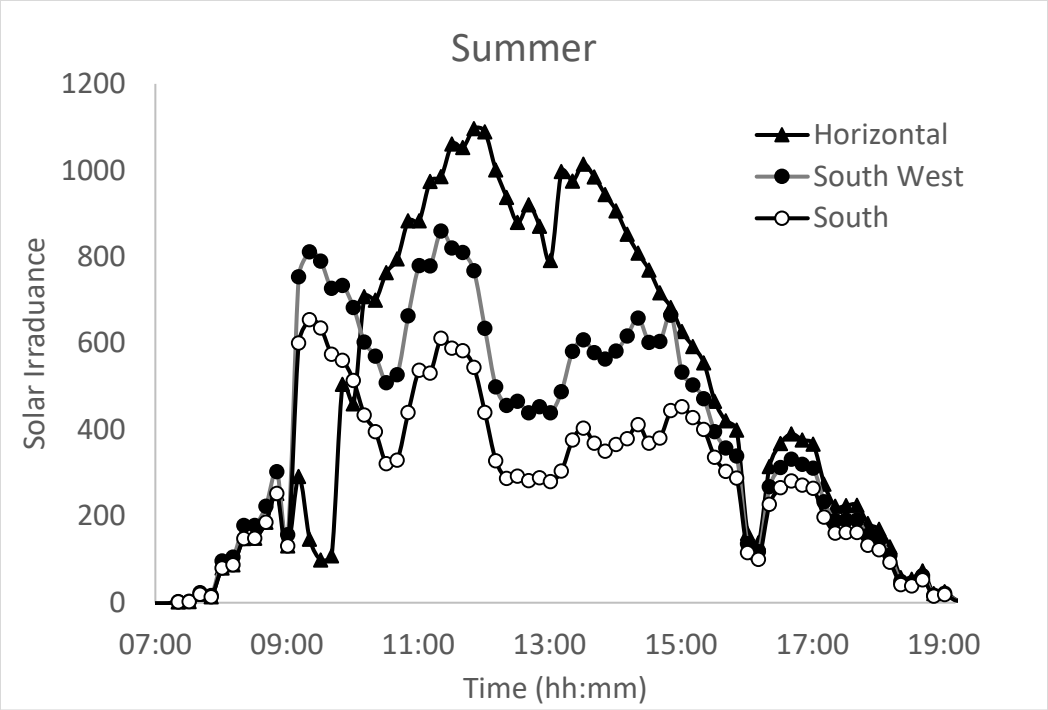

Figure 3.24 Vertical south, vertical South West and horizontal solar irradiances in summer season, July 14th, 2017

Summer season, July 14th, 2017, Figure 3.24 showed the maximum value of horizontal solar irradiance and South West vertical irradiance among all other seasons reaching values of about 1100 W/m^2 and 850 W/m^2 respectively, however this was not the case for South vertical irradiance as they had values of 650 W/m^2.

Based on the analysis of seasonal conditions measurements, September 25th was selected to be the day in which analysis will be performed. This is because the irradiances have high values. Also, the vertical solar irradiances of South and South West orientations have close values. This means that the test enclosures will be exposed to similar conditions. This makes performance analysis of STPV glazing in both orientations measurably valid and useful comparison.

The measurements of global horizontal solar irradiance and diffuse horizontal solar irradiance were taken and presented in Figure 3.25 and Figure 3.26. Results showed that on a sunny day, diffuse solar irradiance accounts for a small portion of the global irradiance, however, on a cloudy day the diffuse solar irradiance is almost equal to global irradiance.

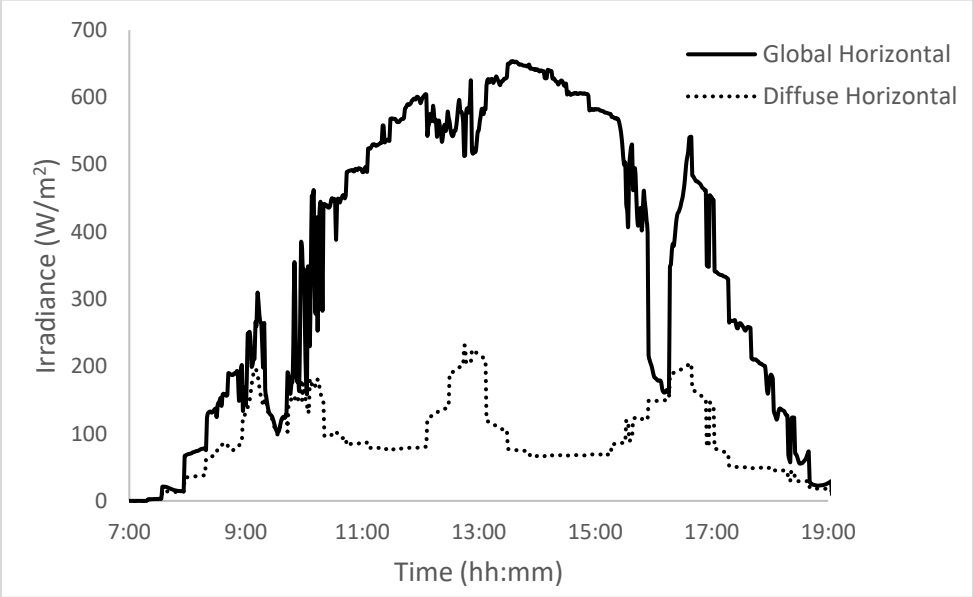

Figure 3.25 Diurnal variation of global and diffuse horizontal irradiances on a sunny day, September 25th, 2017

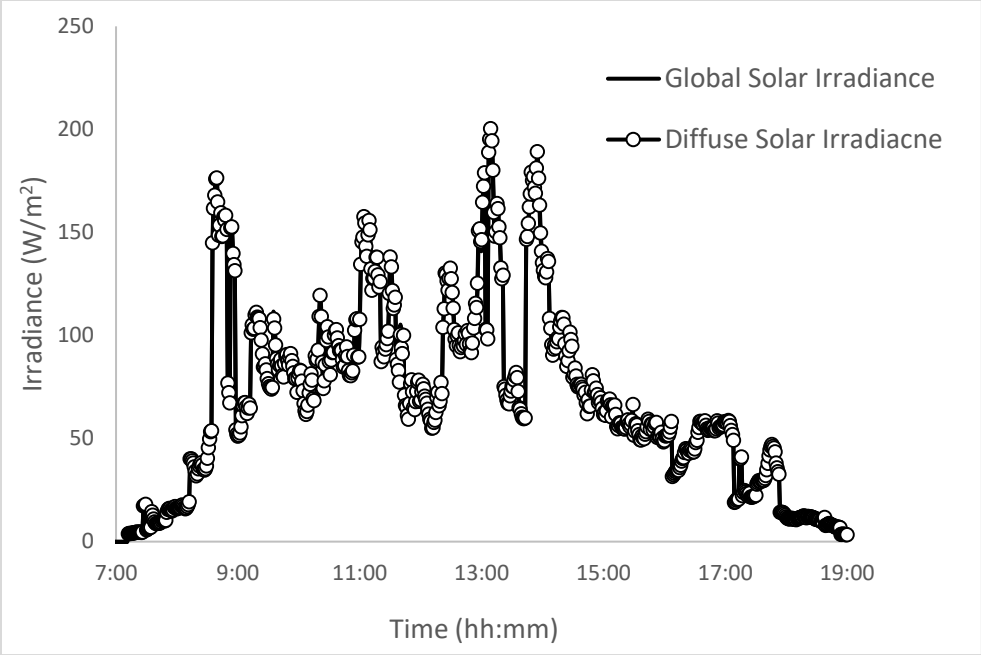

Figure 3.26 Diurnal variation of global and direct horizontal irradiances on a cloudy day, September 20th, 2017

3.4.2 Semi-transparent photovoltaic glazing power generation and efficiency

The diurnal variation of solar irradiance of a sunny day are plotted in the Figure 3.27. The diurnal variation of power generation of thin-film based semi-transparent photovoltaic glazing with different transparencies are also plotted on the same chart. Results demonstrate the similar behaviour of solar irradiance and STPV glazing power generation of all tested cells. Also, it was shown that the cells with lower transparencies generate more power. Nevertheless, Figure 3.28 shows that the relation between solar irradiance and STPV glazing power generation is linear.

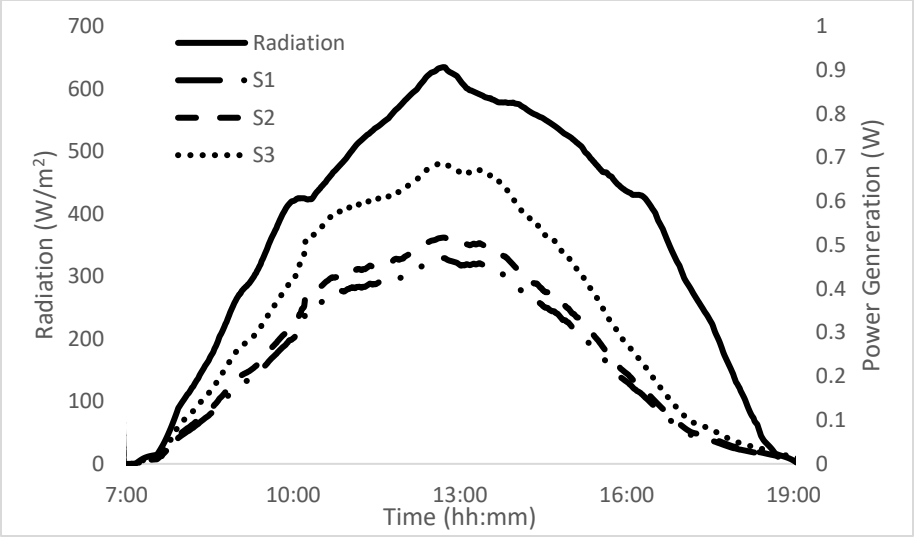

Figure 3.27 Diurnal variation of STPV glazing power generation and horizontal irradiance in a sunny day, September 25th

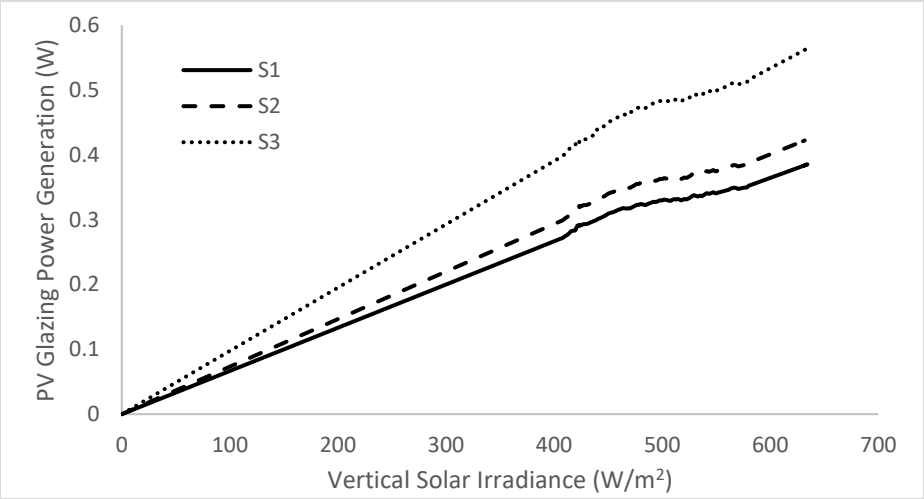

Figure 3.28 Relation between vertical solar irradiance and STPV glazing power generation

The efficiencies of the tested semi-transparent photovoltaic glazing with different transparencies were calculated based on the measured power generation. These efficiencies were plotted with the diurnal variation of the measured PV glazing surface temperatures and presented in Figure 3.29. Results demonstrate that STPV glazing with lower transparencies have higher efficiencies. Also,

the correlation between STPV glazing surface temperature and STPV glazing efficiency was shown in the chart relating both variables in Figure 3.30. The charts show that as PV glazing temperature increase its efficiency decreases and vice versa.

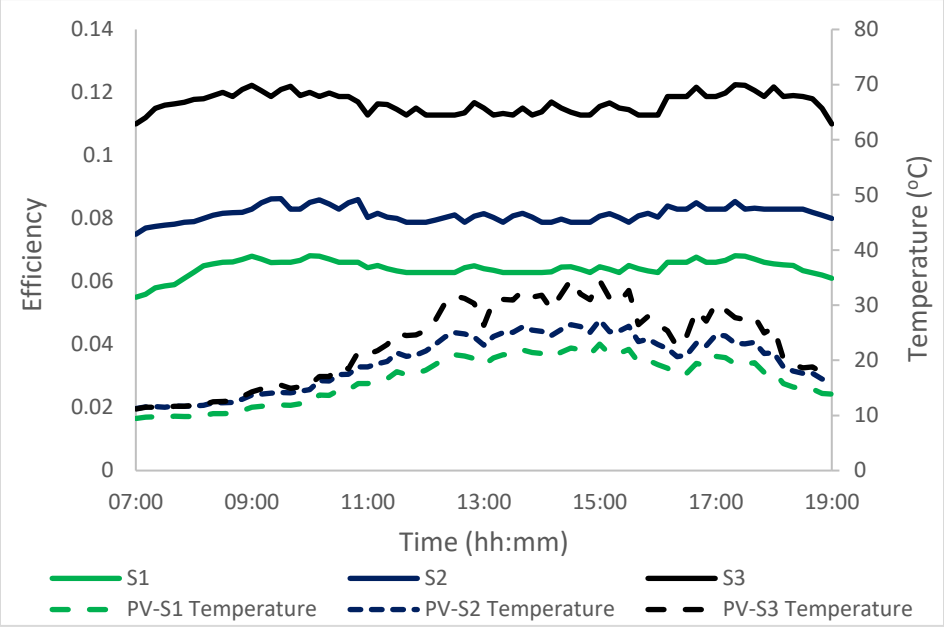

Figure 3.29 Diurnal variation of STPV glazing temperature and efficiency

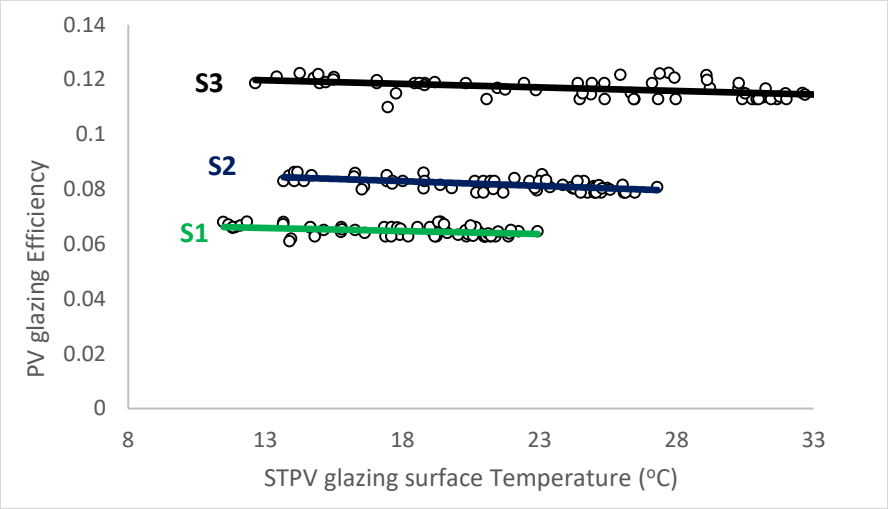

Figure 3.30 Variation of efficiency with STPV glazing surface temperature

The calculated efficiency and temperature coefficient based on the measurements of STPV glazing temperatures and power generation are summarized in Table 3.10. The efficiency of S1 is 6.7%, S2 is 8.5% and S3 is 12%. With respect to temperature coefficient, is 0.42% for S1, 0.35% for S2 and 0.15% for S3.

Table 3.10 Summary of STPV glazing efficiencies and temperature coefficients

STPV glazing	Type and transparency	STPV glazing maximum efficiency	Temperature coefficient
S1	CdTe Thin-film – 25%	6.7%	0.42
S2	CdTe Thin-film – 19%	8.5%	0.35
S3	CdTe Thin-film – 0.5%	12%	0.15

3.4.3 Daylight Measurements

One of the most important properties of a semi-transparent photovoltaic glazing is that it allows the passage of daylight into the enclosure. In tests, luminance was recorded outside and inside the test enclosures using single clear glazing and the STPV glazing of transparency 35% as an example for the purpose of comparing. Other sample transparencies could be used alternatively. The chart shows the identical tendency of the daylight outside and inside. Also, the inside luminance of clear glazing is more than quadruple than that of the STPV glazing as shown in Figure 3.31 and Figure 3.32.

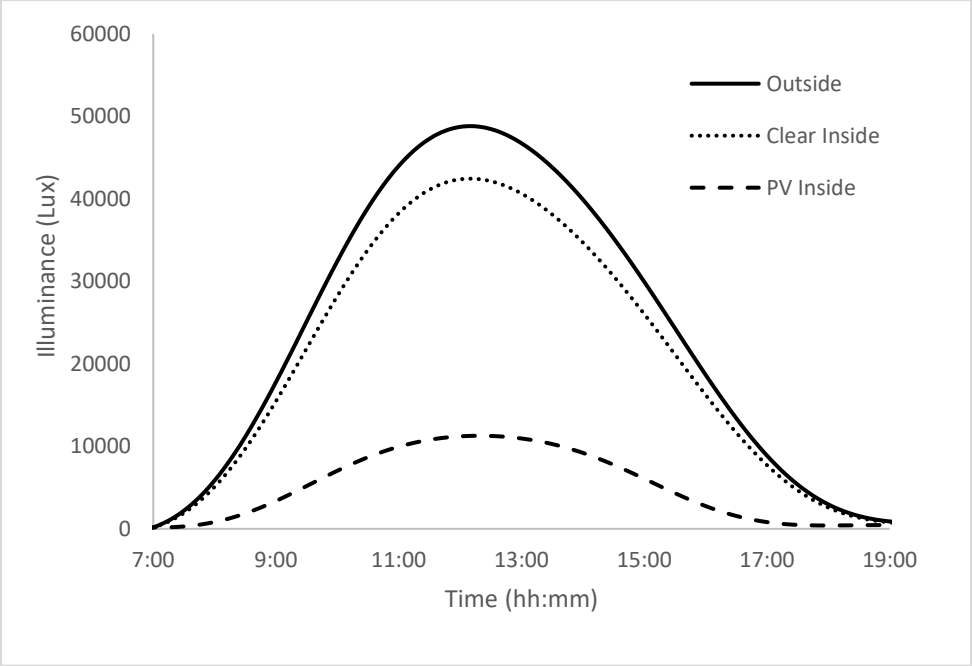

Figure 3.31 Variation of illuminance outside and inside clear glazing and 35% transparency STPV glazing test enclosures

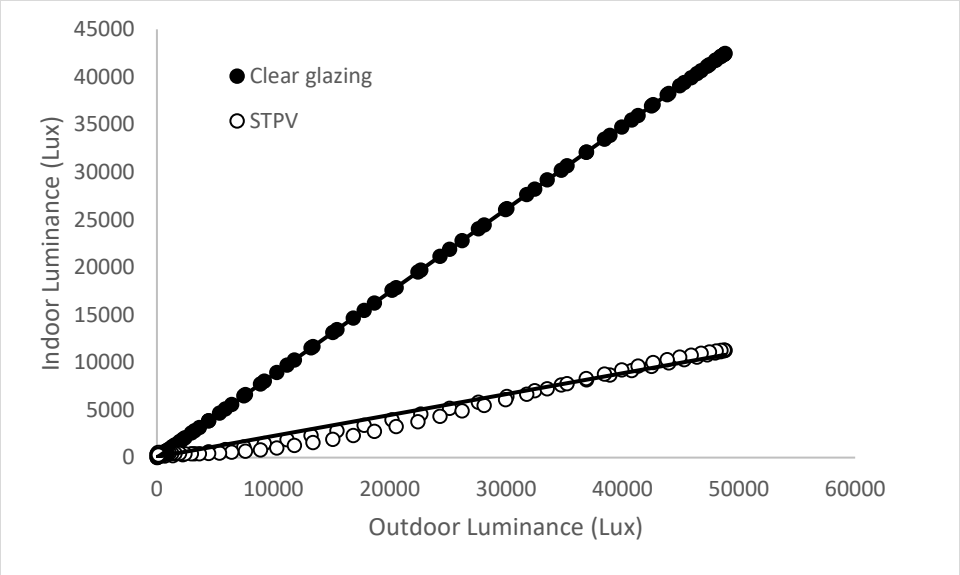

Figure 3.32 Variation of illuminance inside clear glazing and 35% transparency STPV glazing test enclosures with outdoor illuminance

3.5 Conclusion

Outdoor and indoor experimental setups were set in order to evaluate the thermal performance, energy performance and daylight performance of semi-transparent photovoltaic glazing with different transparencies and compare them to clear glazing. The data of the STPV glazing such as material, size and transparency were defined.

The test enclosures were equipped with instruments which provide the reliable measurements needed in order to calculate the thermal, energy and daylight performance. The instruments were well calibrated and have clearly defined parameters such as accuracy and measurement ranges.

The ambient conditions of the outdoor experiment were studied in terms of temperature and solar irradiance. Suitable days and orientations were selected accordingly for efficient evaluation of STPV glazing performances. Also, basic correlations were made to understand the dependence of the behaviour of different parameters.

Chapter 4 Thermal Performance Evaluation of Cadmium Telluride Semi-Transparent PV Glazing

The aim of this chapter is to investigate the thermal performance of Cadmium telluride (CdTe) thin-film based semi-transparent photovoltaic glazing of different transparencies. The thermal performance is evaluated in terms of temperature behaviour inside the test enclosures in addition to overall heat transfer coefficient (U-value) and solar heat gain coefficient (SHGC) evaluation. Different experiments were set and installed to achieve validation of results. Calculations were performed based on the readings taken from each experiment.

4.1 Introduction

In order to achieve the thermal performance evaluation of CdTe thin-film based semi-transparent photovoltaic (STPV) glazing, different experimental setups were installed and oriented to face South and South West. The experimental conditions used were as follows:

1**. Experiment 1**: An outdoor experimental setup consisting of eight test enclosures was deployed in an outdoor environment. This experiment was used for investigating temperature behavior at glazing surface and inside the test enclosures and for evaluating U-value and SHGC. Further details regarding the test enclosures and the experiment's installation are presented in Chapter 3 - section 3.2.

2. **Experiment 2**: A similar experimental set-up as described above was tested indoors. A solar simulator with a constant irradiance was used to emulate the solar irradiance and a constant speed fan was used to emulate the wind speed so that the convection heat transfer is not underestimated in an indoor environment as recommended by Robinson [101]. This experiment was used for U-value calculation. According to the knowledge of the 1st author, this experimental set-up has not

been performed before, so similar results as experiment 1 setups would validate the results and the experiment.

3. **Experiment 3**: A heat flux sensor was fitted at each of the test enclosures. This experiment was used for U-value evaluation using temperature and heat flux measurements.

Details about the experiments' locations and test enclosure sizes are presented in chapter 3 – section 3.2. The forthcoming sections are explaining about the results and their relevant discussions.

Figure 4.1 Photograph of the test enclosures used for thermal performance evaluation

4.2 Evaluation of Overall Heat Transfer Coefficient (U-value)

4.2.1 Experiment 1: Outdoor test enclosures

Eight outdoor test enclosures were installed. Four of the were oriented towards the South. Clear glazing S0 (90% transparency) and STPVs S1 (25% transparency), S2 (19% transparency) and S3

(0.5% transparency) were installed at each of the South-oriented test enclosures. Another four identical test enclosures with the attached glazing were installed and oriented towards the South West.

4.2.1.1 Governing Equations for U-value Calculation

Heat is transferred via three methods: conduction, convection and radiation. In order to quantify the heat transfer through a system, the methods of heat transfer involved have to be identified and presented in the form of equations so that the total heat transfer coefficient (U-value) can be calculated. In the present study, the heat is said to be radiated from the sun. It then experiences convection from the atmospheric air outside the test cell. After that, it is conducted through the insulation board and the STPV glazing in order to penetrate the test cell where it experiences convection again due to air inside the test cell. Heat is then stored inside the test cell resulting in an increase of temperature to reach a value higher than ambient temperature. This leads to heat transfer from inside the test cell to the outside via the same heat transfer methods of convection and conduction as prescribed above. It is to be noted that the glazing absorbs part of the heat going out of the test cell to generate power.

The equations presented in this section are as proposed by Ghosh et al. [102] based on the assumptions of steady state and one directional heat transfer from a test enclosure to the outside. The assumption of steady state heat transfer is valid for outdoor experiment held for a long period of time [103] whereas the assumption of one directional heat transfer is valid because of the high insulation property of the polyisocyanurate insulation board (thermal conductivity $K = 0.02\ W/mk$) that makes heat transfer through it negligible compared to the glazing. The behaviour

of the incident heat from solar irradiation to the test enclosure can be represented as in equation (4.1).

$$Q_{in} = Q_g + Q_{tc} + Q_w + generated\ power \quad (4.1)$$

Where;

Q_{in} is the incident solar heat to the glazing in (W) and it is represented through equation (4.2),

$$Q_{in} = I_{ver,global} A\tau\alpha \quad (4.2)$$

Where;

$I_{ver,global}$ is the global vertical solar irradiance measured by the pyranometer (in W/m^2).τ and α are the transmittance and absorbance of the glazing respectively.

Q_{tc} is the heat stored inside the test enclosure and it is related to mass of air inside the test enclosure, heat capacity of air and variation of the inside temperature with time as presented in equation (4.3).

$$Q_{tc} = M_{tc} C_{tc} \frac{dT_{in}}{dt} \quad (4.3)$$

C_{tc} is the heat capacity of air = 1.005 kJ/kg ^{o}C.

The mass of air inside the test enclosure (M_{tc}) can be obtained from equation (4.4).

$$M_{tc} = \rho_{air} V_{tc} \quad (4.4)$$

Where, ρ_{air} is the density of air = 1.23 kg/m^3

V_{tc} is the inner volume of the test enclosure in (m^3)

Q_w is the heat transfer through inside and outside air convection and conduction through the insulation board wall. It can be calculated through equations (4.5) and (4.6).

$$Q_w = U_w A_w (T_{in} - T_{ambient}) \quad (4.5)$$

$$U_w = [\frac{1}{ho} + \frac{L}{K} + \frac{1}{hi}]^{-1} \quad (4.6)$$

Where,

U_w is the combined U-value of the test enclosure's wall with inside and ambient air. It is evaluated in (W/m^2K)

A_w is the area of the polyisocyanurate insulation board

$T_{ambient}$ is the ambient temperature in (^oC)

T_{in} is the temperature inside the test enclosure in (^oC)

K is the thermal conductivity of the polyisocyanurate insulation board and it is equal to 0.02 W/mK

L is the thickness of the insulation board which is 0.025 m

h_o and h_i are outside and inside convection heat transfer coefficients respectively in (W/m^2K) and they are evaluated using equation (4.7) and (4.8)

$$h_o = 5.7 + 8.8V_{wind} \text{ [104]} \quad (4.7)$$

$hi = 7\ W/m^2K$ [105] (4.8)

$generated\ power$ represents the power generated by the STPV in (W).

Solving equations (4.2) to (4.8) leaves only one unknown in equation (4.1) which is Q_g that represents the heat conducted through the glazing.

Hence, it is possible to find the U-value of the glazing as shown in equation (4.9)

$$U = \frac{Q_g}{A(T_{in} - T_{ambient})} \quad (4.9)$$

The transmittance and reflectance of each glazing were measured using a Perkin Elmer Lambda 1050 spectrometer and are shown in Figure 4.2 and Figure 4.3.

Radiation has only three behaviours when passing through a glazing, namely reflection, transmission and absorption. Hence, the summation of percentages of the three behaviours gives a value of 100% signifying full incident radiation, thus the absorbance of the above PVs can be calculated and its variation with wavelength can be drawn out as shown in Figure 4.4. Table 4.1 summarizes the optical and power generation properties of the tested glazing.

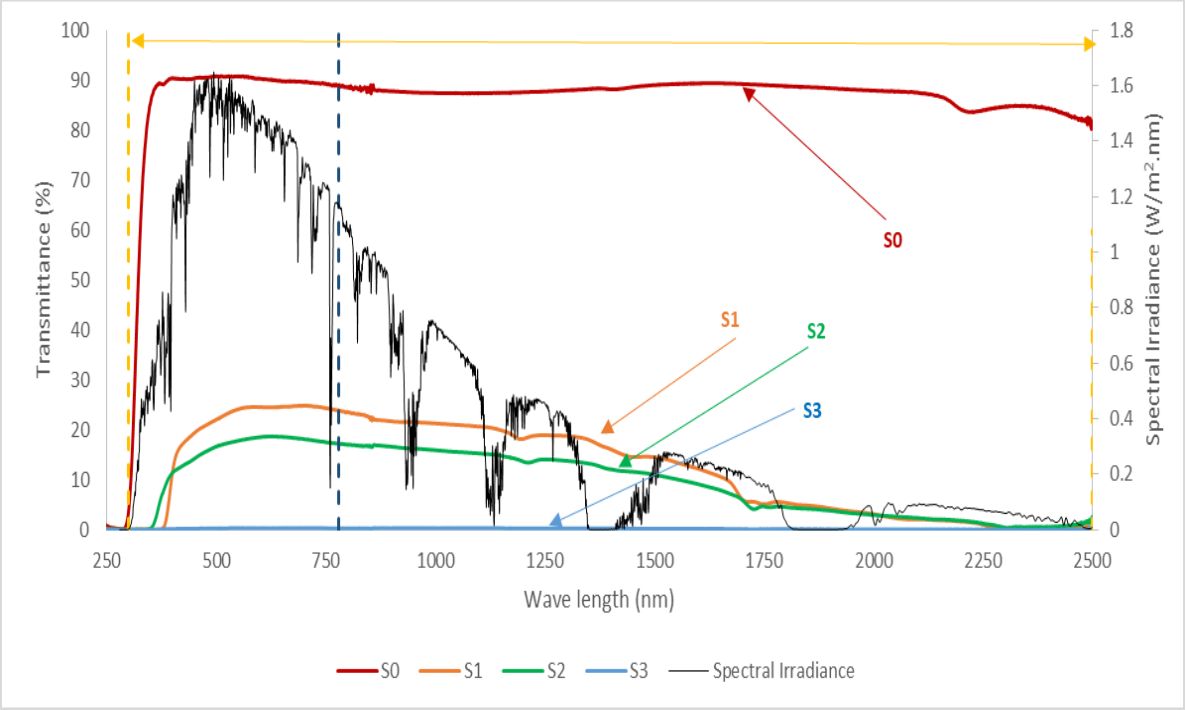

Figure 4.2 Variation of S0, S1, S2 and S3 transmittance and spectral irradiance with wavelength

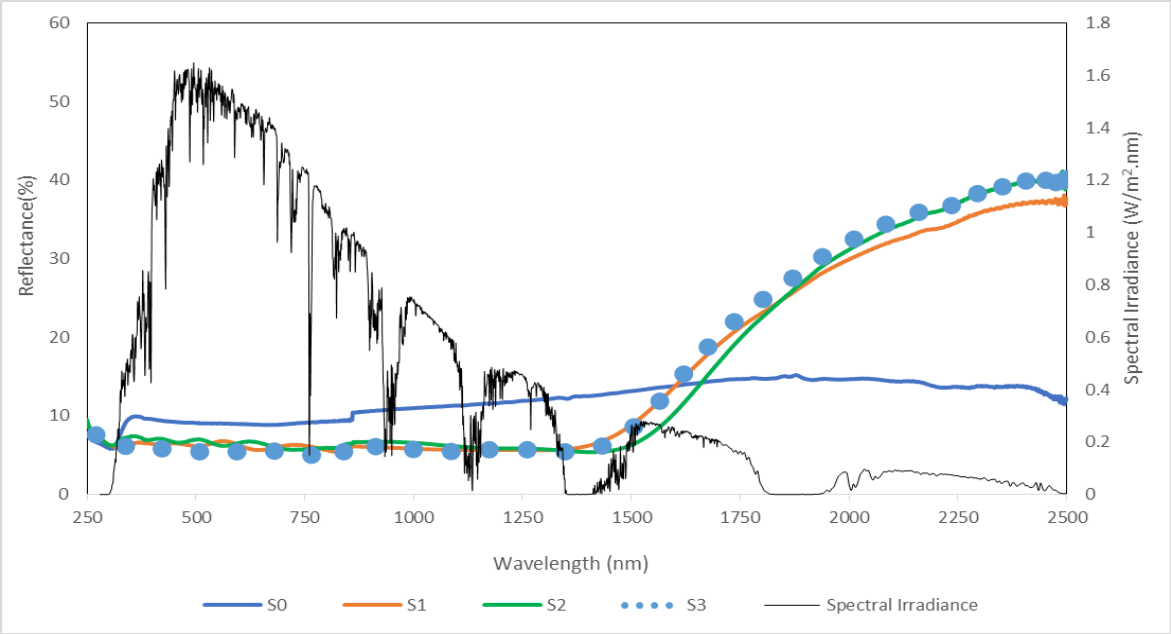

Figure 4.3 Variation of S0, S1, S2 and S3 reflectance and spectral irradiance with wavelength

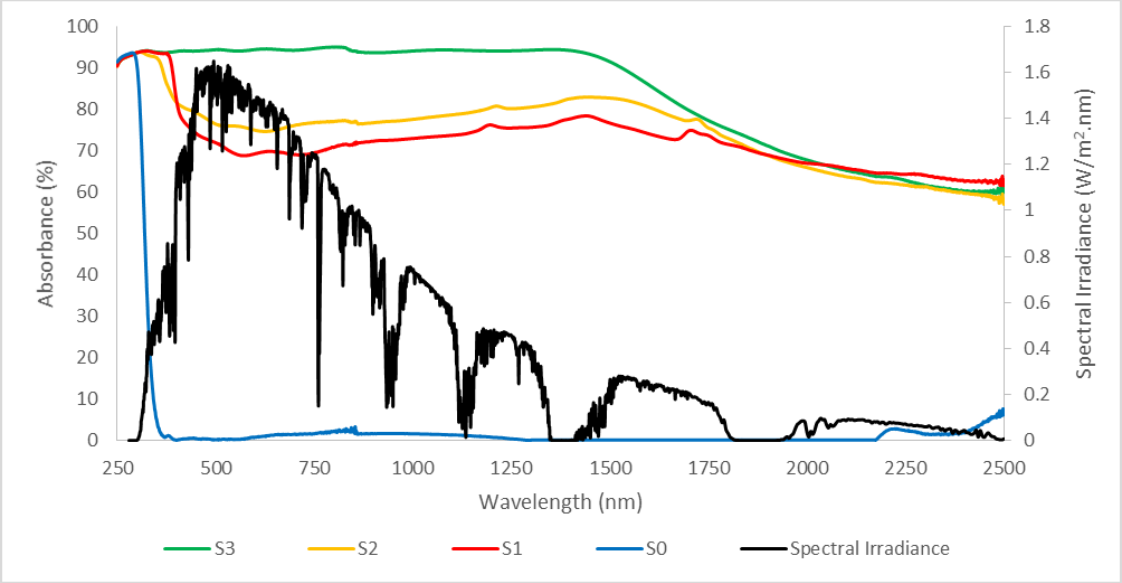

Figure 4.4Variation of S0, S1, S2 and S3 absorbance and spectral irradiance with wavelength

Table 4.1 Optical and power generation properties of glazing S0, S1, S2 and S3

	S0	**S1**	**S2**	**S3**
Maximum Transmittance	90%	24.83%	18.66%	ffa%
Average Transmittance	85%	12%	9.3%	0.157%
Maximum Reflectance	15.2%	41.12%	40%	40.37%
Average Reflectance	11.97%	15.6%	15.9%	16.12%
Maximum Absorbance	93.6%	94.11%	93.78%	95.02%
Average Absorbance	3.9%	72.3%	74.7%	83.6 %
Maximum Power Generation	-	0.45 W	0.5 W	0.68 W

It is to be noted that the solution of equations (4.1-4.9) were based on the measurement of solar irradiation and temperatures throughout the day. This leads to finding a U-value for glazing at each time step of the day.

4.2.1.2 Experimental Results

Readings were taken in different weather conditions during cloudy, intermittently cloudy and sunny days from August 2017 until August 2018. Chapter 3 – section 3.4 justifies the selection of the season of autumn for performing calculations. Figure 4.5 shows the weather conditions in terms of ambient temperature and clearness index for three different days of September; sunny day (September 25th), intermittently cloudy day (September 22nd) and cloudy day (September 20th). Clearness index is a parameter used to quantify the ratio of horizontal global irradiance to the irradiance available at the atmosphere.

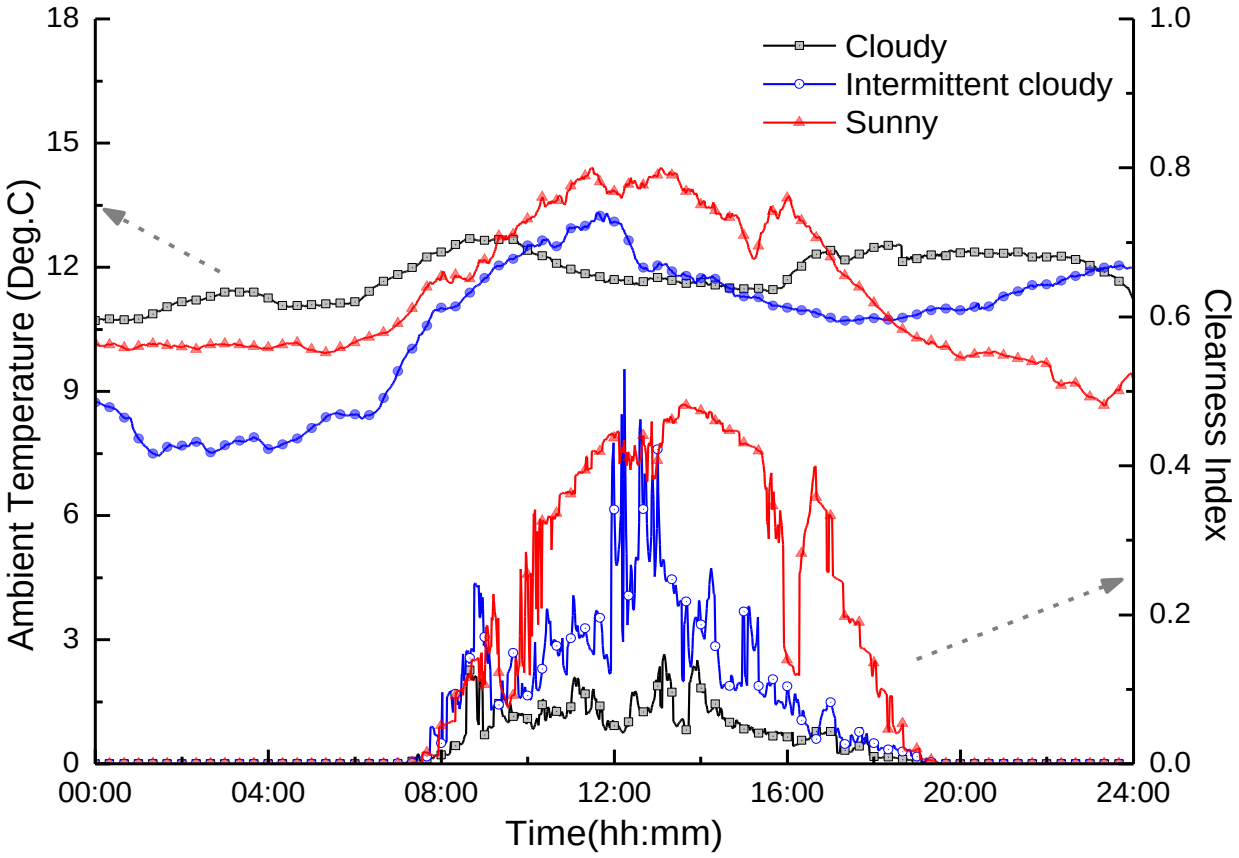

Figure 4.5 Diurnal Variation of Ambient Temperature and Clearness Index of three different days

The measurement of day conditions presented in Figure 4.5 shows that on the cloudy day the ambient temperature ranged between 11 ^{o}C and 13 ^{o}C and clearness index reached a maximum of 0.12. On the intermittently cloudy day the ambient temperature showed a fluctuation between 7.5 ^{o}C to 13^{o}C and clearness index had a maximum value of 0.52 only at 12:00 p.m. Moreover, the sunny day showed the highest values for ambient temperature and clearness index throughout the day reaching 14^{o}C and 0.48 respectively. Therefore, in order to get the best characterization of thermal performance, calculations and analysis were performed based on the sunny day's conditions, (25th September), as this was the day in which most heat transfer occurred.

Temperature clearly reflects the behaviour of a system with respect to heat transfer. In order to assess the thermal performance of STPVs S1, S2 and S3 and compare them to that of clear glazing, the temperatures inside the test enclosures and at the inner surfaces of the glazing were recorded in both orientations.

The inside temperatures of all test enclosures were monitored and presented in Figure 4.6. Results show that all glazing had almost equal temperatures at night, this continued until about 8:00 a.m. where all tested glazing responded to temperature change due to sun rise. The temperatures reached their peak values during the period between 12:00 p.m. and 05:00 p.m. for South West orientation and between 11:00 p.m. and 04:00 p.m. for South orientation. South West orientation has a time interval of peak temperatures shifted one hour later than the South orientation because as time comes close to sun set, the west orientation becomes directly exposed to solar radiations. The clear single glazing (S0) test enclosure was shown to have the highest temperature among all reaching 43^{o}C in South West orientation and 40^{o}C in South orientation, the thing that indicates the occurrence of higher heat transfer than semi-transparent photovoltaic (S1, S2 and S3) test enclosures. Whereas S1, S2 and S3 have shown maximum inside test enclosure temperatures of 34.3^{o}C, 32.7^{o}C and 31.1^{o}C respectively for South West orientation and 33.7^{o}C, 31.8^{o}C and 31.3^{o}C respectively for South orientation respectively. At 08:00 p.m. as the sun sets, the temperature goes back to its initial settings with almost equal values of 11^{o}C for both South and South West orientations. Both test enclosure orientations resulted in the same diurnal variation of inside temperatures for all tested glazing with South orientation having slightly higher temperature because South orientation is exposed to sun for a more extended period of time.

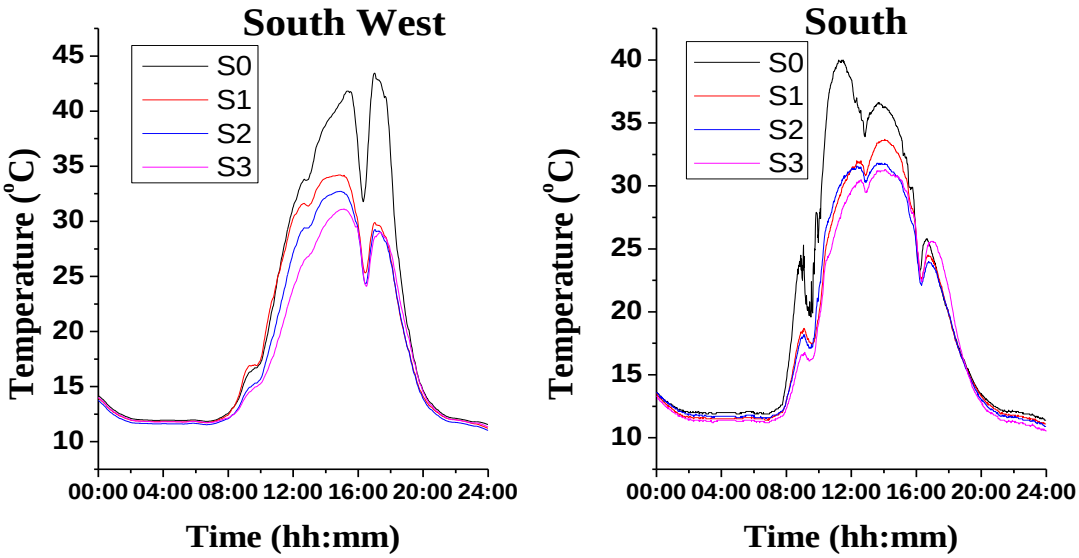

Figure 4.6 Diurnal variation of all test enclosures inside temperatures with different glazing installed to each

Figure 4.7 shows the diurnal variation of inner surface temperature of tested glazing S0, S1, S2 and S3. The temperatures showed similar behaviour as the test enclosure inside temperatures in terms of diurnal variation profile and peak time hours. Although the temperature inside the STPV test cell was higher than that of the single glazing, the inner surface temperature of STPV was shown to be lower. The lowest recorded temperature was for single glazing that reached a maximum of 33.2°C in South West orientation and 30.2°C in South orientation. As for S3, S2 and S1 they showed maximum temperatures of 46.4 °C, 44.3 °C and 42.4°C in the South West oriented test enclosures and 44.3 °C, 43.5 °C and 38.7 °C in the South oriented test enclosure respectively. The STPVs have higher inner surface temperature than single glazing, this is because PVs absorb heat in order to generate electric power. The absorbed heat at the surface of the PV results in an increase in temperature.

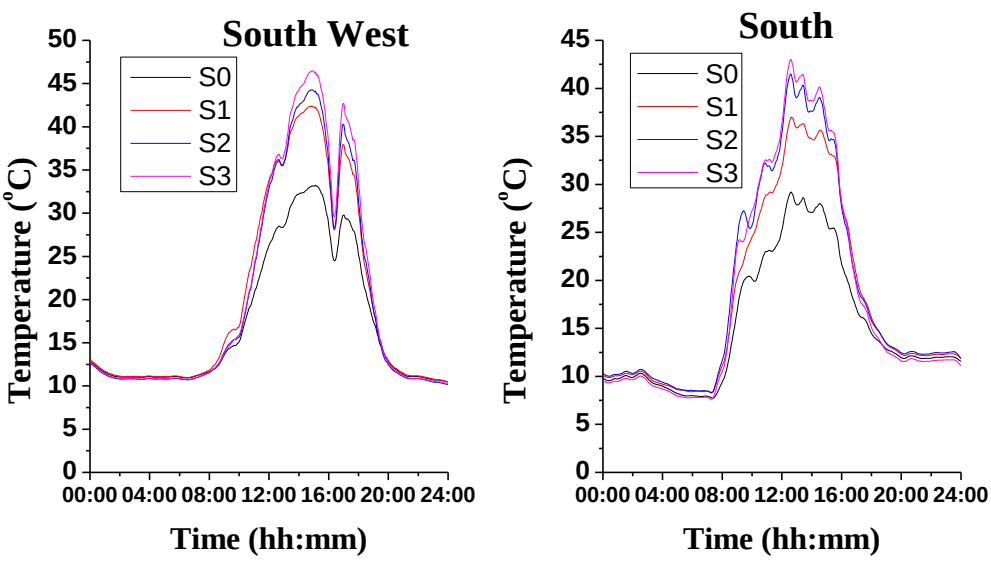

Figure 4.7 Diurnal variation of all inner test enclosures temperatures with different glazing installed to each

Temperature of CdTe-BIPV internal surface was relatively higher than test cell temperature while reverse behavior was achieved for single glazing. This can be explained by thermal diffusivity and effusivity of glass and CdTe material. Thermal effusivity is related to the ability of the material to absorb heat, while diffusivity is the speed to reach thermal equilibrium. CdTe BIPV had two glass panes and CdTe material was sandwiched between them. Thus, enhanced heat flow and then reserved it in glass increased the internal glass temperature for CdTe BIPV while for single glass heat was transferred into the internal text cell.

The analysis of thermal behaviour demonstrates that STPVs S1, S2 and S3 have better insulation properties than the single clear glazing S0, U-value quantifies this insulating property. Figure 4.8 to Figure 4.15 show the diurnal variation of U-value of all tested glazing along with temperature difference and vertical global solar irradiance in both orientations South and South West.

In Figure 4.8, the diurnal variation of temperature difference between ambient and inside the test cell holding S0 glazing at South direction, showed a pattern similar to the vertical global solar irradiance. This is because of the response of inside temperature to the increase of solar irradiance during the day. As solar irradiance increases, the heat is transferred from outside to inside the test cell leading to an increase in its temperature. The U-value was found to be fluctuating with time with an average of 5.6 W/m^{2}K.

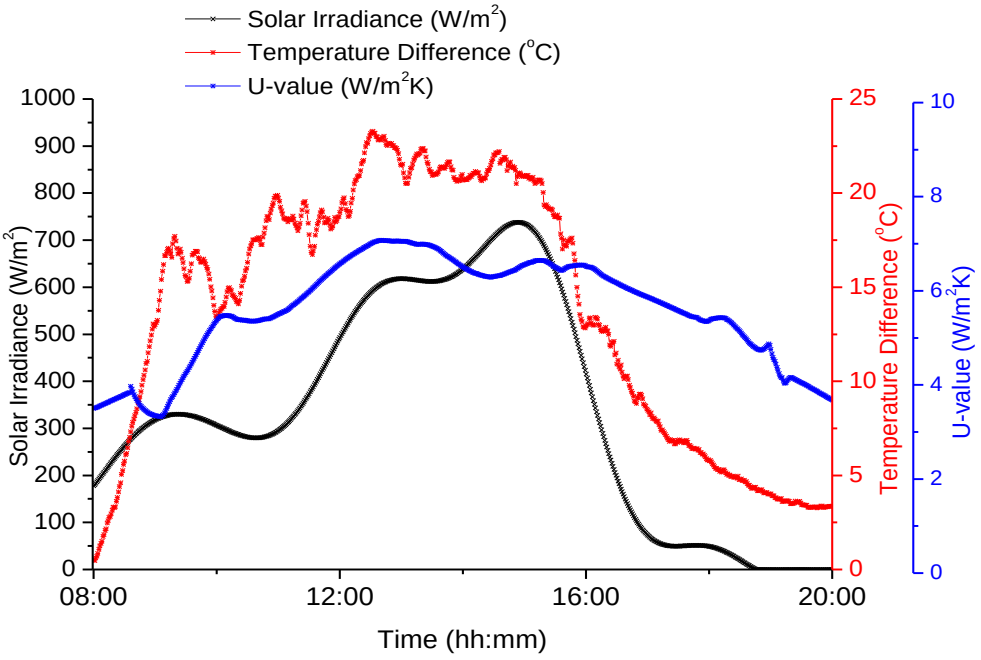

Figure 4.8 Diurnal Variation Solar irradiation, Temperature Difference, and U-value in S0 glazing Test Enclosure in South Orientation

Results of S0 glazing in South West orientation are presented in Figure 4.9. The figure shows that the behaviour of temperature difference also matches that of the global vertical irradiance while the U-value is fluctuating. The average U-value is 5.67 W/m^{2}K. The small difference between the U-values of S0 in south and south west orientation is because of the experimental measurements.

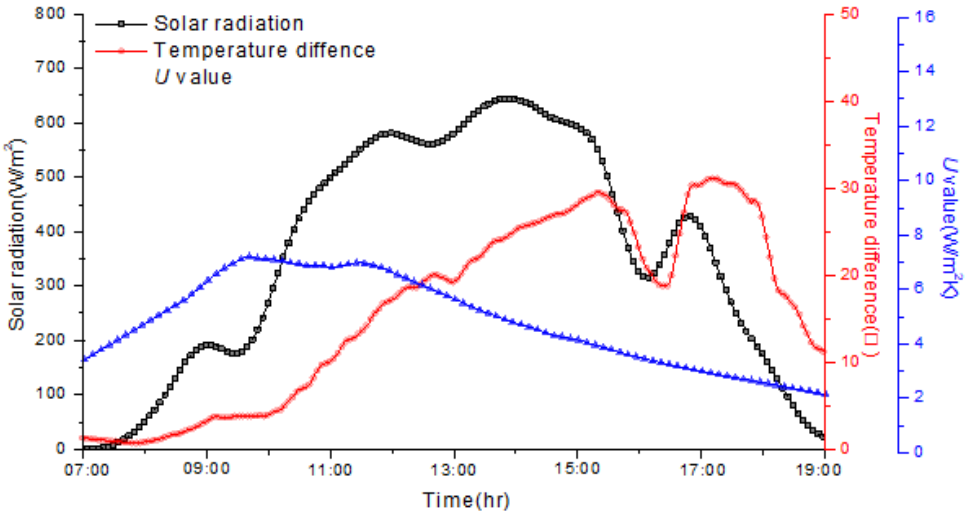

Figure 4.9 Diurnal Variation Solar irradiation, Temperature Difference, and U-value in S0 glazing Test Enclosure in South West Orientation

In

Figure *4.10*, the behaviour of South oriented S1 STPV glazing was presented. Results have shown a fluctuating U-value and a similar behaviour for temperature difference and vertical global irradiance. The average U-value was 2.64 W/m^{2}K.

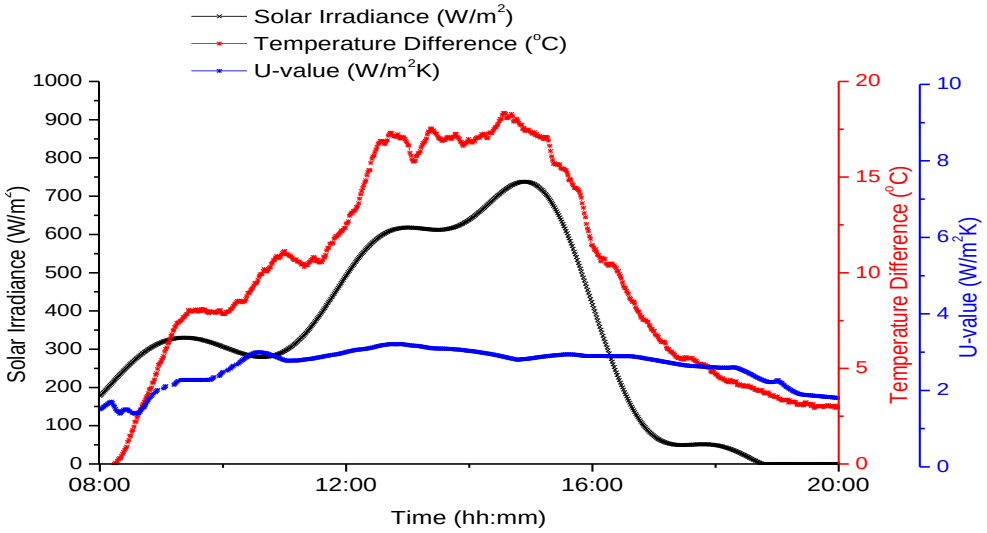

Figure 4.10 Diurnal Variation Solar irradiation, Temperature Difference, and U-value in S1 glazing Test Enclosure in South Orientation

In Figure 4.11, results of irradiance, temperature difference and U-value of S1 glazing oriented to South West are presented. The U-value is again fluctuating throughout the day and temperature difference is showing response to the changes of solar irradiance. The average U-value of S1 STPV glazing was found to be 2.7 W/m^{2}K.

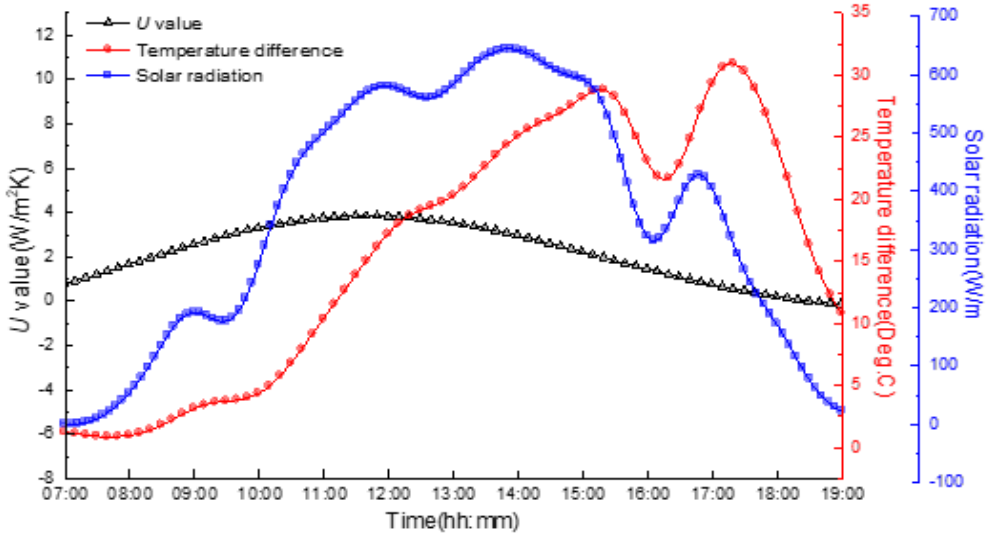

Figure 4.11 Diurnal Variation Solar irradiation, Temperature Difference, and U-value in S1 glazing Test Enclosure in South West Orientation

Results of S2 glazing test cell are presented in Figure 4.12 that shows similar pattern as previous cells in terms of fluctuation of U-value and the increase of temperature difference with the increase of solar irradiance. The average U-value of S2 glazing in South orientation is 2.35 W/m^{2}K.

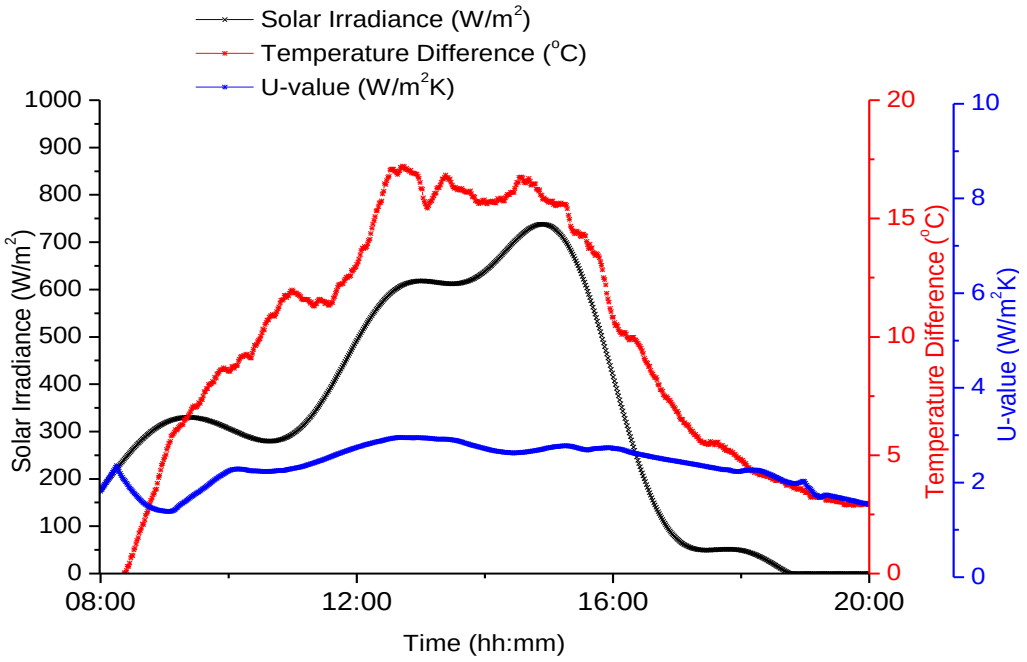

Figure 4.12 Diurnal Variation Solar irradiation, Temperature Difference, and U-value in S2 glazing Test Enclosure in South Orientation

As for South West orientation of S2 glazing, results of Figure 4.13 show similar behaviour as described in figure 12 for temperature difference and U-value. The average U-value of S2 glazing is 2.3 W/m^{2}K that is approximately equal to the value registered for S2 glazing in south orientation.

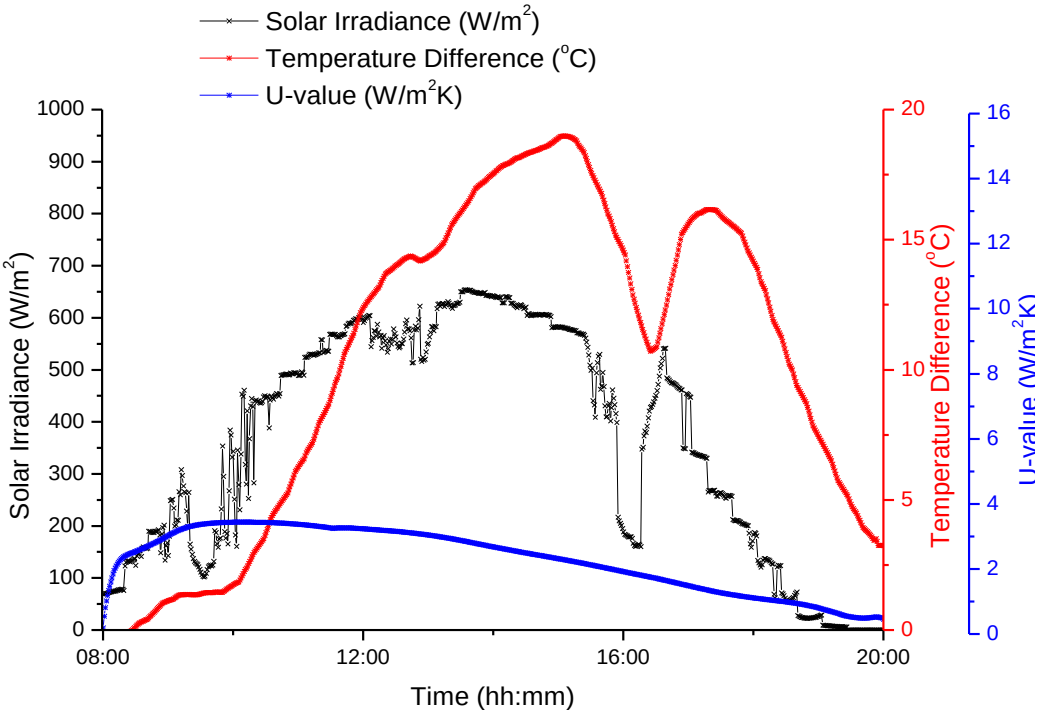

Figure 4.13 Diurnal Variation Solar irradiation, Temperature Difference, and U-value in S2 glazing Test Enclosure in South West Orientation

Results for S3 glazing are presented in Figure 4.14 show a low U-value with an average of 0.248 W/m^{2}K. However, this low U-value does not prevent the temperature difference to respond to the changes of solar irradiance. This is because the heat transferred into the test cell is stored leading to an accumulated increase in temperature.

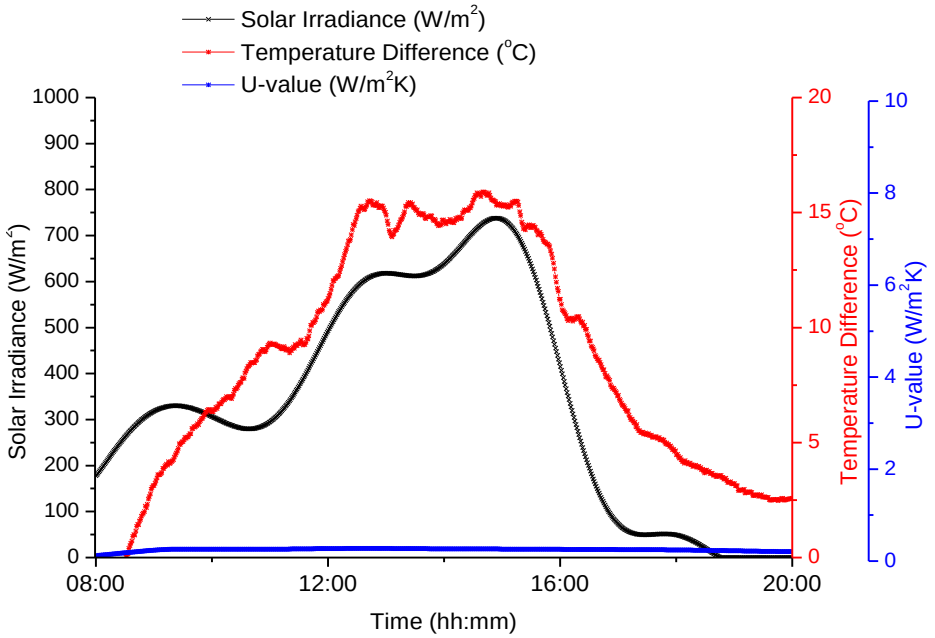

Figure 4.14 Diurnal Variation Solar irradiation, Temperature Difference, and U-value in S3 glazing Test Enclosure in South Orientation

The same pattern described in Figure 4.14 was present in Figure 4.15 for S3 glazing oriented towards South West orientation. The U-value was found to be low with an average of 0.24 W/m^{2}K, and the temperature difference between inside test cell and ambient was found to have similar pattern.

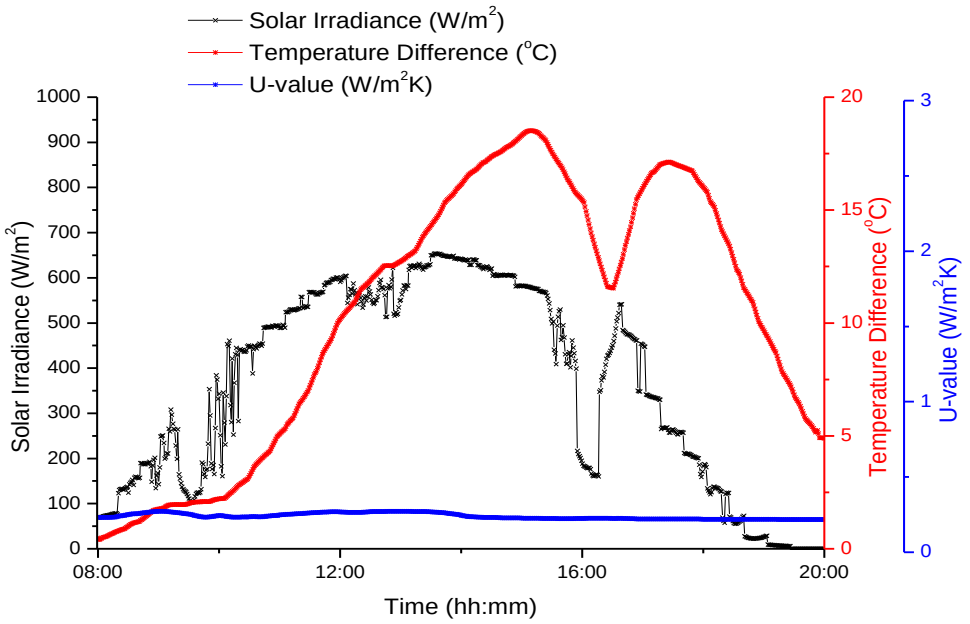

Figure 4.15 Diurnal Variation Solar irradiation, Temperature Difference, and U-value in S3 glazing Test Enclosure in South West Orientation

4.2.1.3 Results Discussion

In this experiment the U-value did not show a constant value throughout the day, as the steady state heat transfer can hardly be achieved in outdoor conditions. This is because the U-value is not a constant parameter and it varies with environment parameters such as temperature and wind speed [101]. However, taking the average value is efficient for describing the overall heat transfer coefficient U-value of the tested glazing according to BS ISO 9869-1:2014 [103], because a steady state heat transfer assumption is valid when performing an outdoor experiment for a long period of time. This was proven true in the case presented in this thesis as results of similar glazing have shown similar average U-values in South and South West orientations.

It was clear that glazing with higher transparency have higher U-values. This agrees with Figure 4.2 shows that low transparency-glazing limits the irradiance for the whole range of wavelengths not only for visible range of solar irradiance. Clear single glazing was shown to have the highest U-value above other glazing having an average of 5.6 W/m^2K in South orientation and 5.67 W/m^2K in South West orientation respectively. Semi-transparent photovoltaic S1 has the second highest U-value as it has an average of 2.64 W/m^2K in South direction and 2.7 in South West direction. Whereas results of STPV S2 showed an average U-value of 2.35 W/m^2K and 2.3 W/m^2K in South and South West orientations respectively. The lowest registered U-value was for STPV 3 whose average U-value was 0.248 W/m^2K and 0.24 W/m^2K when the glazing was oriented towards South and South West respectively. The low U-values of STPV glazing give them the advantage of achieving thermal comfort with low cooling power in hot weather conditions. Table 4.2 summarizes the resulting U-values of the tested glazing in experiment 1.

Table 4.2 Summary of U-values calculated using outdoor experiment (Experiment 1)

Glazing	U-value in South Direction (W/m^2K)	U-value in South West Direction (W/m^2K)	Average U-value (W/m^2K)
S0	5.6	5.67	5.64
S1	2.64	2.7	2.67
S2	2.35	2.3	2.33
S3	0.248	0.240.	0.244

4.2.2 Experiment 2: Indoor test enclosures

A similar experiment to the one presented in "Experiment 1" was carried out in an indoor environment. The purpose of using the indoor experiment is to have a steady heat transfer by using an AAA+ type constant irradiance solar simulator in addition to a constant speed fan. This leads to a constant U-value over time. The tested glazing S0, S1, S2 and S3 were exposed to a constant solar irradiance of 300 W/m^2 which is equivalent to the averages of vertical global solar irradiance in South and South West orientations. Also, the constant speed fan was set to generate an air flow with a speed of 1.5 m/s. Readings were taken for 8 hours so that steady heat transfer can be achieved. It is to be noted that the experiment does not require the glazing to be tested simultaneously because of the fact that the solar irradiance and ambient conditions of temperature and wind speed can be kept constant. Further details of the experimental setup are presented in Chapter 3 - section 3.2. The equations used for calculating the U-value are the same equations used in "Experiment 1".

Temperatures inside the test enclosures and at ambient conditions around the test enclosures were monitored each minute throughout the experiments and presented in Figure 4.16. Results show that test enclosures' temperature changes sharply at the beginning of the experiment then becomes nearly flat for the rest of the experiments' duration. This indicates the occurrence of steady heat transfer. The test enclosure that was equipped with clear single glazing S0 had the highest inside temperature reaching 33 ^{o}C. Following this result were the S1, S2 and S3 test enclosures with maximum temperatures of 31.5 ^{o}C, 29 ^{o}C and 27 ^{o}C respectively. As for ambient temperature around the test cell, this showed an increasing pattern with the continuous constant solar irradiance. It is to be noted that the temperature difference between inside the test enclosure and the ambient

is almost constant. The behaviour of inside temperature in the indoor experiment matches that of the outdoor experiment as the glazing with higher transparency has a higher inside test enclosure temperature.

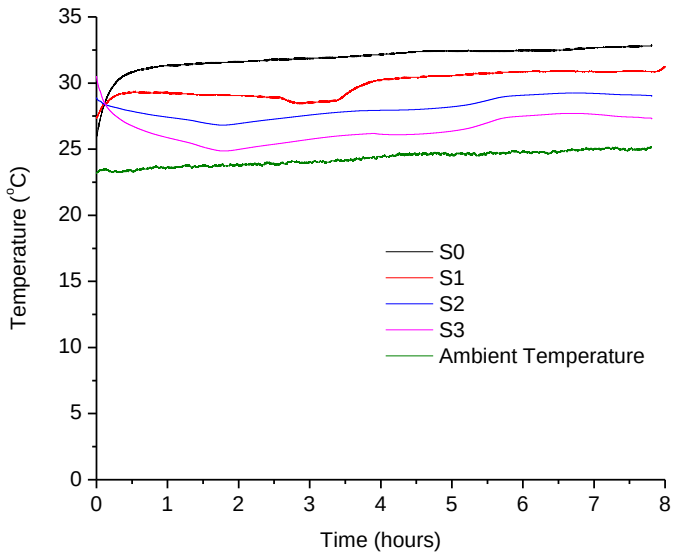

Figure 4.16 Variation of temperatures inside the test enclosures in indoor experiment

Figure 4.17 shows the variation of inner surface temperature of glazing S0, S1, S2 and S3 with the duration of the indoor experiment time. Results show that a time of about 40 minutes was needed for the increase of temperature with the continuous radiation to become flat. This time interval is when transient heat transfer occurs before reaching steady state heat transfer. Glazing S0 showed the lowest surface temperature among other tested glazing with a maximum temperature reaching 37 ^{o}C. Then the glazing can be ordered from lower surface temperature to higher surface temperature as S1, S2 and S3 with maximum temperatures of 38.5 ^{o}C, 40 ^{o}C and 42 ^{o}C respectively. The inner surface temperature of STPV glazing is higher than that of clear glazing

and this can again be illustrated by the fact that STPV glazing absorbs heat to generate electric power.

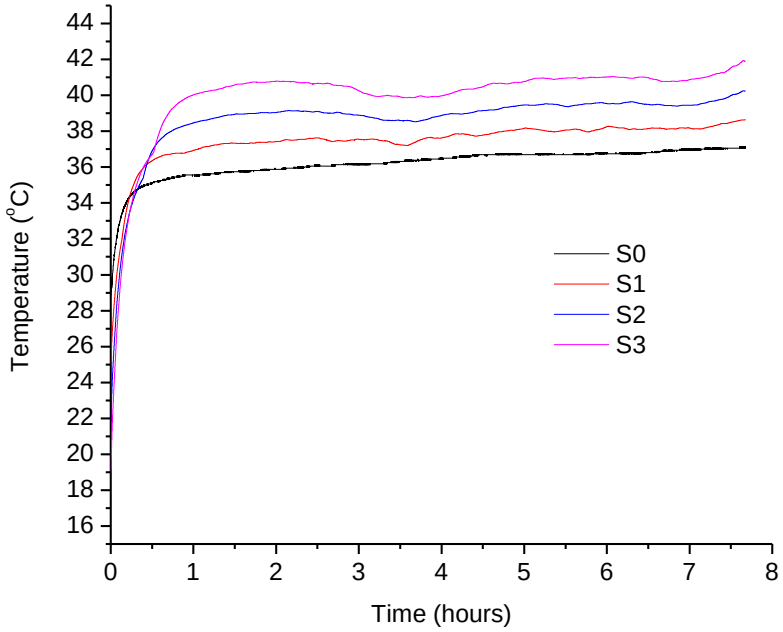

Figure 4.17 Variation of inner surface temperature of tested glazing in indoor experiment

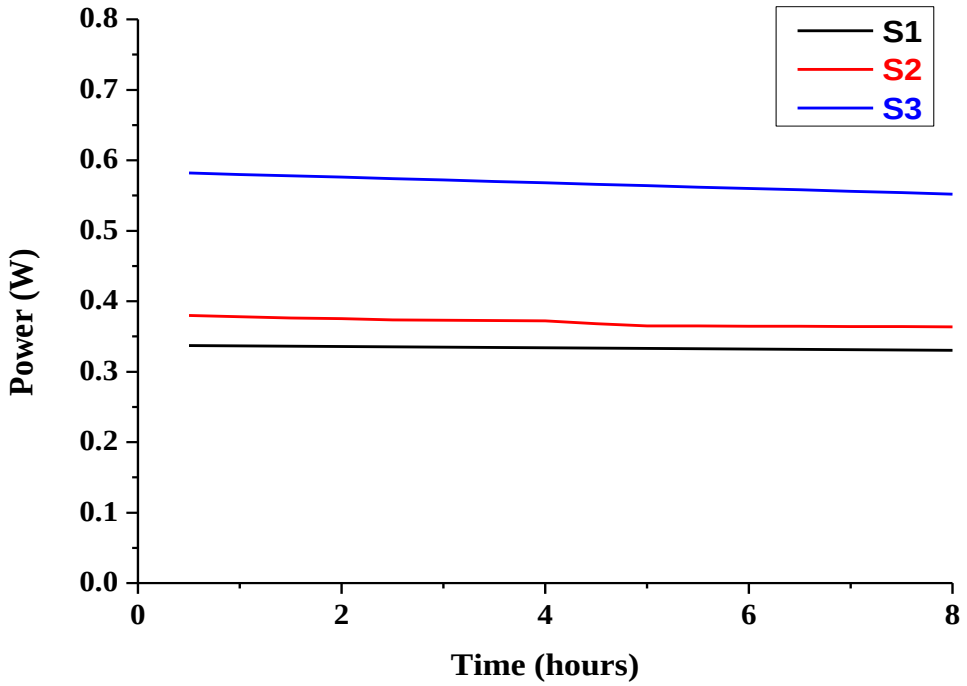

Figure 4.18 Power generated from STPV glazing in indoor experiment

The generated power was monitored to be used in equation 4.1 and in order to calculate the U-value of STPV glazing S1, S2 and S3. Results were presented in Figure 4.18. The highest power was shown to be generated from STPV S3 with a maximum value of 0.58 W, the second highest generated power was from STPV S2 with a maximum of 0.38 W and the lowest power generation was from STPV S1 with a maximum of 0.33 W. It is to be noted that power generated by STPV glazing decreases over time because their surface temperatures increase due to the continuous applied solar irradiance and this decreases their efficiencies.

The U-values of glazing S0, S1, S2 and S3 were calculated based on the results of the indoor experiment and were shown in figure 4.18. Steady and constant U-values were obtained because steady heat transfer could be achieved in the indoor environment. The highest U-value (5.7

W/m^{2}K) is achieved by S0. STPV S1 has the second highest U-value reaching 2.7 W/m^{2}K while S2 and S3 have U-values of 2.3 W/m^{2}K and 0.25 W/m^{2}K respectively. Results were found to be similar to those obtained in the outdoor experiment (Experiment 1). This proves that the assumption of steady state heat transfer in outdoor experiment "experiment 1" is true. In addition, it is clear that in indoor experiment that almost a constant U-value could be obtained. This is because constant environmental parameters were set for the experiment such as solar irradiance and fan wind speed.

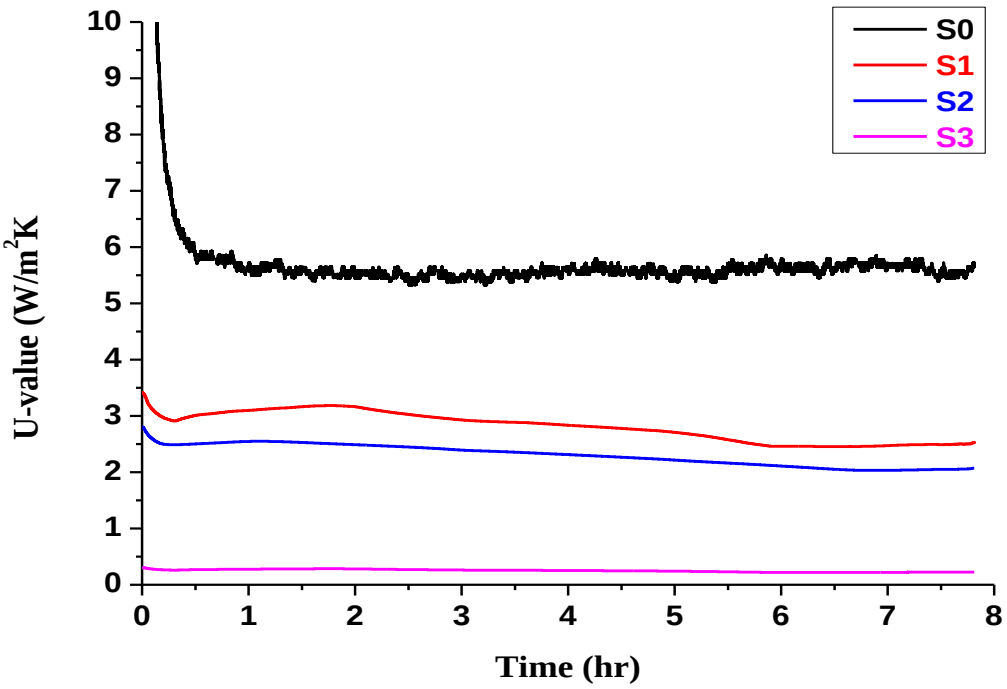

Figure 4.19 Results of U-values of glazing S0, S1, S2 and S3 from indoor experiment

4.2.3 Experiment 3: Using heat flux sensor

Heat flux is defined as the heat transferred per unit area. A heat flux sensor was used to evaluate the U-value of STPV S5 and compare it to single clear glazing S4 which is similar to S0 but with

larger dimensions. The reason S4 and S5 were not tested in the outdoor and indoor experiments (Experiments 1 and 2) is that it is of a larger size (30 cm x 30 cm) and cannot fit to the designed test enclosures. So, they were fitted to two cooler/warmer units test enclosures presented in chapter 3. A 30 cm x 30 cm clear glazing S4 was used for results validation and physical interpretation.

The experiment was set based on the recommendations of BS ISO 9869-1:2014 [103]. A heat flux sensor was attached to the inner wall of the glazing. Two thermocouples were placed at a distance 5 cm away from inner and outer surfaces of the glazing. The temperature inside each test enclosure was controlled to meet a set point of 23 ^{o}C to create a temperature difference between inside and ambient conditions. The test enclosures were set in outdoor conditions and measurements were taken at night to avoid any influence of solar radiation on the heat flux sensor measurements. Measurements were taken from 15th February 2018 to 3rd March 2018. The maximum allowable standard deviation in U-value results must be in the range of 5% for three consecutive days for the measurements to be accepted as recommended by BS ISO 9869-1:2014 [103]. Equation 4.10 was used to calculate the U-value of the glazing.

$$U_g = \frac{Q}{A} \times \frac{1}{T_{in} - T_{ambient}} \tag{4.10}$$

Where $\frac{Q}{A}$ is the heat flux in (W/m^2) measured by the heat flux sensor.

U_g is the U-value of the glazing and T_{in} and $T_{ambient}$ are temperatures inside the test cell and at ambient outdoor condition respectively.

Measurements of inside temperature, ambient temperature and heat flux as well as the calculated U-value for test enclosure holding S4 glazing are presented in Figure 4.20. The figure shows the

results of three consecutive nights from February 20th to February 23rd from 18:00 to 06:00. Results show a steady U-value for the three nights with an average of 5.6 W/m^{2}K and a standard deviation below 5%. The calculated U-value is equal to that calculated for clear glazing S0 in experiments 1 and 2. This validates the results of the measurements.

Figure 4.21 shows the measurement of inside temperature, ambient temperature and heat flux and calculated U-value on three consecutive nights from February 15th to February 18th for the test enclosure holding STPV S5 in the time range between 18:00 to 06:00. Results reveal a steady, almost constant U-value over the three nights with an average value of 3.1 W/m^{2}K and a standard deviation not exceeding 5%.

Results of U-values match the pattern deduced in experiments 1 and 2; that higher transparency glazing has higher U-values. Table 4.3 summarizes the U-values of S4 and S5.

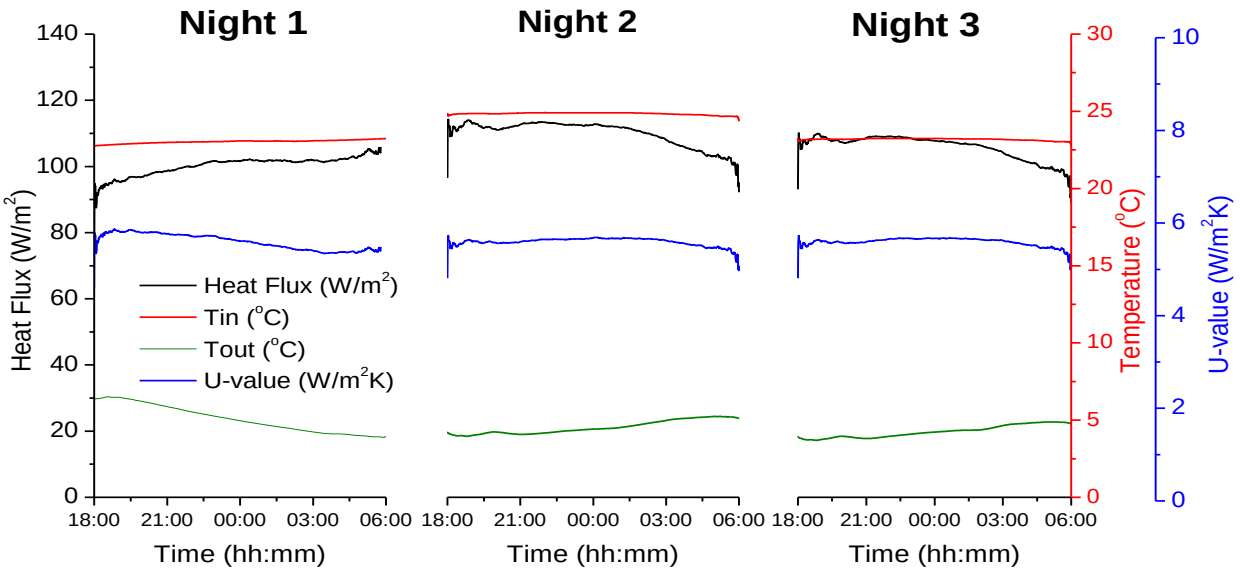

Figure 4.20 Variation of U-value, inside temperature, ambient temperature and heat flux in three nights for S4 test enclosure

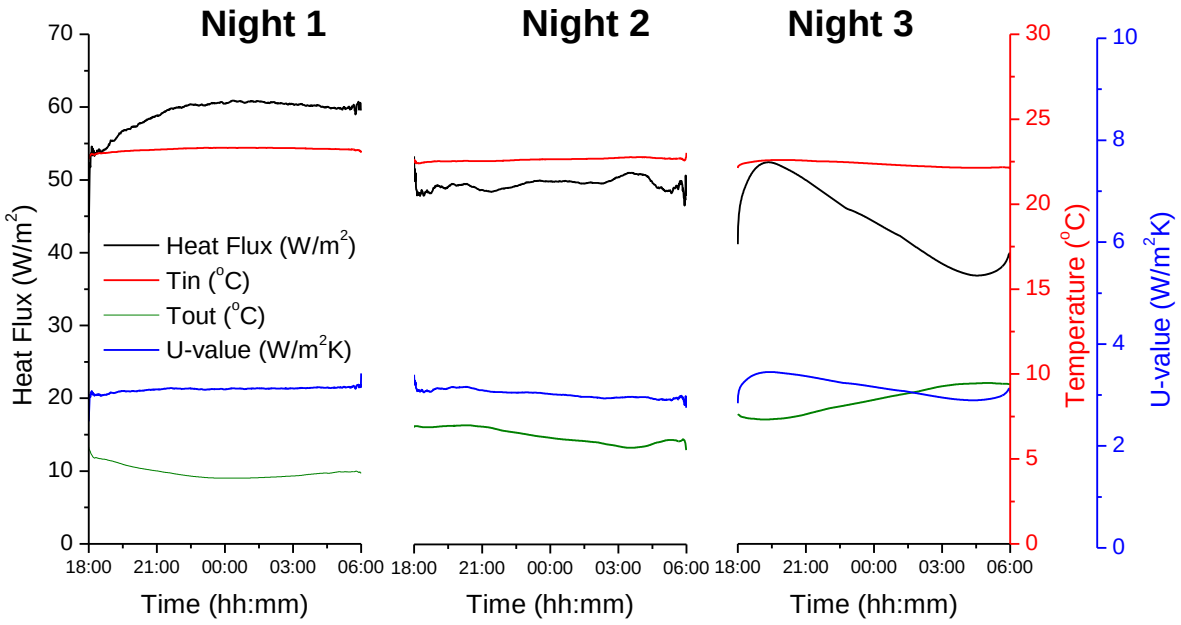

Figure 4.21 Variation of U-value, inside temperature, ambient temperature and heat flux in three nights for S5 test enclosure

Table 4.3 U-values of S4 and S5 glazing

	S4		S5	
	U-value	Standard deviation	U-value	Standard deviation
Night 1	5.6 W/m^{2}K	3%	3.1 W/m^{2}K	1.6%
Night 2	5.6 W/m^{2}K	1.6%	3.04 W/m^{2}K	2.5%
Night 3	5.59 W/m^{2}K	1.7%	3.16 W/m^{2}K	4.8%

4.3 Evaluation of Solar Heat Gain Coefficient (SHGC)

Solar heat gain coefficient (SHGC) measures the fraction of solar radiation that passes through the glazing as a fraction from vertical global solar radiation [90]. Higher SHGC indicates higher transmission of solar radiation through the glazing by being directly transmitted or by being stored and released again.

4.3.1 Equations for calculating SHGC

Considering the beam component of radiation being transmitted at an incident angle (θ), the solar heat gain coefficient (SHGC) can be calculated through the following series of equations [90].

$$SHGC = \frac{TSE}{I_{ver,global}} \tag{4.11}$$

Where, TSE is the transmitted solar energy in (W/m^2) and $I_{ver,global}$ is the vertical global irradiance in (W/m^2)

$$TSE = \left(I_{hor,dir} + I_{hor,diff} \times A_i\right) \times \tau_{dir} R_b + I_{hor,diff}(1 + A_i) \times \tau_{diff} \frac{(1+\cos\beta)}{2} + I_{hor,global} \times \rho_g \times \tau_g \frac{(1-cos\beta)}{2} \tag{4.12}$$

Where $I_{hor,dir}$, $I_{hor,diff}$ and $I_{hor,global}$ are horizontal direct irradiance, horizontal diffuse irradiance and horizontal global irradiance respectively in (W/m^2).

τ_{dir}, τ_{diff} and τ_g are direct, diffuse and global transmittance respectively.

R_b is the factor of beam radiation, ρ_g is the solar reflectance of glazing and β is the the angle between the panel and the horizontal. A_i is the anisotropic index and it can be calculated through equation 4.13 [99]

$$A_i = \frac{I_{hor,dir}}{I_o} \tag{4.13}$$

where I_o is the extraterrestrial solar irradiance in (W/m^2) and it can be calculated through equation (4.14)

$$I_o = I_{sc}(1 + 0.033\cos(\frac{360\,Nd}{365})(cos\varphi \times cos\delta \times cos\omega + sin\varphi \times sin\delta) \tag{4.14}$$

I_{sc} is the solar constant irradiance that is equivalent to 1360 W/m^2, Nd is the day number, φ is the azimuth angle, δ is the declination angle presented in equation (4.15) and ω' is the hour angle included in equation (4.16)

$$\delta = 23.45\sin(\frac{360}{365} \times (284 + Nd)) \tag{4.15}$$

$$\omega' = \frac{AST\ (in\ minutes) - 720}{4} \tag{4.16}$$

AST is the apparent solar time and can be calculated using equation (4.17)

$$AST = LST + 4 \times (LSTM - Longitude) + ET \tag{4.17}$$

Where, LST is the local solar time, $LSTM$ Local longitude of standard time meridian calculated through equation (4.18), and ET is the equation of time calculated through equation (4.19).

$$LSTM = 15 \times (\frac{Longitude}{15})_{round\ to\ an\ integer} \tag{4.18}$$

$$ET = 9.87sin\left(2 \times 360\left(\frac{N_d-81}{365}\right)\right) - 7.53cos\left(360\left(\frac{N_d-81}{365}\right)\right) - 1.5sin(360\left(\frac{N_d-81}{365}\right)) \quad (4.19)$$

Transmittances τ_{dir}, τ_{diff} and τ_g included in equation (4.12) can be calculated through equation (4.20) [106]:

$$\tau = \frac{1}{2}\left(\frac{1-\left(\frac{\sin(\theta-n)}{\sin(\theta+n)}\right)^2}{1+(2n_g-1)\left(\frac{\sin(\theta-n)}{\sin(\theta+n)}\right)} + \frac{1-\left(\frac{\tan(\theta-n)}{\tan(\theta+n)}\right)^2}{1+(2n_g-1)\left(\frac{\tan(\theta-n)}{\tan(\theta+n)}\right)}\right) \times \exp\left(^{-K_g N_g t_g}/_{cos\theta}\right) \quad (4.20)$$

K_g is the extinction coefficient, N_g is the number of the glass pane and t_g is the thickness of glazing in (m)

θ is the incident angle that can be calculated through one of the equations (4.21), (4.22) or (4.23).

The suffixes “dir", "diff" and “g” after the transmittance in equation (4.12) are dependent on the value of incident angle θ as follows:

$$\theta_{diff} = 59.68 - 0.1388\beta + 0.001497\beta^2 \quad (4.21)$$

$$\theta_g = 90 - 0.5788\beta + 0.002693\beta^2 \quad (4.22)$$

$$\cos(\theta_{dir}) = \sin(\delta) \times \sin(\varphi) \times \cos(\beta) - \sin(\delta) \times \cos(\varphi) \times \sin(\beta) \times \cos(\gamma) + \cos(\delta) \times \cos(\varphi) \times \cos(\beta) \times \cos(\omega') + \cos(\delta) \times \sin(\varphi) \times \sin(\beta) \times \cos(\gamma) \times \cos(\omega') + \cos(\delta) \times \sin(\beta) \times \sin(\gamma) \times \sin(\omega') \quad (4.23)$$

4.3.2 Results of SHGC

Figure 4.22 shows the results of the calculated SHGC for glazing S0, S1, S2, S3 and S5. The highest SHGC belongs to clear single glazing S0 with a maximum value of 0.728. This value

agrees with the value published by the Royal Institute of British Architectural (RIBA) [27]. The second highest SHGC was for 35% transparent STPV S5 with a maximum value of 0.28. As for STPVs S1, S2 and S3, their SHGC had maximum values of 0.2, 0.14 and 0.0291 respectively. These values are unique as the SHGC of CdTe thin-film PV glazing was not calculated before, according to the author's knowledge. However, the results signify that glazing with higher transparencies have higher solar heat gain coefficients and this matches the behaviour of results published by Chae et al. [87]. This reveals that different transparencies of STPV glazing have the advantage of solar heat gain control. It was also noted that as incident angle increases the SHGC decreases for all tested glazing.

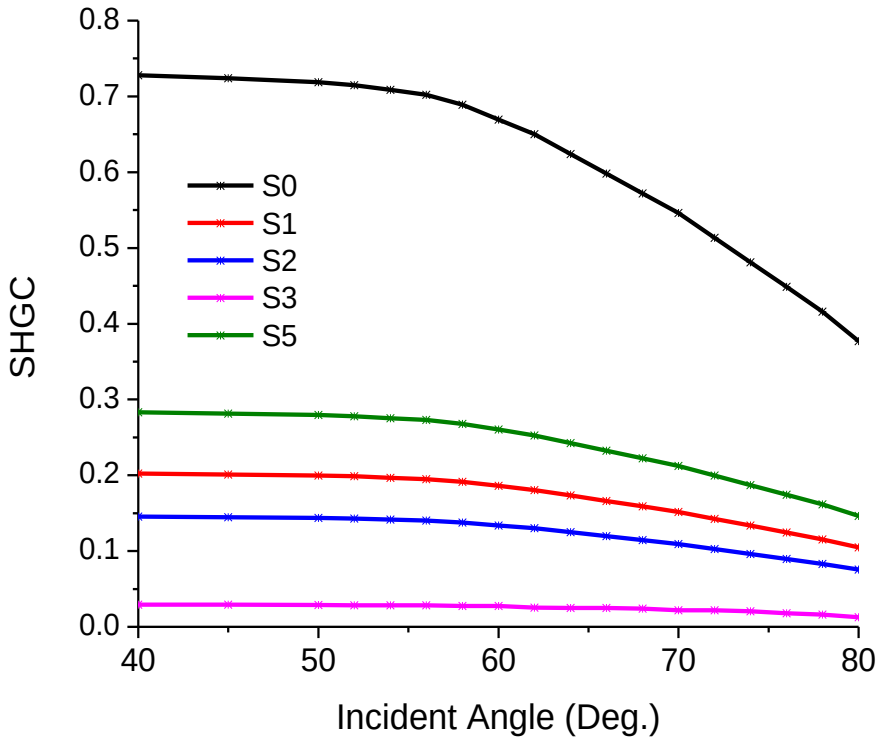

Figure 4.22 Variation of SHGC of glazing S0, S1, S2, S3 and S5 with incident angle

4.4 Conclusion

Thermal performances of semi-transparent photovoltaic S1, S2, S3 and S5 were evaluated and compared to single clear glazing S0 and S4. U-values were calculated in three different experiments for results validation. Among the three experiments used for evaluating U-value, using the heat flux sensor delivered the steadiest results. Indoor experiment is the one that can be performed in a short time with reliable results, whereas the outdoor experiment shows the actual behaviour of glazing in realistic conditions.

The outdoor experiment showed that STPV glazing can limit the heat transfer transmitted through them compared to clear single glazing in both tested orientations, South and South West. Also, STPVs have similar U-values in both orientations. This indicates that they have constant thermal properties. Nevertheless, both outdoor and indoor experiments revealed similar results in terms of temperature behaviour inside the test enclosures and evaluating U-values. This indicates that the results are validated.

It was also shown that glazing with higher transparencies have less ability to limit the temperature rise inside the test enclosures. They also have higher U-values and SHGC compared to other less transparent glazing. Also, all semi-transparent photovoltaic glazing has shown lower U-values and SHGC than single clear glazing. This proves the good insulating properties of CdTe thin-film based STPV compared to conventional single glazing. These insulating properties make them able to reduce cooling loads if used as windows or facades in BIPV applications. Table 4.4 summarizes the U-values obtained from the three experiments used.

Table 4.4 Summary of calculated U-values

	S0 (W/m^2K)	S1 (W/m^2K)	S2 (W/m^2K)	S3 (W/m^2K)	S4 (W/m^2K)	S5 (W/m^2K)
Experiment 1	5.64	2.67	2.33	0.244	-	-
Experiment 2	5.7	2.7	2.3	0.25	-	-
Experiment 3	-	-	-	-	5.6	3.1
Average	5.67	2.69	2.32	0.247	5.6	3.1

Chapter 5 Performance of Cadmium Telluride Semi-Transparent PV Glazing for Power Saving in Façade Buildings

This chapter provides the performance assessment of CdTe Semi-Transparent PV glazing (S1, S2 and S3) for power saving in façade buildings in comparison with conventional clear single glazing (S0). The performance was evaluated in terms of net energy performance that include air conditioning energy consumption, artificial lighting energy consumption and STPV façade energy generation. The assessment was achieved using outdoor experimental setups of test enclosures oriented to face South and South West orientations.

5.1 Introduction

In order to investigate the energy performance of CdTe thin-film based STPV glazing under realistic weather and solar irradiance conditions, outdoor experimental setups were installed holding STPV glazing S1, S2 and S3 and single clear glazing S0.

Energy consumption of Façade buildings, which are generally highly glazed, is even more significant when air conditioning (AC) is considered. Energy is saved by more heat being reflected resulting in less AC power consumption with the STPV thermal properties. In addition, the optical and electrical properties provide indoor sunlight with power generation. This chapter investigates the net potential energy saving via applying cadmium telluride (CdTe) STPV glazing of different transparencies in Façade buildings. The impact of PV glazing facade orientation was studied by implementing outdoor experiments facing South and South West orientations.

5.2 STPV Glazing Electrical Propertie

The electrical properties of the STPVs were investigated using WACOM AAA+ solar simulator. The IV curves for STPVs used are presented in Figure 5.1. The I-V curves reveal that the maximum power point (MPP) of S3 is the highest compared to S2 and S1, which has the lowest

value of MPP. Detailed results of STPVs properties are presented in Table 5.1. The results show that the efficiency and power generation were found to be inversely proportional to transmittance. The maximum efficiency and power generation for both orientations was registered for S3 whereas S1 showed the lowest efficiency and power generation.

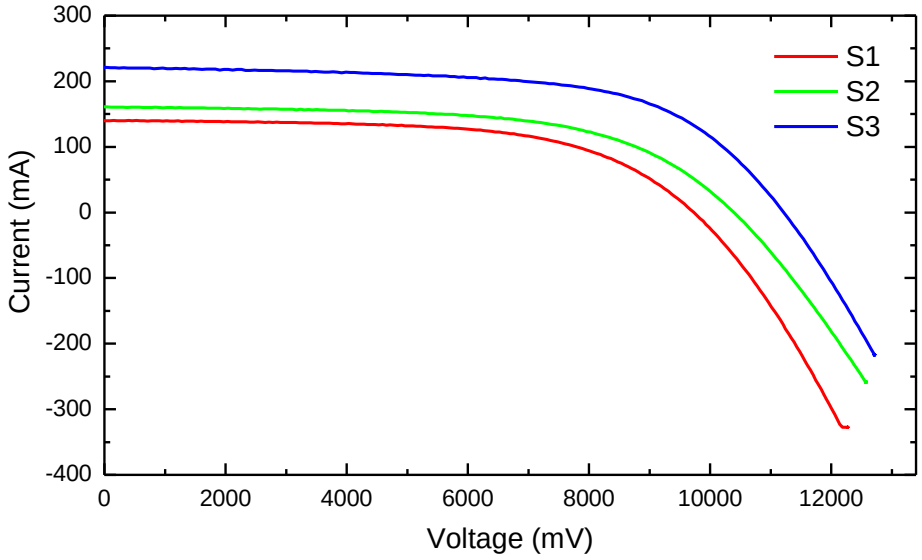

Figure 5.1 The I-V curve of STPVs used in south-west-oriented test cell

Table 5.1 Electrical properties of STPV cells

Parameters	**South West Orientation**			**South Orientation**		
	S3	**S2**	**S1**	**S3**	**S2**	**S1**
Nominal Power [Pm] (W)	1.53	0.99	0.815	1.41	0.987	0.815
Short Circuit Current [Isc] (A)	0.22	0.16	0.14	0.21	0.16	0.14
Open Circuit Voltage [Voc] (V)	11.21	10.39	9.734	11.14	10.08	9.734
Current at Maximum Power Point [Imp] (A)	0.18	0.13	0.115	0.163	0.13	0.115
Voltage at Maximum Power Point [Vmp] (V)	8.49	7.57	7.05	8.65	7.43	7.05
Efficiency [η] (%)	12.6	8.23	6.7	11.69	8.15	6.7

5.3 Energy and Power Measurement

In order to establish a performance assessment for all cells under the same conditions, an experimental setup had been built consisting of eight sample enclosures. A data acquisition and logging system had been used to gather data and save it in an excel sheet. The setup was installed at ESI building, Exeter University, UK as described in section 3.2.

The design had two identical sets of four enclosures set to the south and south-west directions. Because of the constraint of a fixed size of the available STPV (20 X 20 cm^2) the enclosures had been designed with dimensions of 20 X 20 cm^2. It is worth mentioning that the active area of the STPV is within the 10 X 10 cm^2.

The enclosures utilized Peltier-based cooling systems for mimicking the AC units in the buildings. Also, each enclosure was equipped with:

- K-type temperature inside the enclosure for thermal evaluation
- voltage and current sensors for AC power consumption measurements
- a voltage sensor for the STPV power generation measurement

All enclosures are installed in a box provided by ventilation holes and fans. Figure 5.2 shows the completed experimental setup.

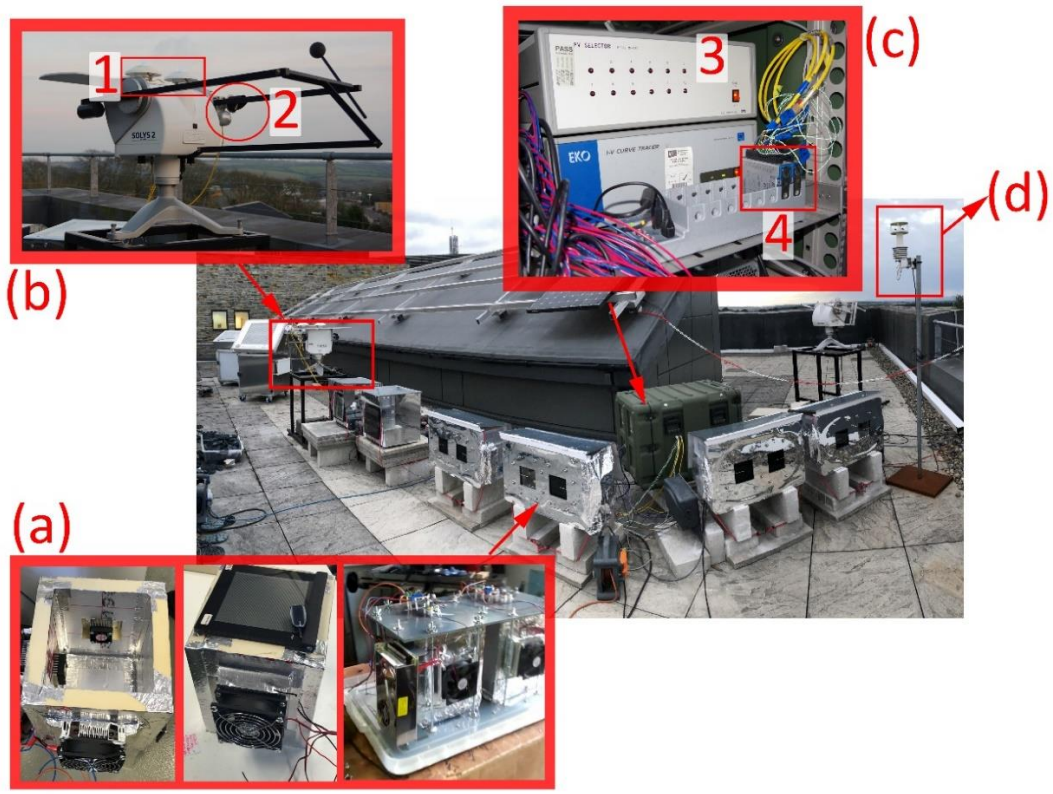

Figure 5.2 The Completed view of the whole setup: (a) test cell (b) solar tracker (1) global and diffuse radiation (2) the direct radiation (c) data logger (3) IV-tracer (4) thermocouple data logger (d) weather station

Outdoor experiments were dedicated to the overall system energy evaluations in real weather. The evaluations included orientation aspects, wind and shading disturbances, and inside-light measurement when the facades were vertically assembled.

5.4 Enclosure temperature and Air conditioning

As per Lomas and Kane [107], the range of comfort temperature in winter and summer seasons is below 24°C. Also according to Seppanen et al. [108], the performances increase with temperatures up to 22°C and decreases with temperatures above 24°C. In this trial, the thermostat was set at 20°C for cooling to calculate the AC loads. According to the UK weather, keeping the inside temperature of the enclosure below 20°C is not hard. However, in hot countries, for example in the Middle East, it needs the AC to work for a longer time with higher capacity to achieve the 20°C regulation.

Figure 5.3, Figure 5.4 and Figure 5.5 depict the temperature profiles for three different days; 6 May 2018, 23 NOV 2017, and 12 DEC 2017 respectively. Different days are tested to provide an evidence of the selected days later and to test the cells under the conditions which are proportionate to achieve the aim of this thesis. These figures show that for hot days in May the AC units needed to work harder and longer than the other days in November and December. On those days in November, Figure 5.4, and December, Figure 5.5, the AC units were hardly required or not at all as the temperature is below the AC unit operating threshold. On the November 23rd sample, the AC in enclosures with S0 and S1 ran for a short period during the day, while enclosures with S2 and S3 kept the temperature below 20°C all time. This contributes to the objective of the paper and the feasibility of using STPV. On the DEC sample, the temperature is below 12°C and no power consumed by the AC units for all glazing. To emphasis the value of saving even more,

sample days that has relatively higher temperature profiles will be selected between May to September over the year.

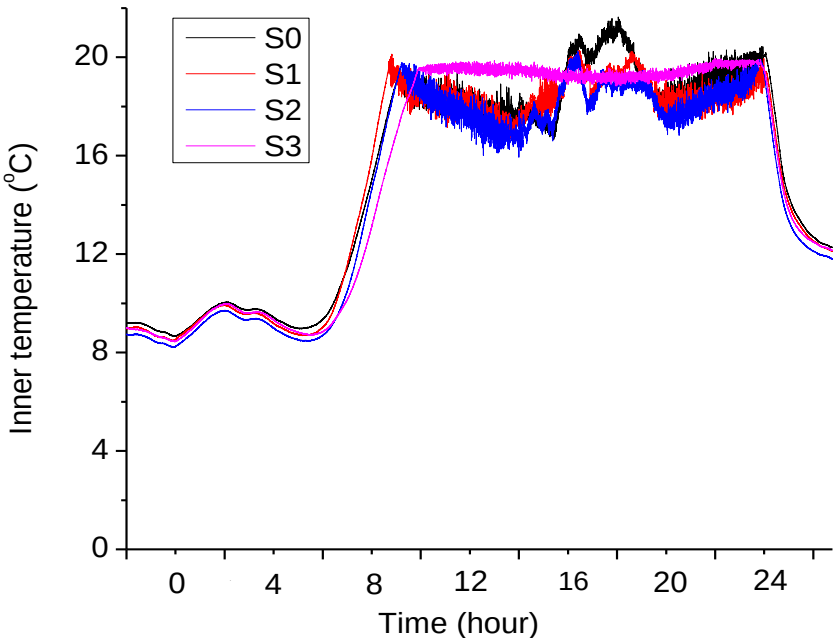

Figure 5.3 The inner-temperature profiles of the south-facing enclosures on 6 May 2018

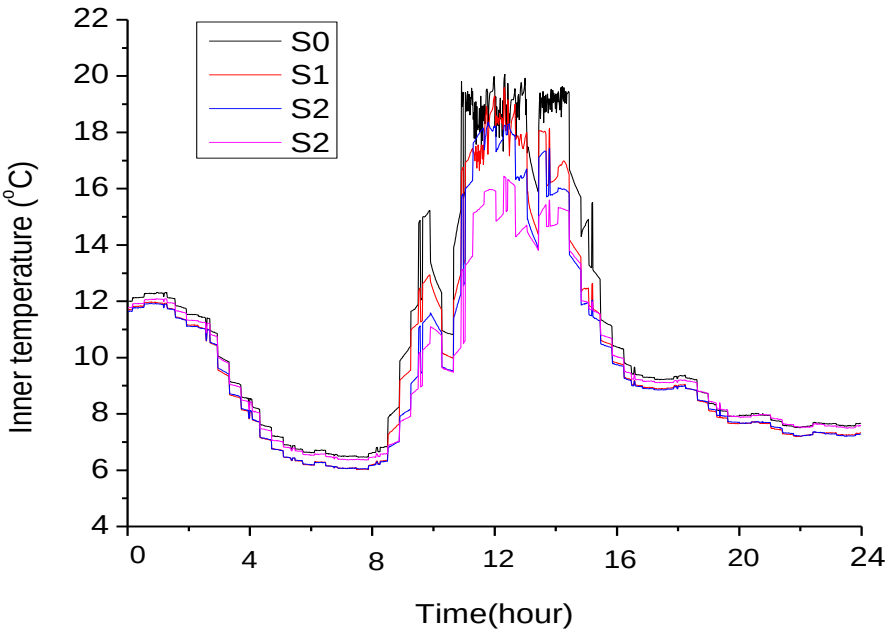

Figure 5.4 The inner-temperature profiles of the south-facing enclosures on 23 November 2017

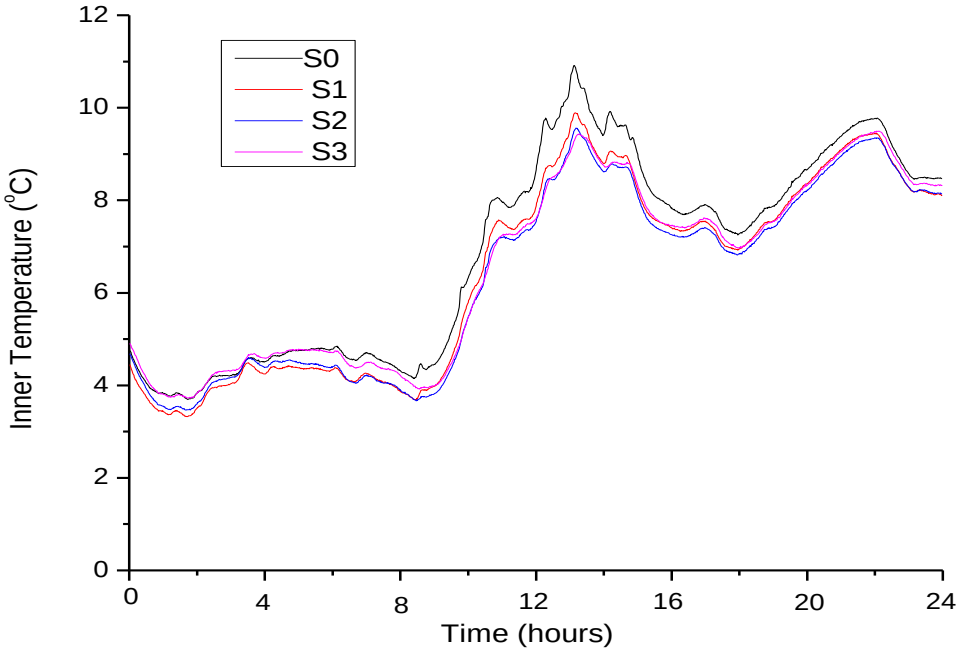

Figure 5.5 The inner-temperature profiles of the south-facing enclosures on 12 December 2017

5.5 Results and discussion

5.5.1 AC power consumption

The power consumption data has been recorded during the May sample day for the four enclosures in both directions: south and south-west. Figure 5.6 shows the accumulated energy consumption over the twenty-four-hour period for both orientations with the various transparencies. The consumption of the S0 enclosure in both orientations is proven to be the most while S3 is the least. Respectively, the energy savings for S1, S2, and S3 compared to the reference enclosure S0 are 4.8%, 8.6%, and 11.6% for the south orientation and 7.9%, 14.4%, and 23.2% for the south-west-oriented enclosures.

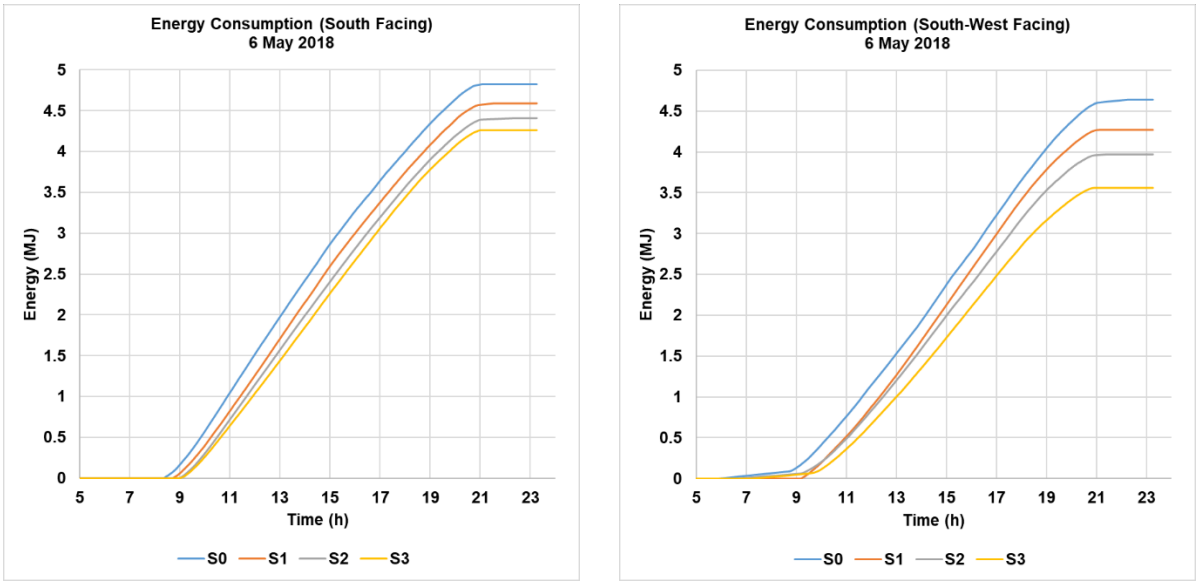

Figure 5.6 The AC energy consumption for different orientations and different transparencies on 6 May 2018

It was noticed that the consumption of the south-west oriented S0 enclosure is slightly less than the south-oriented, which is close to the south-west oriented S1 enclosure. This is because the

south enclosures are facing the sun for more extended periods of time with higher radiation, which transfer more heat inside the enclosures. Therefore, the south enclosures require more cooling energy for all STPVs.

A caveat can be concluded for very hot weathers and south-facing facades, but the savings could be insignificant. This is also shown for the power consumption on 24 November in Figure 5.7, which is a relatively colder day. The energy saving figures for that day are 43.5%, 54.5%, and 61.1% for the south-facing S1, S2, and S3 enclosures respectively.

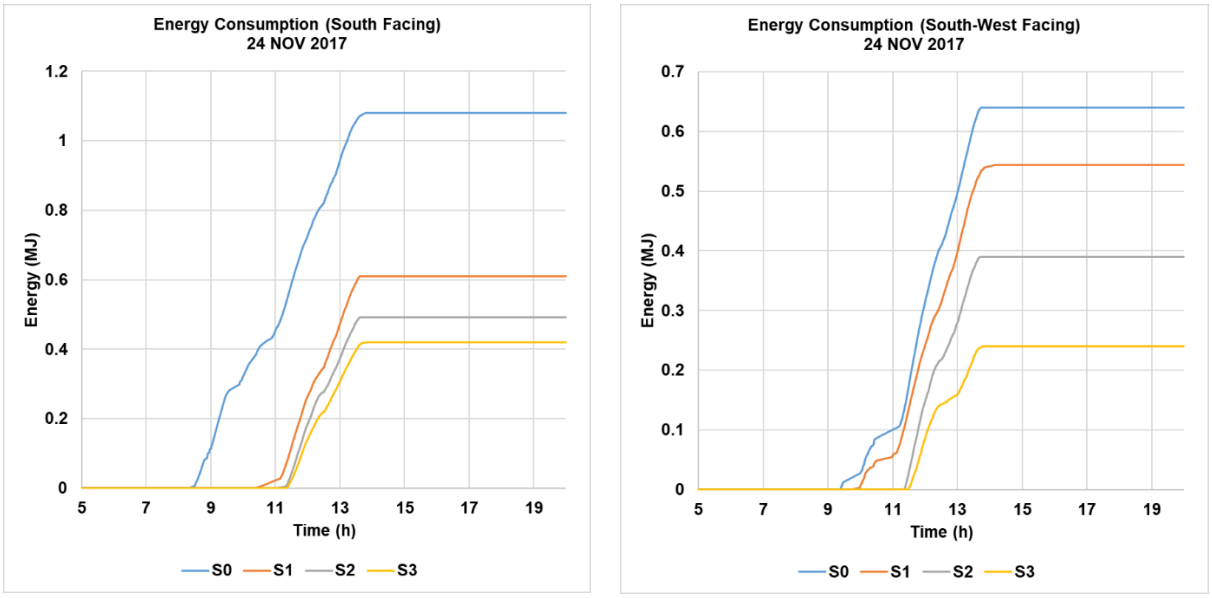

Figure 5.7 The AC energy consumption for different orientations and different transparencies on 24 Nov 2017

Furthermore, the working hours for the AC units in May is about thirteen hours while it is six hours in November. This contributes to more savings in November than May. According to the finding by Barman et al. [14], the determining factors for cooling loads, U-value and SHGC, for

window systems are higher than for the opaque wall. Therefore, as the window to wall ratio (WWR) increases, the thermal load of the building rises.

5.5.2 STPV generation

Instead of the clear glazing, using STPV introduces more reflectance and absorption to the visual light penetrating the windows. Therefore, less sunlight will serve the interior lighting during the working hours and more artificial light consumption will be required. Figure 5.8 illustrates the direct, diffused, and global irradiance on 6 May, which reflects a relatively sunny day.

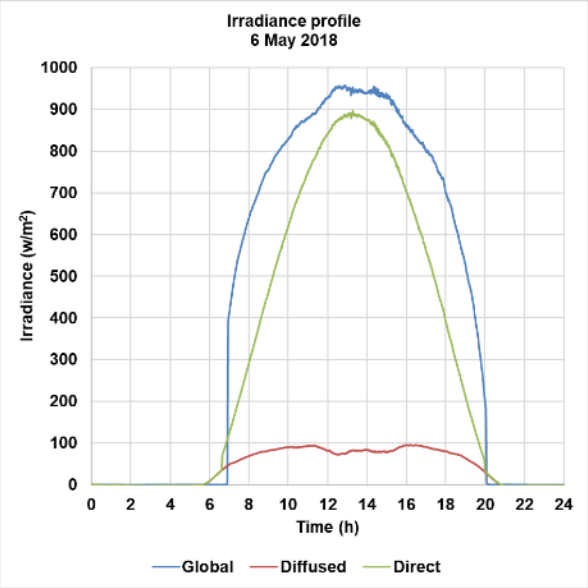

Figure 5.8 The direct, diffused, and global irradiance on 6 May 2018

As the STPVs are used to decrease the heat transfer to the building and save cooling energy, they also contribute to power generation. For example, the S1 STPV sample can generate 30 kJ of energy, which can be directly used by some loads or stored in energy storage systems. This amount of energy is small when it is compared with the AC power consumption, which on the same day,

exceeded the 4.5 MJ as shown in Figure 5.6. The calculated average power and accumulated energy generation of the S1 STPV results are shown Figure 5.9. Moreover, the solar PV module has the same area and reflectance as the STPVs, but because of the modules lesser transmittance it absorbs more radiation. This is subsequently converted into electrical energy. Therefore, the S2 and S3 are expected to provide more power of up to 70% of the S1 production, which is limited to 51 kJ. These energy generations are expectable from the finding in a previous research work [109].

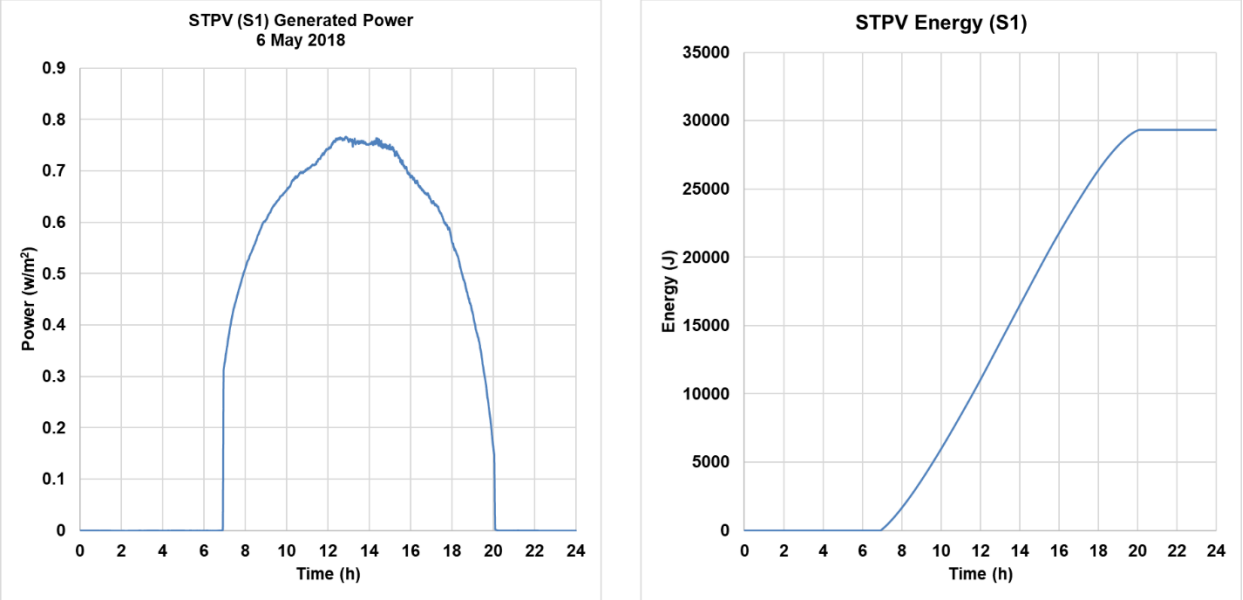

Figure 5.9 The generated power and energy of the S1 STPV enclosure

5.5.3 Interior lighting compensation

In UK standards, the lighting requirement for a façade building for offices is about 500 lumen/m^2 [110]. This can be translated into 9 – 13 W/m^2 if tubular fluorescent lighting is used [111]. For twelve hours (7 am to 7 pm) a 10 W/m^2 had been chosen as the average required value. With an artificial lighting dimming control system introduced the artificial lighting will be activated and

reach the required illuminance level, with the extra electricity consumption calculated when the daylight illuminance level is below 500 Lux.

Figure 5.10 shows the required irradiance and the available interior irradiance for one of the enclosures, which has window S1 with the highest STPV transparency. It is evident that the available light can meet the required value for a short time on that sunny day (6 May 2018). However, it does need some artificial lighting to satisfy the entire duration. Also, for cloudy days or winter days, the expectations from the penetrated sunlight is less.

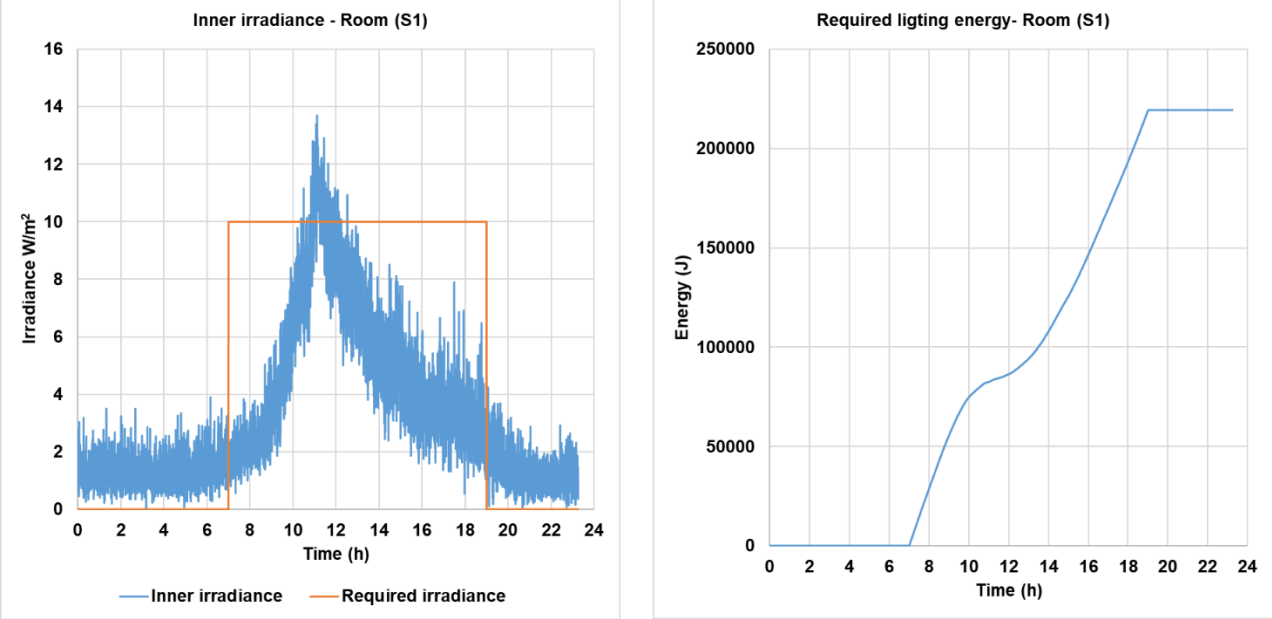

Figure 5.10 The inner irradiance of the enclosure (S1) and the required lighting energy

The required lighting energy using 10 W/m^2 as a reference, has been calculated during the twelve hours as shown in Figure 5.10. In total, 220 kJ is needed. The generated energy from S1 STPV as shown in Figure 5.9 might be used to cover a portion of this consumption, which represents

13.1%. This saving will be less with the lower transparency STPV (S2 and S3) as less sunlight is allowed to penetrate.

5.5.4 Net energy performance

The effects of the STPV window systems on the net energy performance has been analyzed by using the following relation:

Net energy performance = AC energy consumption + Artificial lighting energy consumption − STPV energy generation.

Figure 5.11 shows the net energy performance for both orientations and all STPV transparencies-based enclosures considering the enclosures (S0) as references. The AC power consumption decreases with lower transparency PVs. For the south-facing enclosures, the S1, S2, and S3 consumption relative to S0 are 4.85%, 8.6%, and 11.6% less respectively, while the figures are 7.97%, 14.4%, and 23.27% for the south-west oriented-enclosures. Furthermore, more details are found in Table 5.2.

The clear glazing allows more sunlight to serve the interior lighting of the enclosures, while STPV introduces shading and reflection so that less sunlight penetrates. Thus, more lighting consumption is observed to be used relative to the S0 enclosures. The results are 33.3%, 60.4%, and 82.9% more for the S1, S2, and S3 south enclosures respectively. The south-west enclosures figures are 67.3%, 82.2%, and 83.7% more for S1, S2, and S3.

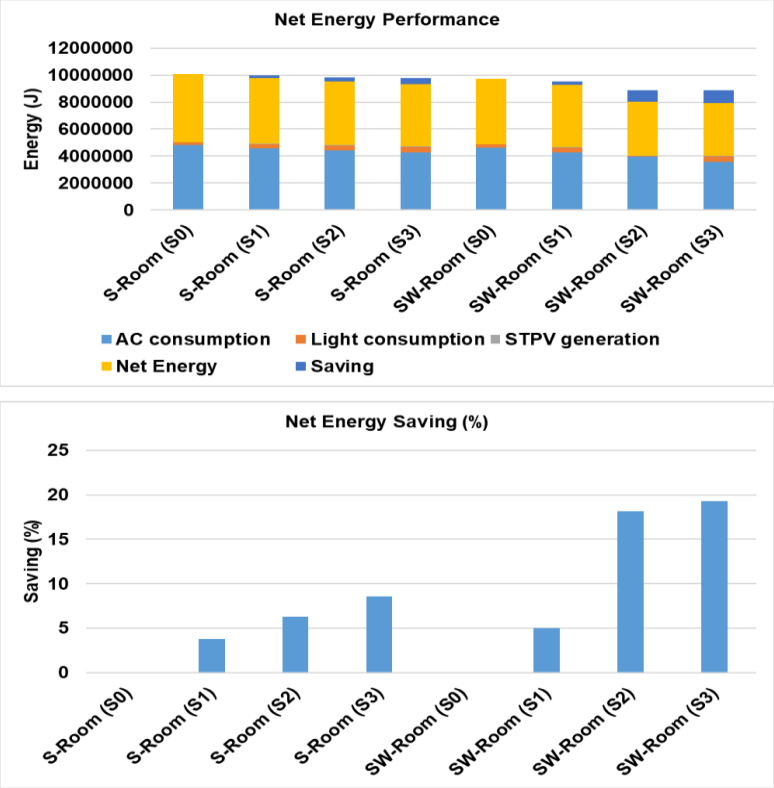

Figure 5.11 Net generation performance

Table 5.2 The net energy saving

	South-facing Enclosures				***South-West-facing Enclosures***			
	(S0)	(S1)	(S2)	(S3)	(S0)	(S1)	(S2)	(S3)
AC consumption (MJ)	4.825	4.591	4.410	4.263	4.640	4.270	3.970	3.560
Light consumption (kJ)	219.3	292.4	352.0	401.2	222.2	371.8	395.9	408.3
STPV generation (kJ)	0	293.3	348.3	524.2	0	234.6	278.6	419.4
Net Energy (kJ)	504.4	485.4	472.7	461.1	486.2	461.8	398.1	392.6
Saving (kJ)	0	190.1	317.1	432.5	0	243.8	880.5	935.8
Saving (%)	0	3.77	6.28	8.57	0	5.01	18.10	19.24

Compared to the total power consumption of the single glazing S0 case, the energy savings for S1 is about 3.77%, S2 is 6.28%, and S3 is 8.5% for the south facing enclosures while the savings are 5% for S1, 18.1% for S2, and 19.2% for S3 south-west facing enclosures. The saving of the south-west enclosures compared to the south enclosures are 4.86% for S1, 15.77% for S2, and 14.86% for S3. Therefore, installing this technology is promising for south-west faces.

Lastly, it is essential to consider the friendly environment and health sides for the residents. Using low transparency PVs might affect health issues and mental states [112]. As a trade-off, using the S1 sample on the south-west facing windows might be a good choice according to the results in Table 5.2.

5.6 Conclusion

In this chapter, a thermal performance analysis and electrical power saving assessment have been carried out for a CdTe-based STPV integrated window system in the climate of the UK. The experimental results of the power and thermal performance testing were presented in detail. The thermal performance, which was quantified as solar heat gain coefficient (SHGC) and U-value, for the STPVs promoting them as good insulators compared with the single glazing case. The south-west facing enclosures introduced more savings when it is compared to the south facing enclosures. The saving is higher when the transparency is lower. A trade-off can be achieved by using a 25% STPV on the south-west oriented enclosures to keep the impact on the mental state at a minimum.

Chapter 6 Daylight Performance Analysis of Cadmium Telluride Semi-Transparent PV Glazing

This chapter illustrates the concept and evaluation of daylight performance of CdTe semi-transparent photovoltaic glazing S5 (35% transparency) in comparison to clear single glazing S4 in two orientations under realistic outdoor conditions in Penryn, UK.

6.1 Introduction

Daylight performance refers to the practice in which glazing is placed in order to transmit adequate internal lighting during daylight hours [113]. A sufficient amount of daylight is vital to daily survival as it affects visual performance, energy efficiency, lighting quality, and even human performance. In terms of energy performance, daylight can be a key factor that leads to energy conservation through reduction of artificial energy requirements. The concept of daylight design is intended to maximize utilization of the available lighting from outdoor illuminance without necessarily causing glare or having very low internal illuminance levels.

Different studies have reported different values for the acceptable range of illuminance for occupants' optical comfort and useful daylight illuminance (UDI). In this study, consideration was given to the horizontal illuminance on a work plane located inside two South oriented test enclosures. STPV glazing S5 was fitted to one of the enclosures and single clear glazing S4 was fitted to the other. Three days were considered for measurement and performance evaluation namely a sunny, an intermittently cloudy and a cloudy day. UDI levels as well as daylight glare index (DGI) and daylight factor (DF) (which is defined as the ratio of horizontal inside illuminance to horizontal outside illuminance), were considered.

6.2 Glare and Daylight Factor Evaluation

6.2.1 Glare Index

Table 6.1 lists the different values of comfortable daylight illuminance noted in previous publications. Vine et al. [114] considers daylight illuminance values between 840 lux – 2416 lux as comfortable, while Roache et al. [115][116] go for lower range of values that is between 700 lux – 1800 lux. According to Reinhart [117], comfortable daylight illuminance is achieved once the illuminance exceeds 150 lux. The authors Nabil and Mardaljevic [118] and Berardi and Anaraki [119] have agreed on the same range of values of considering a comfortable daylight illuminance that is 100 to 2000 lux. However for CIBSE [110] the comfortable daylight illuminance is at 500 lux. Figure *6.1* shows these ranges by graph. The illuminance related to the literature with the assigned comfort zone. The difference in these values is due to the fact that comfort ranges may differ upon changes in sun position, sky condition and individual position with respect to the source of illumination such as a window or a glazing façade. However, the useful daylight illuminance (UDI) is between 100 lux to 2000 lux [120]. An illuminance above 2000 lux may lead to discomfort and glare due to the oversupply of natural light. The daylight glare discomfort can be evaluated using the daylight glare index (DGI) whereby a value below 100 lux is insufficient, and another source of light is required to reach the UDI level.

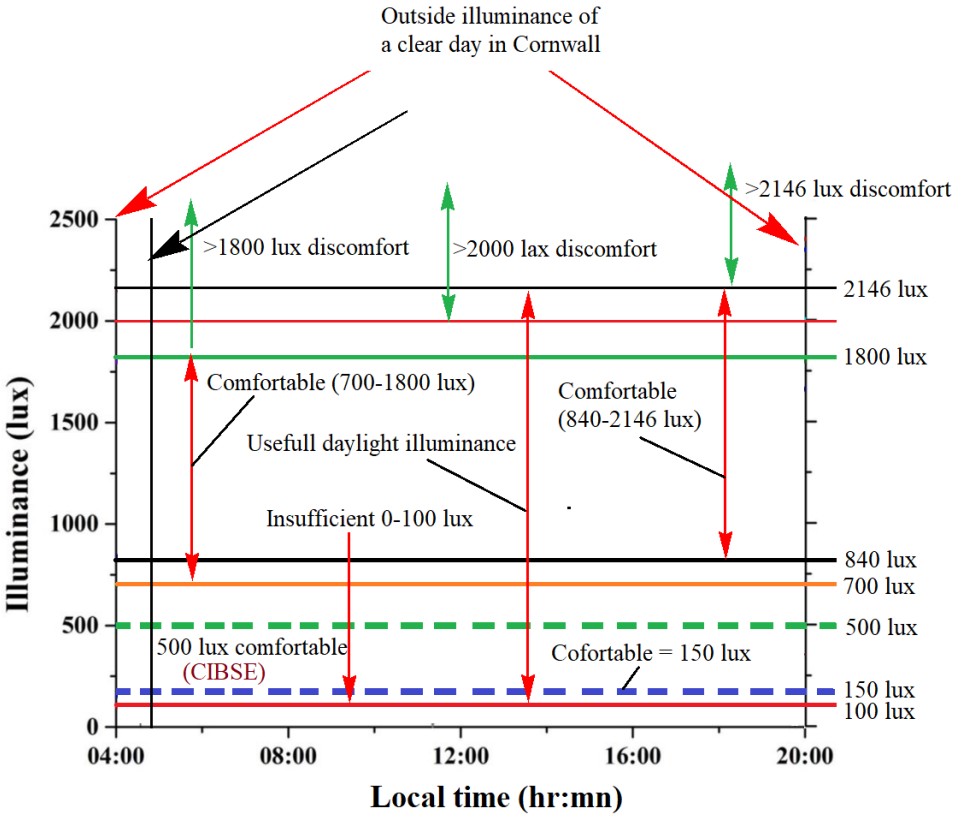

Figure 6.1 Comfortable daylight illuminance

Table 6.1 Ranges of comfortable daylight illuminance

Author (year)	**Comfortable Daylight Illuminance (lux)**
Vine et al.[114]	840 lux – 2416 lux
Roache et al.[115][116]	700 lux – 1800 lux
Reinhart [117]	Greater than or equal 150 lux
Nabil and Mardaljevic [118]	100 lux – 2000 lux
Berardi and Anaraki [119]	100 lux – 2000 lux
CIBSE [110]	500 lux

Different methods are presented for evaluating the daylight glare index (DGI) as shown in equations 6.1 to 6.4.

- British glare index [121]

$$BGI = 10\log_{10} 0.478 \sum_{i=1}^{n} \frac{L_s^{1.6}\omega_s^{0.8}}{L_b P^{1.6}} \quad (6.1)$$

Where, L_s is the source illuminance in (foot-lamberts), $L_b$is the background illuminance (foot-lamberts), ω is the apparent area of source (steradians) and P is a function of the angle between the direction of the light source and the observer's direction of view.

- The Cornell glare equation [122]

$$GI = 10\log_{10} 0.478 \sum_{i=1}^{n} \frac{L_s^{1.6}\Omega^{0.8}}{L_b + 0.07\omega_s^{0.5} L_s} \quad (6.2)$$

Where, L_s, L_b, and ω are is in previous equation 6.1 and Ω is the modified solid angular subtense of the source

- CIE glare index [123]

$$CGI = 10\log_{10} 0.1.\frac{[1+E_d/500]}{E_d+E_i} \sum_{i=1}^{n} \frac{L_s^2\omega_o}{P^2} \quad (6.3)$$

Where, L_s is the source illuminance in (cd/m^2), ω_o is the solid angle of source in steradian, P is Guth position index, E_d is direct vertical illuminance at eye due to all sources in (lux) and E_i is the indirect vertical illuminance at eye due to inter-reflected light in (lux)

- Modified version by Chauvel et al. [124]

$$GI = 10\log_{10} 0.478 \sum_{i=1}^{n} \frac{L_s^{1.6}\Omega^{0.8}}{L_b + 0.07\omega^{0.5} L_s} \quad (6.4)$$

Where, Where, L_s, L_b, ω and Ω are is in previous equation 6.2

Among the abovementioned methods, the CIE glare index method is applicable for artificial or uniform light sources, so it cannot be used in our case. The other methods have complicated measurements for physical and geometrical parameters.

A daylight glare index evaluation equation was developed by Nazzal [125] and is presented in equation 6.5. This equation was formulated for evaluating DGI in daylight applications. It also takes into consideration the observation position and has simpler definitions for geometrical parameters. In addition, the equation considers the adaptation luminance which provides the contribution of the immediate surrounding luminance of the light source, which is recognized to play a key role on the observer's eye adaptation level.

- Daylight Glare Index (DGI)

$$DGI = 10\log_{10} 0.478 \sum_{i=1}^{n} \frac{L_{ext}^{1.6} {\Omega_s}^{0.8}}{L_{adp} + 0.07\omega^{0.5} L_{win}} \quad (6.5)$$

Where, L_{ext} is the exterior luminance level for the outdoor source of light which includes direct sunlight, reflected light from the ground, diffuse skylight as well as other external surfaces (cd/m^2), L_{adp} as the adaptation luminance level from the surroundings such as internal surface reflections (cd/m^2), L_{win} as window luminance level (cd/m^2), ω is the solid angle subtended by the window and Ω_s angle subtended by the light glare source.

Glazing luminance level (L_{win}), exterior luminance level (L_{ext}) and adaptation luminance level (L_{adp}) can be calculated as in equations (6.6) to (6.8).

$$L_{win} = \frac{E_{v,win}}{2\pi\varphi} \quad (6.6)$$

$$L_{ext} = L_{neag} = \frac{E_{v,neag}}{2(\pi-1)} \quad (6.7)$$

$$L_{adp} = \frac{E_{v,adp}}{\pi} \quad (6.8)$$

Where $E_{v,win}$, $E_{v,neag}$ and $E_{v,adp}$ are window vertical illuminance (lux), near glazing vertical illuminance (lux) and adaptation vertical illuminance (lux) and are measured using light sensors.

Solid angles subtended by the glare source (Ω) and solid angle subtended by the window (ω) are calculated through the following equations

$$\Omega = 2\pi\varphi' \quad (6.9)$$

$$\omega = \frac{[ab\cos(\tan^{-1}X)\cos(\tan^{-1}Y)]}{d^2} \quad (6.10)$$

Where (φ) is the configuration coefficient and it was calculated using the dimensions of the glazing through the following series of equations presented below [126].

$$\varphi' = \frac{A\tan^{-1}B + C\tan^{-1}D}{\pi} \quad (6.11)$$

$$A = \frac{X}{\sqrt{1+X^2}} \quad (6.12)$$

$$B = \frac{Y}{\sqrt{1+X^2}} \quad (6.13)$$

$$C = \frac{Y}{\sqrt{1+Y^2}} \quad (6.14)$$

$$D = \frac{X}{\sqrt{1+Y^2}} \quad (6.15)$$

Where dimensionless parameters X and Y are as below

$$X = \frac{a}{2d} \quad (6.16)$$

$$Y = \frac{b}{2d} \tag{6.17}$$

Where, a is the width of the glazing, b is the height of glazing and d is the direct distance from point of observation to the centre of glazing.

The level of light related to the DGI figure is shown in Table 5.2. An average value of 22 is considered as acceptable according to [127] and [128].

Table 6.2 Ranges of comfortable daylight illuminance

Level of light	**DGI**
Just perceptible	16
Perceptible	18
Just acceptable	20
Acceptable	22
Just uncomfortable	24
Uncomfortable	26
Just intolerable	28

6.2.2 Daylight factor

Daylight factor (DF) is defined as the ratio of horizontal inside illuminance to the horizontal outside illuminance. It can be evaluated as a percentage through the equation presented below

$$DF = \frac{L_i}{L_o} \times 100 \tag{6.18}$$

Where, L_i is the horizontal inside illuminance in (lux) and L_o is the outside illuminance in (lux) and they are measured using daylight sensors.

6.3 Daylight Illuminance Measurement

In order to evaluate the DGI and DF, an experimental setup was installed. Figure 6.2 shows the cooler/warmer test enclosures that were oriented to the south direction and holding clear glazing S4 (to the left) and STPV glazing S5 (to the right). Figure 6.3 shows the inside vertical daylight sensor. Details of the experimental setup are presented in Chapter 3 – section 3.2.

Figure 6.2 Test enclosures holding glazing S4 and S5

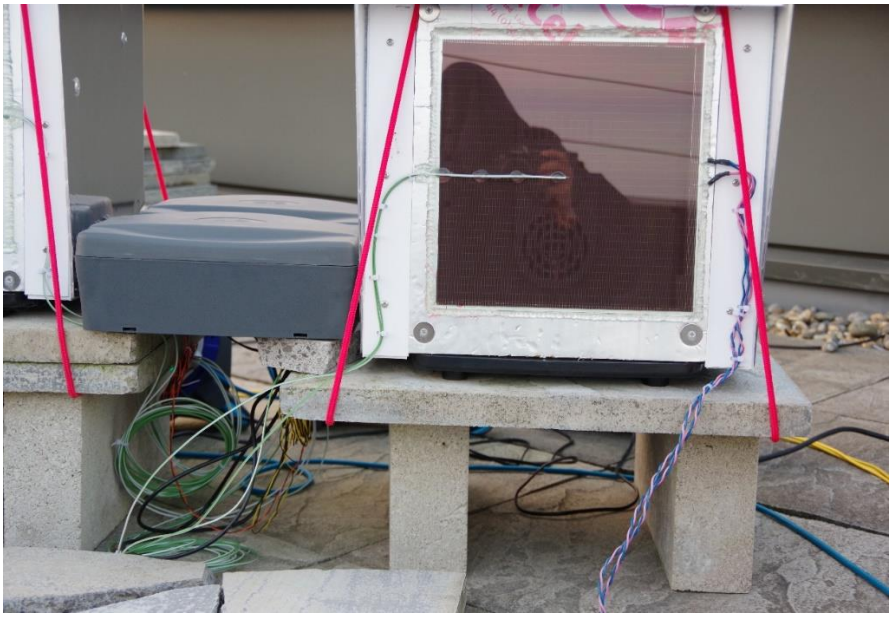

Figure 6.3 Test enclosure holding glazing S4 with light sensor shown inside

Four light sensors were fitted to each of the test enclosures. One sensor was fitted one cm away from the glazing in order to measure the vertical illuminance near the glazing ($E_{v,neag}$). Another sensor was installed facing the center of the glazing at a distance 18 cm away from the glazing with a restricted field of view using a pyramid shaped black shield in order to measure the window vertical illuminance ($E_{v,win}$). The black pyramid shield was used to prevent any effect of light reflection coming from walls. A third sensor was installed just below the pyramid cone in order to measure the adaptation illuminance ($E_{v,adp}$). The location and installation of the three sensors mentioned above were set based on A. Nazzal's recommendations [125]. A fourth sensor was fitted 12 cm away from the front wall at a height of 20 cm from the ground to measure the horizontal illuminance (E_H). Figure 6.4 shows a schematic diagram of the experiment with sensors locations and Figure 6.5 clarifies the dimensions of the glazing and distance from measurement point.

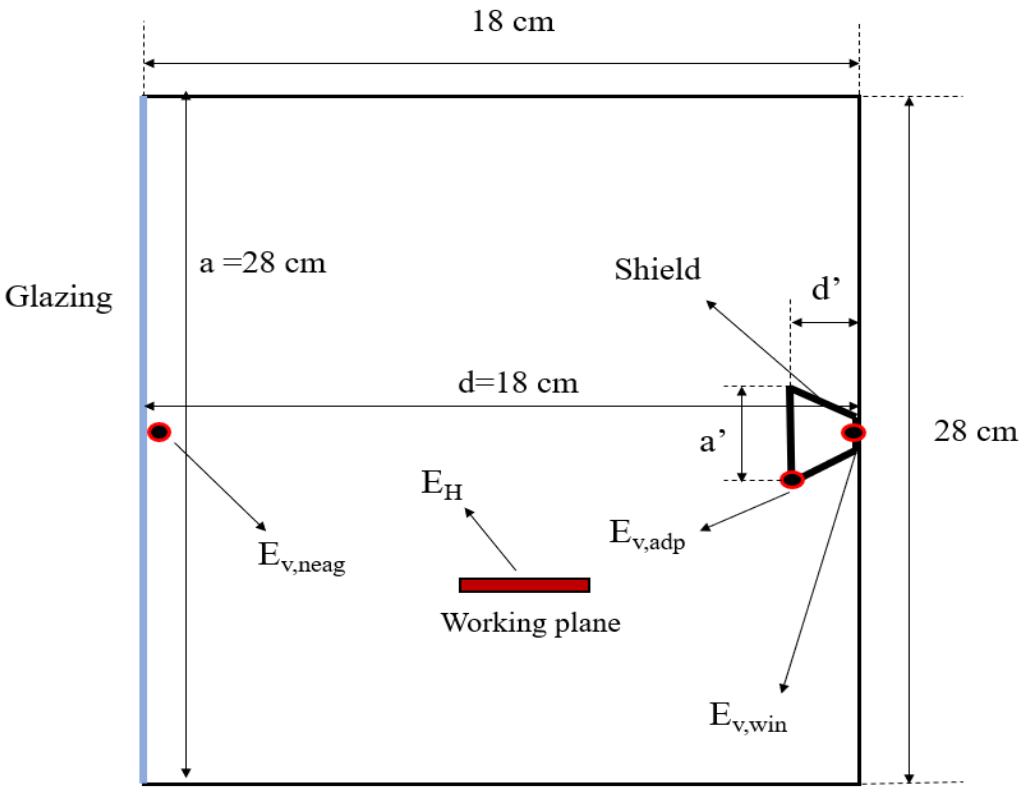

Figure 6.4 Schematic diagram of the experiment used for determining DGI

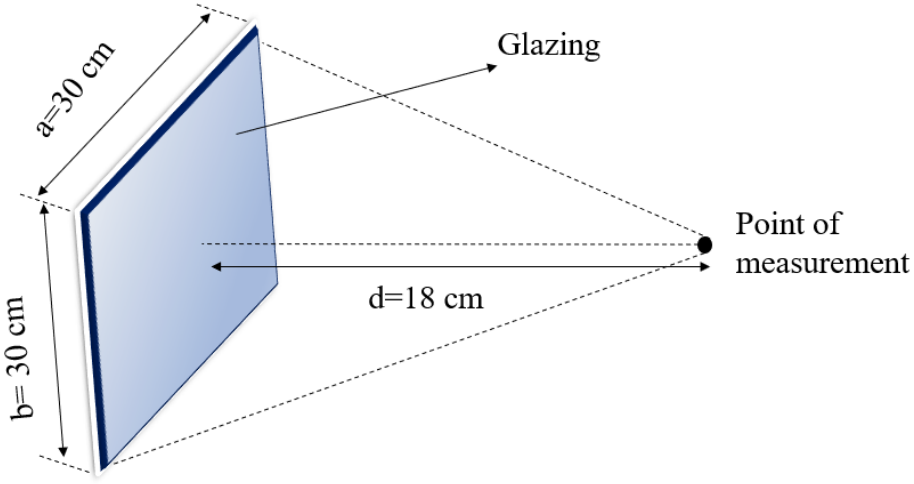

Figure 6.5 Schematic drawing showing the dimensions of the glazing and the distance from measurement point

Dimensions a', b' and d' of the restriction shield are shown in Figure 6.4 and Figure 6.6 and were selected based on equation 6.19.

$$\frac{a}{a\prime} = \frac{b}{b\prime} = \frac{d}{d\prime} \tag{6.19}$$

Where a' is the width of the pyramid, b' is the height of the pyramid and d' is the distance between $E_{v,win}$ sensor the opening of the pyramid as shown in Figure 6.6 [123].

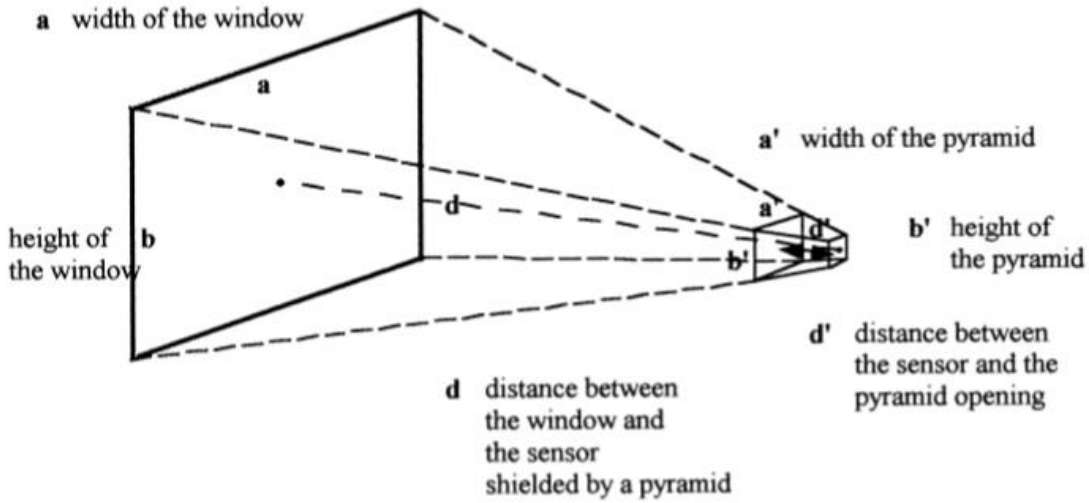

Figure 6.6 Dimensions of the pyramid-shape restriction shield

6.4 Results

6.4.1 Daylight Glare Index for South facing facade

The daylight glare index of the glazing under test were calculated for each of a sunny, an intermittently cloudy and an overcast day using equation 6.5.

Figure 6.7 illustrates the measured illuminance for the three differently positioned illuminance sensors as described in the previous section for the STPV and clear glazing respectively on a sunny day. The luminance is calculated from the equations 6.6 to 6.8 using the measured values and then the daylight glare index is calculated and shown in Figure 6.8. It is clear that the STPV is able to provide acceptable glare levels ranging between 18 and 23 over the time slot of interest between 08:00 and 17:00. On the other hand, the clear glazing provides high glare levels which are considered as unacceptable and uncomfortable over the whole time slot. In hot countries this situation is the norm over the year and for that, a usage of associated technologies, for example shading, might be utilized to decrease these levels. In Façade buildings where the glazing is used on the entire front, the glare might increase even more. However, the STPV will keep it within the comfortable zones. Consequently, STPV glazing is very promising for Façades in hot countries where the light is much more intense and for a longer duration of time.

Similarly,

Figure 6.9 illustrates the measured illuminance on an intermittent cloudy day and the daylight glare index was calculated and shown in Figure 6.10. Again, it is clear that the STPV is the superior solution when it is compared with the clear glazing. It provides the comfortable glare levels over 89% of the time slot in which we are interested. That means, this solution is passively suitable for office enclosures. The clear glazing still provides uncomfortable levels even with intermittently cloudy weather. As far as Facade is concerned, the STPV in hot countries works more effectively. However, the transparency should be considered to obtain the desirable levels.

The same is repeated for the data obtained on a cloudy day and the measured illuminance is shown in Figure 6.11. The daylight glare index was calculated and shown in Figure 6.12. The clear glazing

is still struggling to provide the acceptable levels while the STPV glazing, again, provides an average of 18 DGI which is just acceptable and can be considered in the acceptable zone.

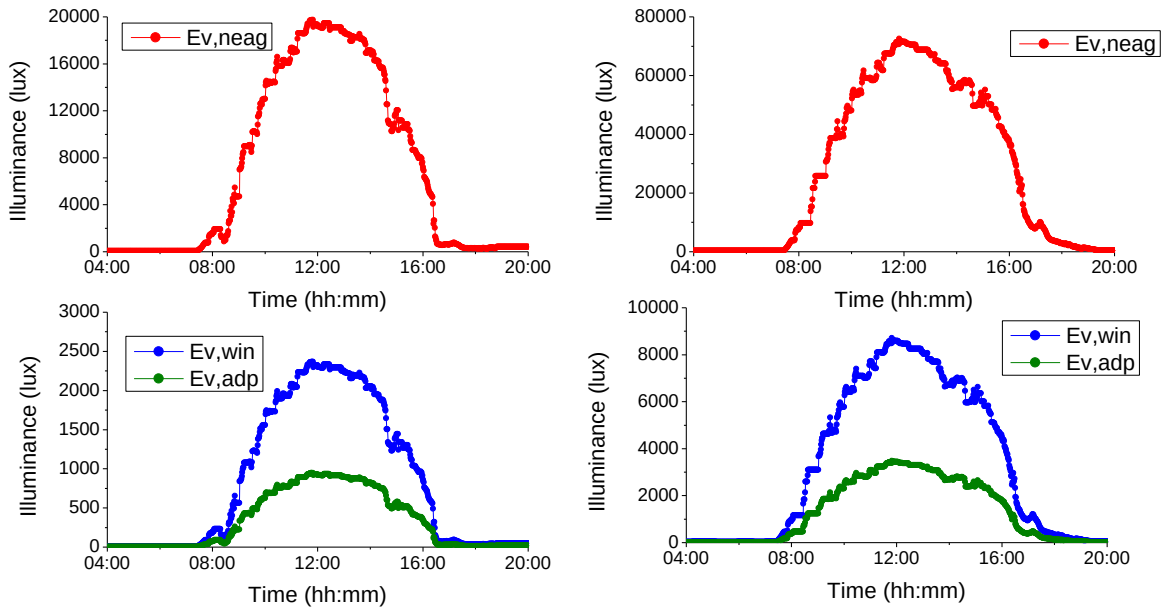

a. Illuminance level for STPV S5

b. Illuminance level for clear glazing S4

Figure 6.7 Sunny day Illuminance level for STPV S5 and clear glazing S4

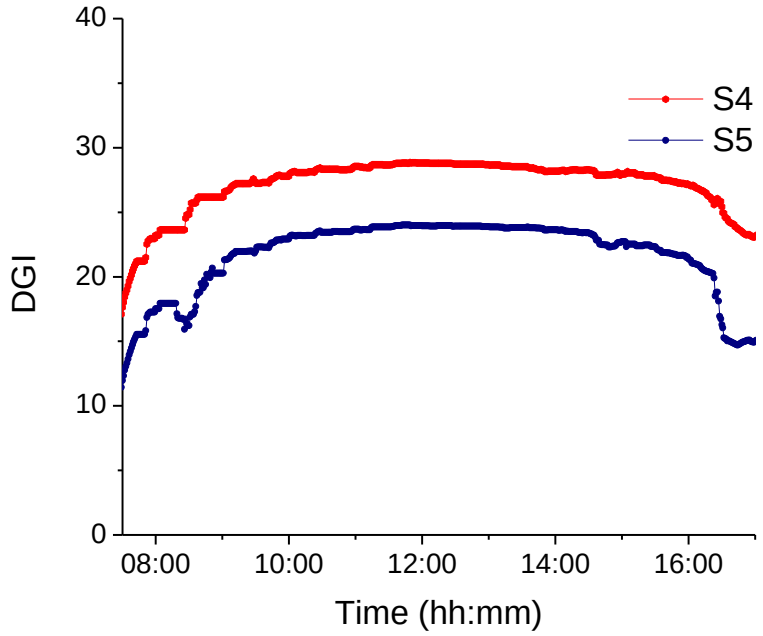

Figure 6.8 DGI of clear glazing and STPV for a sunny day

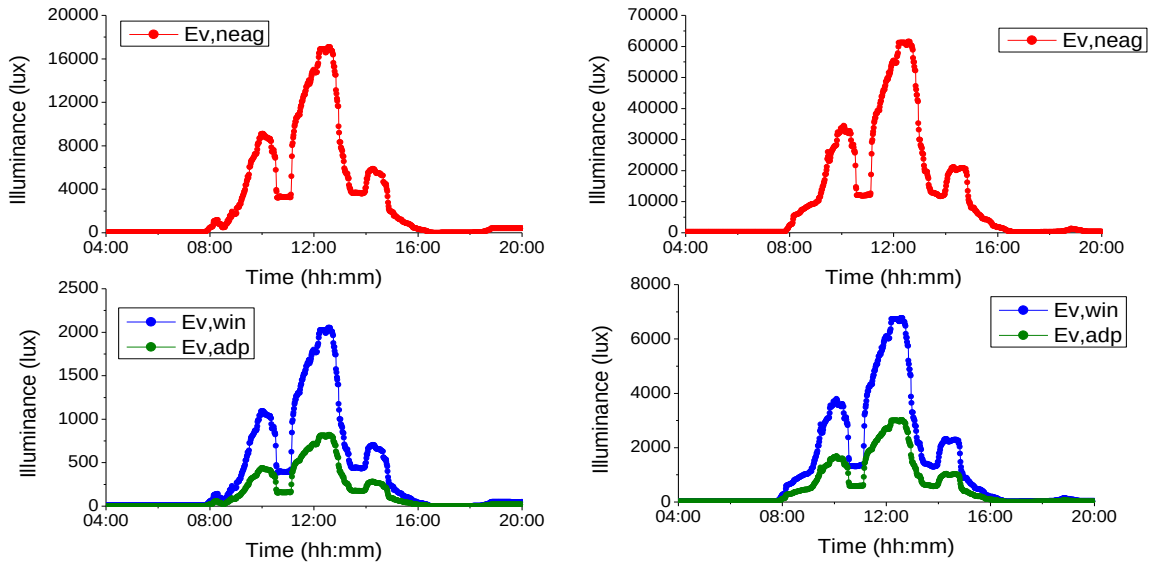

a. Illuminance level for STPV S5

b. Illuminance level for clear glazing S4

Figure 6.9 Intermittent cloudy day Illuminance level for STPV S5 and clear glazing S4

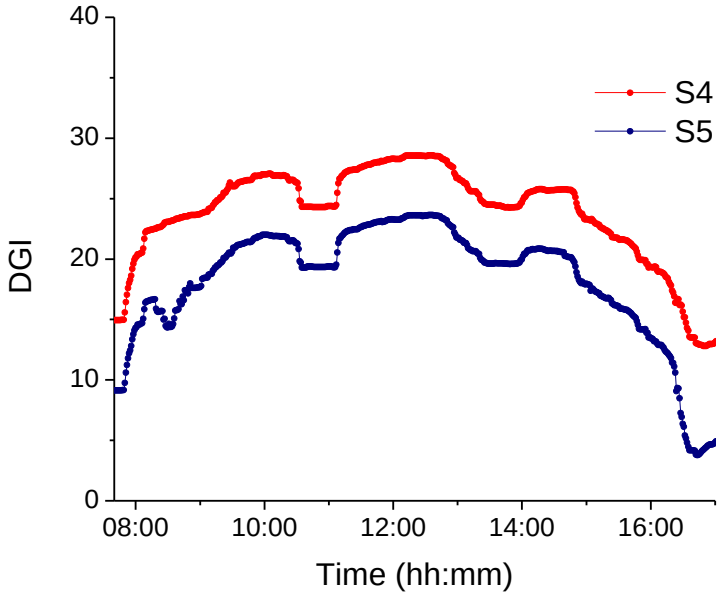

Figure 6.10 DGI of clear glazing and STPV for an intermittent cloudy day

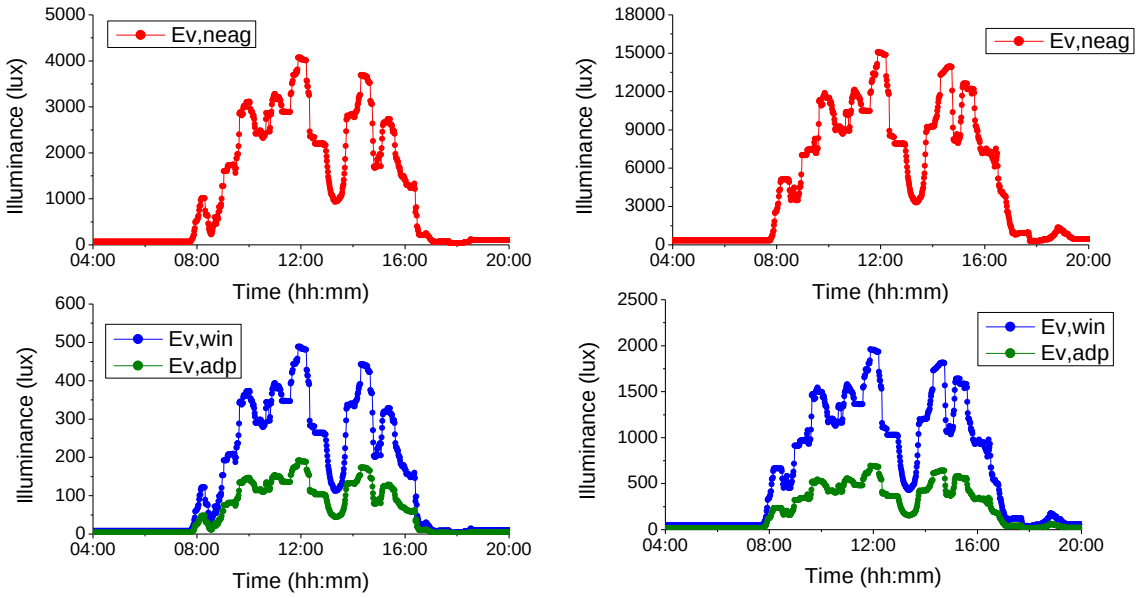

a. Illuminance level for STPV S5

b. Illuminance level for clear glazing S4

Figure 6.11 Cloudy day Illuminance level for STPV S5 and clear glazing S4

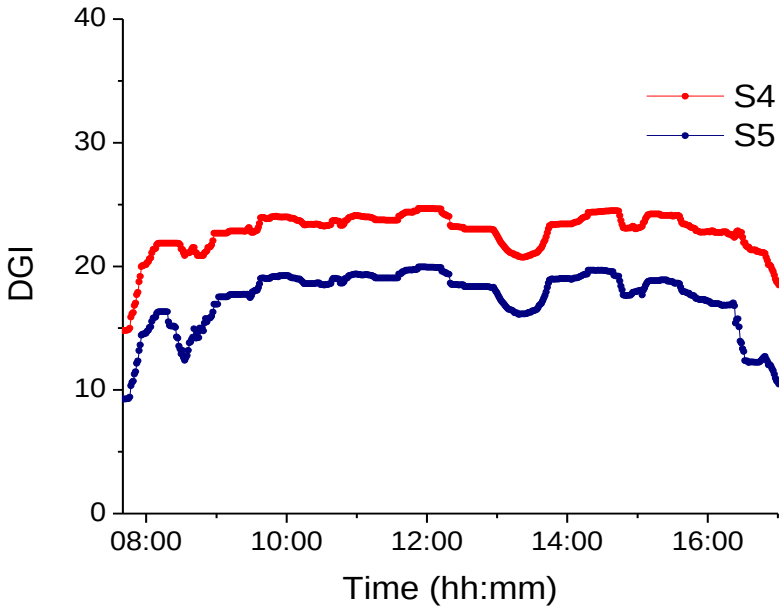

Figure 6.12 DGI of clear glazing and STPV for a cloudy day

6.4.2 Daylight Glare Index for South-West facing façade

The same experiment has been carried out for the same glazing but with a south-west-oriented enclosure. All measurements have been recorded over three distinct days to provide a comprehensive study.

Figure 6.13 illustrates the measured illuminance on a sunny day while the daylight glare index is calculated and shown in Figure 6.14. It is clear that the STPV is able to provide less glare levels than the clear glazing ranging between 15 and 24 over the time slot of interest between 8:00 and 17:00. These levels for short time are over the acceptable levels. On the other hand, the clear glazing provides high glare levels which are considered as unacceptable and uncomfortable over the whole time slot. Again, STPV glazing is very promising for Façades in hot countries where the light is much more and for long duration of time.

Similarly, Figure 6.15 illustrates the measured illuminance in an intermittent cloudy day and the daylight glare index was calculated and shown in Figure 6.16. Again, it is clear that the STPV is the superior solution when it is compared with the clear glazing. It provides the comfortable glare levels over 90% of the time slot of interest.

The same is repeated for the data obtained on a cloudy day and the measured illuminance is shown in Figure 6.17. The daylight glare index was calculated and shown in Figure 6.18. The clear glazing succeeds to provide the acceptable levels while the STPV glazing provides an average of 17 DGI which is within the perceptible zone.

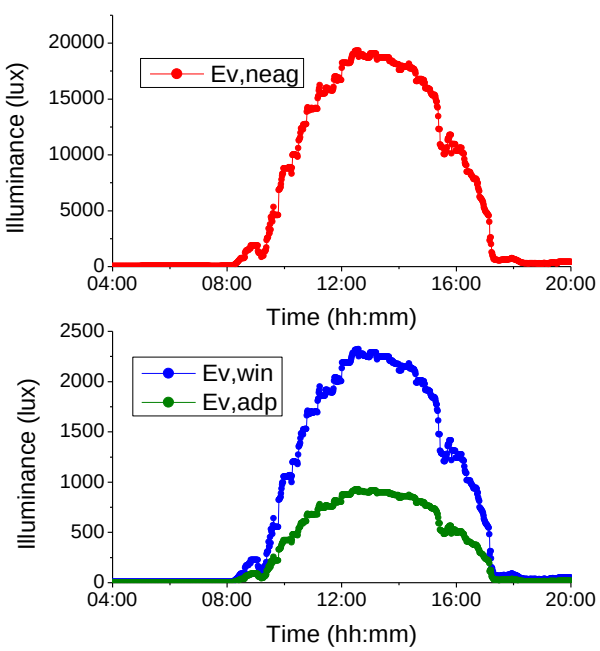

a. Illuminance level for STPV S5

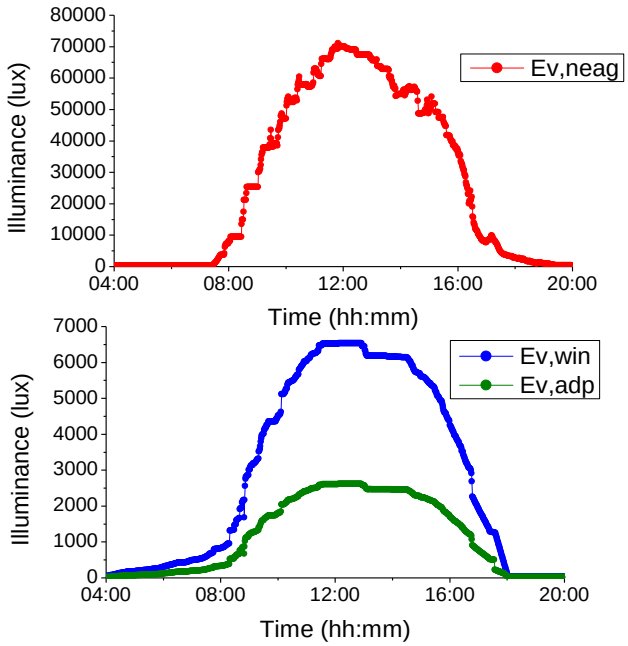

b. Illuminance level for clear glazing S4

Figure 6.13 Sunny day Illuminance level for south-west-facing STPV S5 and clear glazing S4

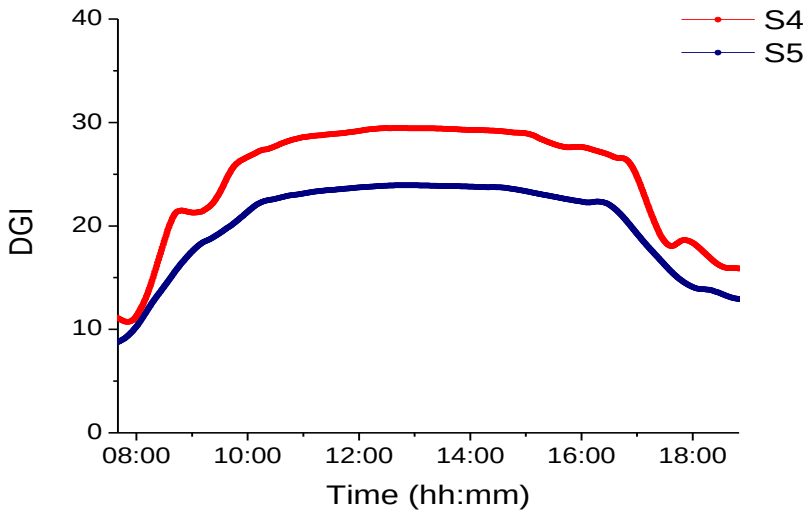

Figure 6.14 DGI of south-west facing clear glazing and STPV for a sunny day

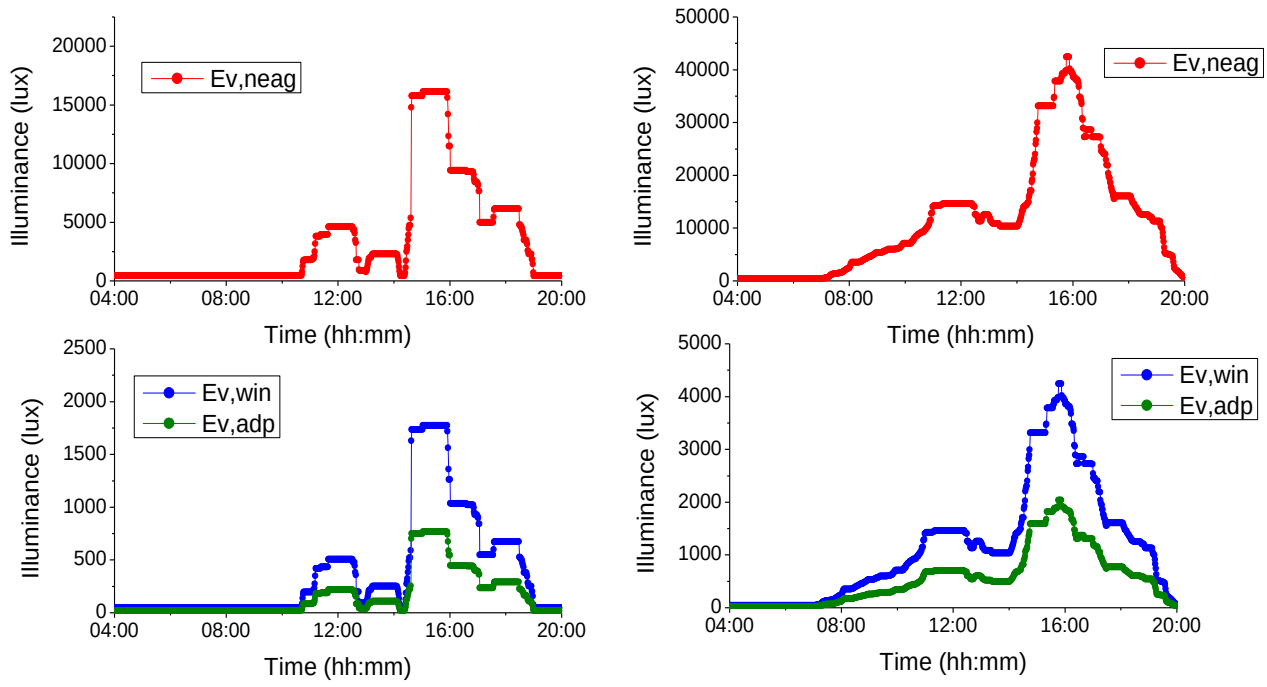

a. Illuminance level for STPV S5

b. Illuminance level for clear glazing S4

Figure 6.15 Intermittent cloudy day Illuminance level for south-west-facing STPV S5 and clear glazing S4

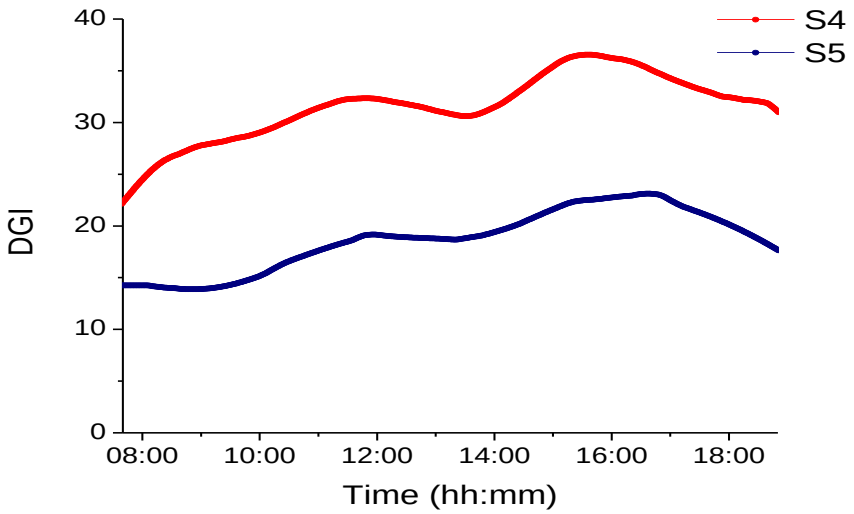

Figure 6.16 DGI of south-west-facing clear glazing and STPV for an intermittent cloudy day

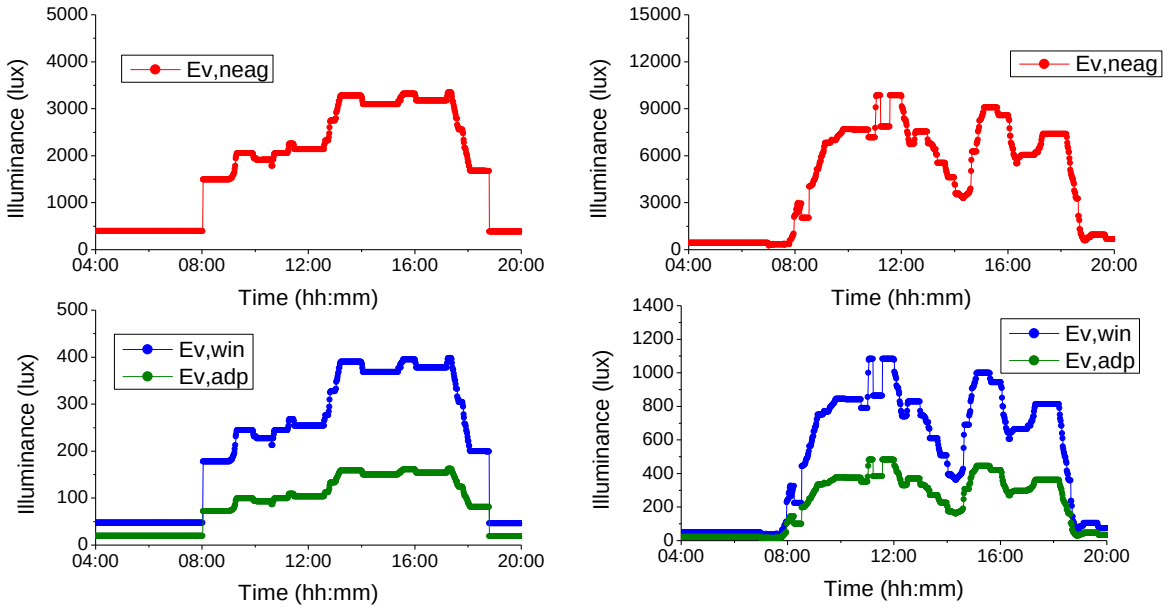

a. Illuminance level for STPV S5

b. Illuminance level for clear glazing S4

Figure 6.17 Cloudy day Illuminance level for south-west-facing STPV S5 and clear glazing S4

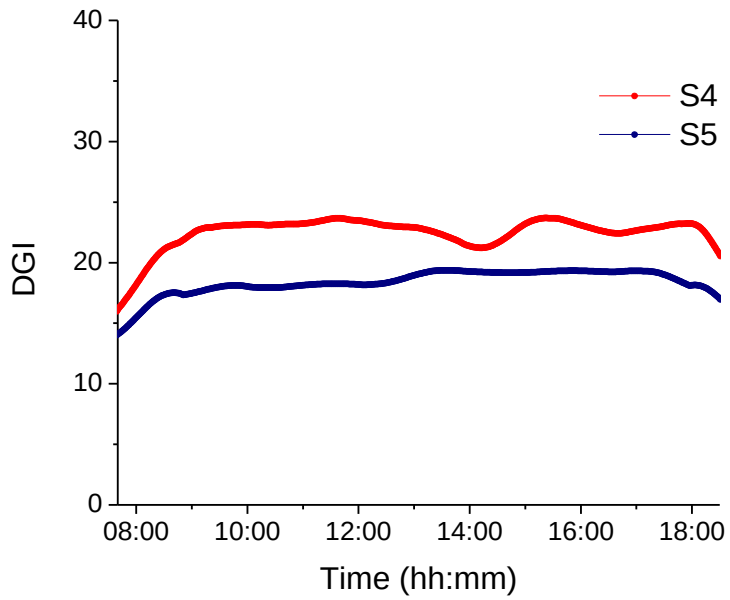

Figure 6.18 DGI of south-west-facing clear glazing and STPV for a cloudy day

6.4.3 Daylight factor

As stated in the equation 6.18, the daylight factor can be calculated using the measured horizontal illuminance of the interior and exterior sides of the glazing. Figure 6.19 indicates the daylight factor (DF) for the clear glazing and the STPV units. The value should be equal for any day as it referred to the material structure. A range of 2% to 5% DF is considered as usable daylight, while DF higher than 5% is considered as a fully daylight environment [129].

Figure 6.19 shows that the STPV can meet the zone of the usable daylight along the time slot of interest over the day. On the other hand, the clear glazing, S4, attains a result way above the targeted value reaching over 20% which means achieving an environment that is fully reliable on daylight. However, daylight glare index (DGI) results showed that the enclosure where clear glazing S4 was used is over lit and exposed and is considered as uncomfortable. As Façade in hot countries is a concern, the clear glazing would require other means of shading to reduce the DF while the STPV passively provides the acceptable range. Similarly, Figure 6.20 illustrates the

expected values for both clear and STPV glazing. The daylight factor for the STPV slightly exceeds 5% for a short period which is acceptable while the clear glazing shows higher values that are over lit as illustrated in DGI analysis in section 6.4.2.

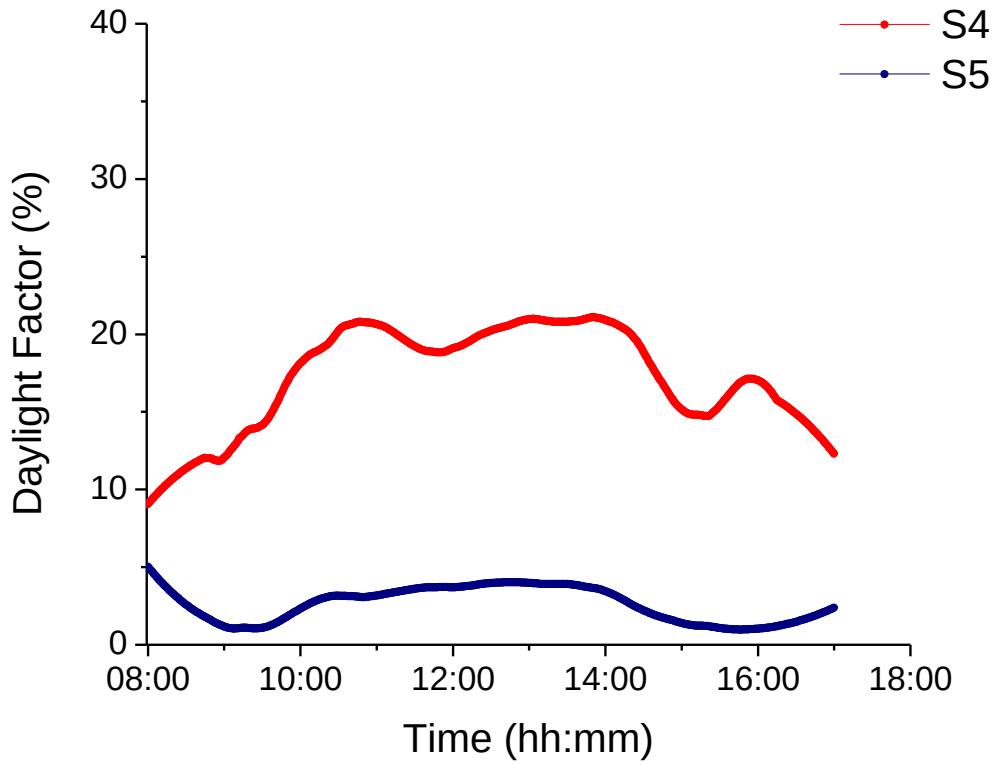

Figure 6.19 Daylight Factor (DF) for south-facing clear glazing and STPV

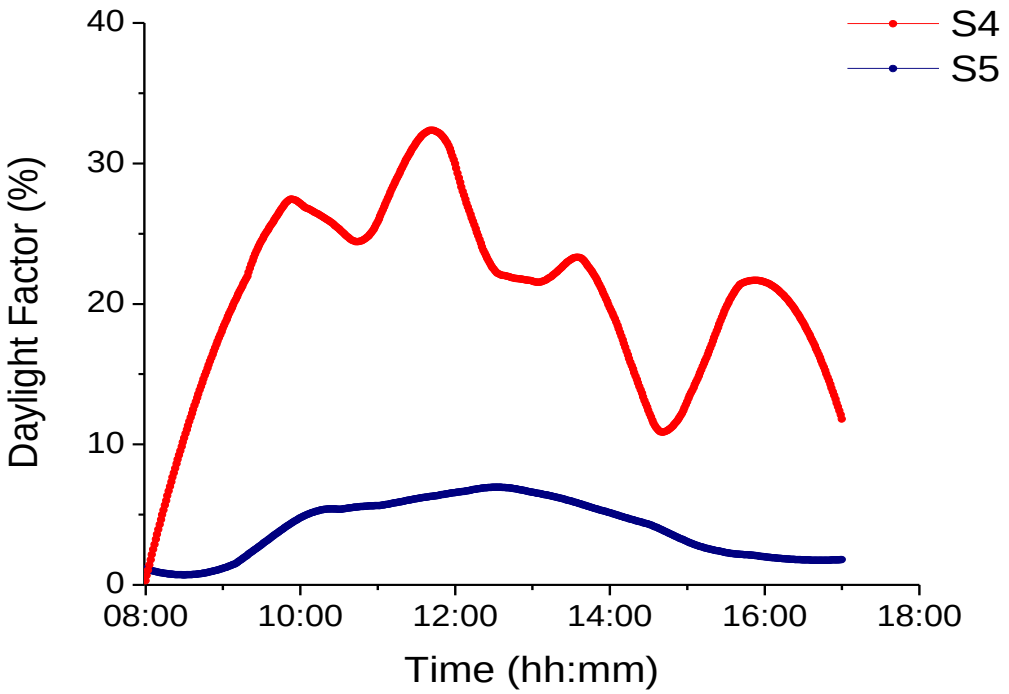

Figure 6.20 Daylight Factor (DF) for south-west-facing clear glazing and STPV

6.4.4 Advantages of using CdTe STPV glazing

In addition to what has been found, that the STPV is a passive solution which contributes towards creating a comfortable environment, the STPV can also generate energy compared with the clear glazing and with the suspended particle devices which consume energy to react. In some cases where the glare or daylight is lower than the desirable values, artificial lighting might be used. If it is assumed that the CdTe glazing of 1 m^2 is able to generate 240Wh per day, the artificial light to maintain 4% DF for 12h will be 720Wh if a 60W light bulb is used. Consequently, a greater area of CdTe is needed to cover the lighting needs and that would be achievable in Facades buildings.

6.5 Conclusion

An outdoor experimental setup was installed to evaluate the daylight performance of a 35%-transparency CdTe thin-film based STPV glazing and compare it to clear single glazing in two different orientations. Daylight performance was represented by daylight glare index (DGI) and daylight factor (DF).

Results showed that CdTe thin-film based STPV glazing can be a good solution for daylight glare control if suitable transparency has been chosen. It provides glare reduction as it mitigates the high sunlight and brings it within the acceptable ranges. This property can be more beneficial in sunny and hot countries because glazing is exposed to high illuminance levels.

In addition, results of daylight factor revealed that using STPV glazing leads internal illuminance to reach a usable daylight level for a large portion of the targeted time slot. For the periods when internal daylight is not sufficient, artificial lighting will be needed. However, power generation from the STPV glazing can compensate for lighting power consumption especially if glazing is of larger areas such as facades.

Chapter 7 Conclusions and Future Work

This chapter aims to summarize the work explained throughout the thesis showing a background knowledge of the topic and the contribution of this work in the specified field of study. It also clearly shows the drawn-out findings as well as suggestions for future work.

7.1 Contribution

The study contributes to the body of knowledge of BIPV applications as it considers full performance analysis of using a PV glazing which little research has targeted. It shows a realistic outdoor thermal, energy and daylight performances for CdTe thin-film based PV glazing. In

thermal performance analysis, different experimental methods have been used and compared for evaluating the overall heat transfer coefficient (U-value. Also, the solar heat gain coefficient (SHGC) was calculated. Moreover, a practical net energy performance has been assessed through the analysis of air conditioning power consumption, artificial lighting power consumption and PV power generation. In addition, daylight performance of the semi-transparent CdTe PV glazing was analysed and quantified and this, to 1st author's knowledge, has not been performed before.

7.2 Findings

The findings revealed by this study are highlighted below

1. Small test enclosures were designed and implemented in order to evaluate the thermal, energy and daylight performances of semi-transparent CdTe thin-film based PV glazing of various transparencies and oriented towards South and South West orientations.

2. Thermal performance of the STPV glazing under study was evaluated. It was concluded the CdTe STPV glazing can limit temperature rise inside the test enclosures better than conventional single glazing. However, the STPV glazing have higher inner surface temperature than conventional single glazing because of the absorbed heat that is used for power generation. Also, the calculations have shown that glazing with higher transparencies have lower U-values and SHGCs. The low U-values and SHGCs signifies that lower transparency CdTe STPV glazing have better insulation property than higher transparency ones. U-values were calculated using three different methods, namely, outdoor test enclosure, indoor test enclosure and outdoor heat flux sensor. Outdoor experiment is the one that reflects the real thermal behaviour throughout the day. While indoor experiment has the advantage of achieving steady state heat transfer in short time. Whereas using heat flux sensor is the one that gives the steadiest results. Nevertheless, it was also

concluded that the thermal parameters of CdTe STPV glazing are similar in South and South West Orientations.

3. Energy performance of CdTe thin-film based STPV glazing of different transparencies was investigated under different weather conditions and in South and South West orientations. It was concluded that lower transparency STPV glazing generate higher power. Also, South oriented test enclosures consume more cooling power than south-west oriented ones. This is because at south orientation, the glazing is exposed to solar irradiance for longer time, thus more heat can be transferred into the test enclosures. The saving in cooling power can reach up to 61% compared to conventional single glazing. Nevertheless, net energy evaluation has shown that higher net energy saving can be achieved by using CdTe STPV glazing in cold weather conditions than in hot weather conditions. Compared to conventional clear glazing, the net energy saving can reach up to 8.5% in South and 19.2% in South West orientation.

4. The study of daylight performance of the CdTe STPV glazing has revealed that using CdTe thin-film based STPV glazing offers the ability to control daylight glare to acceptable levels. Moreover, usable daylight level can be achieved using CdTe thin-film based STPV glazing for high percentage of the aimed time slot. The times when daylight is not sufficient, artificial lighting is required. The power consumption of artificial lighting can be compensated by the power generation of the STPV glazing if optimized STPV glazing transparency is selected and used in large areas.

7.3 Future work

The proposed thin-film based semi-transparent PV glazing was found to be effective in cooling load mitigation, net energy saving and daylight comfort. However, more work is necessary to be done for the comprehensive research to reach the end goal of having optimum PV glazing material

in BIPV applications, especially that the material investigated in this study is little targeted in research for such applications. Below is a list of future work that is proposed by the 1st author:

1. The performance of CdTe STPV glazing has to be studied in different locations of different climatic conditions such as desert climate, Mediterranean climate and tropical climate to find the best location it can be used in.

2. The effect of important factors on the performance of CdTe thin-film based STPV glazing can be studied. Such as window-to-wall ratio (WWR), soiling and PV glazing surface temperature

3. Two- and three-dimensional model of finite heat transfer can be developed to compare with the experimental results for further results validation.

4. Comprehensive thermo-optical dynamic model can be developed in order to simulate the thermal comfort level for such applications.

5. Cost analysis, including capital cost and saving in running cost, is required for more realistic findings.

6. Design modifications can be done on the studied CdTe thin-film based STPV such as being double glazing or air flow PV glazing. This helps in achieving the optimum design for maximum benefit of the PV material under study.

7.4 Closure

This study has presented a full performance analysis of a CdTe thin-film based semi-transparent PV glazing of different transparencies using outdoor experimental methods. The objectives that are presented at the beginning of the work has been fully covered and fulfilled. It is hoped that this

study would help in achieving the end goal of further reduction in global energy consumption and environmental pollution.

References

[1] International Energy Agency, “Statistics and Data,” 2018. [Online]. Available: https://www.iea.org/.

[2] C. L. Cheng, L. M. Liao, and C. P. Chou, “A study of summarized correlation with shading performance for horizontal shading devices in Taiwan,” *Sol. Energy*, vol. 90, pp. 1–16, 2013.

[3] B. Petter Jelle *et al.*, “Fenestration of today and tomorrow: A state-of-the-art review and future research opportunities,” *Sol. Energy Mater. Sol. Cells*, vol. 96, pp. 69–96, 2012.

[4] F. Vasilis, “Sustainability of photovoltaics: The case for thin-film solar cells,” *Renew. Sustain. Energy Rev.*, vol. 13, no. 9, pp. 2746–2750, 2009.

[5] Macsun solar, “China Solar Panel BIPV System, Best Quality BIPV System from Shenzhen Wholesaler: Macsun Solar Energy Technology Co., Ltd.” [Online]. Available: https://macsunsolar.manufacturer.globalsources.com/si/6008841773917/pdtl/BIPV-system/1165626737/Solar-Panel-BIPV-System-Best-Quality-BIPV-

System.htm?state_filt=CN_CNFUJ. [Accessed: 29-Apr-2019].

[6] E. Biyik *et al.*, "A key review of building integrated photovoltaic (BIPV) systems," *Eng. Sci. Technol. an Int. J.*, vol. 20, no. 3, pp. 833–858, 2017.

[7] F. A. Shirland, "The history, design, fabrication and performance of CdS thin film solar cells," *Adv. Energy Convers.*, vol. 6, no. 4, pp. 201–221, 2003.

[8] I. Repins *et al.*, "19.9%-efficient ZnO/CdS/CuInGaSe2 solar cell with 81.2% fill factor," *Prog. Photovoltaics Res. Appl.*, vol. 16, no. 3, pp. 235–239, May 2008.

[9] B. A. Andersson, "Materials availability for large-scale thin-film photovoltaics," *Prog. Photovoltaics Res. Appl.*, vol. 8, no. 1, pp. 61–76, Feb. 2000.

[10] F. Solar and A. F. Solar, "First Solar Sets World Record for CdTe Solar Cell Efficiency," *http://investor.firstsolar.com/releasedetail.cfm?ReleaseID=828273*, 2014. [Online]. Available: http://investor.firstsolar.com/releases.cfm.

[11] P. T. Support, "First Solar," *Energy*, 2006. [Online]. Available: http://www.firstsolar.com/en/Modules/Our-Technology.

[12] S. Dubey, J. N. Sarvaiya, and B. Seshadri, "Temperature dependent photovoltaic (PV) efficiency and its effect on PV production in the world - A review," *Energy Procedia*, vol. 33, pp. 311–321, 2013.

[13] S. B. Sadineni, F. Atallah, and R. F. Boehm, "Impact of roof integrated PV orientation on the residential electricity peak demand," *Appl. Energy*, vol. 92, pp. 204–210, Apr. 2012.

[14] A. A. Babatunde, S. Abbasoglu, and M. Senol, "Analysis of the impact of dust, tilt angle and orientation on performance of PV Plants," *Renew. Sustain. Energy Rev.*, vol. 90, pp. 1017–1026, Jul. 2018.

[15] "International Energy Agency, World Energy Statistics and Balances 2017."

[16] A. Eljojo, "Effect of Windows Size, Position and Orientation on the Amount of Energy Needed for Winter Heating and Summer Cooling," *J. Eng. Res. Technol.*, vol. 1, no. 1, 2017.

[17] Siddhartha and Maya Yeshwanth Pai, "Effect of Building Orientation and Window Glazing on the Energy Consumption of HVAC System of an Office Building for Different Climate Zones," *Int. J. Eng. Res.*, vol. V4, no. 09, pp. 838–843, 2015.

[18] A. S. Muhaisen and H. R. Dabboor, "Studying the Impact of Orientation, Size, and Glass Material of Windows on Heating and Cooling Energy Demand of the Gaza Strip Buildings," *J. Archit. Plan.*, vol. 27, no. 1, pp. 1–15, 2015.

[19] A. M. A. Youssef, Z. J. Zhai, and R. M. Reffat, "Design of optimal building envelopes with integrated photovoltaics," *Build. Simul.*, vol. 8, no. 3, pp. 353–366, Jun. 2015.

[20] A. Cannavale, U. Ayr, and F. Martellotta, "Energetic and visual comfort implications of using perovskite-based building-integrated photovoltaic glazings," *Energy Procedia*, vol. 126, pp. 636–643, 2017.

[21] S. Saridar and H. El Kadi, "The impact of applying recent façade technology on daylighting performance in buildings in eastern Mediterranean," *Build. Environ.*, vol. 37, no. 11, pp. 1205–1212, 2002.

[22] A. A. M. Ali and M. F. Ahmed, "Evaluating the Impact of Shading Devices on the Indoor Thermal

Comfort of Residential Buildings in Egypt," in *Fifth National Conference of IBPSA-USA Madison (SimBuild 2012), Wisconsin, August 1-3, 2012.*, 2012, no. 1, pp. 603–612.

[23] K. Jon Chua and S. Kiang Chou, "Evaluating the performance of shading devices and glazing types to promote energy efficiency of residential buildings," *Build. Simul.*, vol. 3, no. 3, pp. 181–194, 2010.

[24] O. Aydın, "Conjugate heat transfer analysis of double pane windows," *Build. Environ.*, vol. 41, no. 2, pp. 109–116, 2005.

[25] E. Cuce, C. H. Young, and S. B. Riffat, "Thermal performance investigation of heat insulation solar glass: A comparative experimental study," *Energy Build.*, vol. 86, pp. 595–600, Jan. 2015.

[26] "Slimlite." [Online]. Available: http://www.slimliteglass.co.uk/slimlite-ultra-clear-self-cleaning-double-glazed-units/insulation-u-value.html.

[27] RIBA, "Efficient windows. Measuring Performance: Solar Heat Gain Coefficient (SHGC)." [Online]. Available: http://efficientwindows.org/shgc.php.

[28] H. Poirazis, Å. Blomsterberg, and M. Wall, "Energy simulations for glazed office buildings in Sweden," *Energy Build.*, vol. 40, no. 7, pp. 1161–1170, 2008.

[29] A. Boyano, P. Hernandez, and O. Wolf, "Energy demands and potential savings in European office buildings: Case studies based on EnergyPlus simulations," *Energy Build.*, vol. 65, pp. 19–28, 2013.

[30] T. Chow, C. Li, and Z. Lin, "Solar Energy Materials & Solar Cells Innovative solar windows for cooling-demand climate," *Sol. Energy Mater. Sol. Cells*, vol. 94, no. 2, pp. 212–220, 2010.

[31] S. Forughian and M. Taheri Shahr Aiini, "Comparative Study of Single-glazed and Double-glazed Windows in Terms of Energy Efficiency and Economic Expenses," *J. Hist. Cult. Art Res.*, vol. 6, no. 3, p. 879, 2017.

[32] S. Ghoshal and S. Neogi, "Advance glazing system - Energy efficiency approach for buildings a review," *Energy Procedia*, vol. 54, pp. 352–358, 2014.

[33] N. Smith and N. Isaacs, "A cost benefit analysis of secondary glazing as a retrofit alternative for New Zealand households," *Built Hum. Environ. Rev.*, vol. 2, no. 1, pp. 69–80, 2009.

[34] "The Best Double Glazed Windows (2019) | GreenMatch." [Online]. Available: https://www.greenmatch.co.uk/double-glazing/double-glazed-windows. [Accessed: 27-Apr-2019].

[35] A. Ghosh and B. Norton, "Advances in switchable and highly insulating autonomous (self-powered) glazing systems for adaptive low energy buildings," *Renew. Energy*, vol. 126, pp. 1003–1031, Oct. 2018.

[36] M. Arici and H. Karabay, "Determination of optimum thickness of double-glazed windows for the climatic regions of Turkey," *Energy Build.*, vol. 42, no. 10, pp. 1773–1778, 2010.

[37] K. A. R. Ismail and J. R. Henríquez, "Two-dimensional model for the double glass naturally ventilated window," *Int. J. Heat Mass Transf.*, vol. 48, no. 3–4, pp. 461–475, 2005.

[38] K. A. R. Ismail and C. Salinas S., "Non-gray radiative convective conductive modeling of a double glass window with a cavity filled with a mixture of absorbing gases," *Int. J. Heat Mass Transf.*, vol. 49, no. 17–18, pp. 2972–2983, Aug. 2006.

[39] K. A. R. Ismail, C. T. Salinas, and J. R. Henriquez, "A comparative study of naturally ventilated

and gas filled windows for hot climates," *Energy Convers. Manag.*, vol. 50, no. 7, pp. 1691–1703, 2009.

[40] P. C. Eames, "Vacuum glazing: Current performance and future prospects," *Vacuum*, vol. 82, no. 7, pp. 717–722, 2008.

[41] N. Baker and K. Steemers, *Daylight Design of Buildings: A Handbook for Architects and Engineers*. 2014.

[42] S. Barkaszi and J. Dunlop, "Discussion of strategies for mounting photovoltaic arrays on rooftops," *Proc. Sol. Forum 2001 Sol. Energy Power to Choose*, pp. 333–338, 2001.

[43] B. Norton *et al.*, "Enhancing the performance of building integrated photovoltaics," *Sol. Energy*, vol. 85, no. 8, pp. 1629–1664, 2011.

[44] Mustafa A. Guner, "BAPV facade in Merchiston Campus, Scotland | BIPV | Solar, Solar geyser, Solar panels." [Online]. Available: https://www.pinterest.es/pin/492862752966079351/. [Accessed: 28-Apr-2019].

[45] Reynaers Aluminium, "BIPV | Reynaers Aluminium." [Online]. Available: https://www.reynaers.com/en/bipv. [Accessed: 28-Apr-2019].

[46] M. D. Archer and R. Hill, *Clean Electricity from Photovoltaics*, vol. 1. PUBLISHED BY IMPERIAL COLLEGE PRESS AND DISTRIBUTED BY WORLD SCIENTIFIC PUBLISHING CO., 2001.

[47] S. Strong, "The dawning of solar electric architecture: feature: photovoltaics in buildings," *Franklin Company Consultants*, 1996. [Online]. Available: https://www.researchgate.net/publication/279755864_The_dawning_of_solar_electric_architecture_Feature_Photovoltaics_in_buildings.

[48] H. M. Lee, J. H. Yoon, S. C. Kim, and U. C. Shin, "Operational power performance of south-facing vertical BIPV window system applied in office building," *Sol. Energy*, vol. 145, pp. 66–77, 2017.

[49] I. Hagemann, "PV in buildings - the influence of PV on the design and planning process of a building," *Renew. energy*, vol. 8, no. 1–4 pt 1, pp. 467–470, 1996.

[50] L. El Chaar, L. Lamont, A, and N. El Zein, "Review of photovoltaic technologies," *Renew. Sustain. Energy Rev.*, vol. 15, no. 5, pp. 2165–2175, 2011.

[51] G. M. I. Inc., "Thin Film Solar Cells Market to Grow at 16% CAGR From 2016 to 2024," *Global Market Insights Inc.*, 2018. [Online]. Available: https://solarmagazine.com/thin-film-solar-cells-market-to-grow-at-16-cagr-from-2016-to-2024/.

[52] P. Heinstein, C. Ballif, and L.-E. Perret-Aebi, "Building Integrated Photovoltaics (BIPV): Review, Potentials, Barriers and Myths," *Green*, vol. 3, no. 2, pp. 125–156, Jan. 2013.

[53] K. Kapsis, "Modelling, Design and Experimental Study of Semi-Transparent Photovoltaic Windows for Commercial Building Applications," 2016.

[54] T. Markvart, *Solar Electricity. 2nd*. 2000.

[55] M. A. Green, "Thin-film solar cells: Review of materials, technologies and commercial status," *J. Mater. Sci. Mater. Electron.*, vol. 18, no. SUPPL. 1, pp. 15–19, Oct. 2007.

[56] P. K. Ng, N. Mithraratne, and H. W. Kua, "Energy analysis of semi-transparent BIPV in Singapore

buildings," *Energy Build.*, vol. 66, pp. 274–281, 2013.

[57] D. L. Taesoo and U. E. Abasifreke, "A review of thin film solar cell technologies and challenges," *Renew. Sustain. Energy Rev.*, vol. 70, no. September 2015, pp. 0–1, 2016.

[58] A. Stanley, "Present Status of Cadmium Sulfide Thin Film Solar Cells," 1967.

[59] X. Wu, J. Keane, … R. D.-… of the 17th, and undefined 2001, "16.5%-efficient CdS/CdTe polycrystalline thin-film solar cell," *James James Ltd. London*.

[60] Bonnet and Robenhorst, "New results on the development of a thin film p-CdTe-n-CdS heterojunction solar cell," in *Proceedings of the 9th Photovoltaic Specialists Conference*, 1972.

[61] M. Powalla and D. Bonnet, "Thin-film solar cells based on the polycrystalline compound semiconductors CIS and CdTe," *Adv. Optoelectron.*, vol. 2007, 2007.

[62] J. M. Kroon *et al.*, "Nanocrystalline dye-sensitized solar cells having maximum performance," *Prog. Photovoltaics Res. Appl.*, vol. 15, no. 1, pp. 1–18, Jan. 2007.

[63] M. K. Nazeeruddin *et al.*, "Combined experimental and DFT-TDDFT computational study of photoelectrochemical cell ruthenium sensitizers," *J. Am. Chem. Soc.*, vol. 127, no. 48, pp. 16835–16847, Dec. 2005.

[64] A. Hinsch *et al.*, "Glass frit sealed dye solar modules with adaptable screen printed design," *Conf. Rec. 2006 IEEE 4th World Conf. Photovolt. Energy Conversion, WCPEC-4*, vol. 1, pp. 32–35, 2007.

[65] A. K. Shukla, K. Sudhakar, P. Baredar, and R. Mamat, "BIPV based sustainable building in South Asian countries," *Sol. Energy*, vol. 170, no. January 2017, pp. 1162–1170, 2018.

[66] G. Y. Yun, M. McEvoy, and K. Steemers, "Design and overall energy performance of a ventilated photovoltaic façade," *Sol. Energy*, vol. 81, no. 3, pp. 383–394, 2007.

[67] P. W. Wong, Y. Shimoda, M. Nonaka, M. Inoue, and M. Mizuno, "Semi-transparent PV: Thermal performance, power generation, daylight modelling and energy saving potential in a residential application," *Renew. Energy*, vol. 33, no. 5, pp. 1024–1036, 2008.

[68] T. Semba, T. Shimada, K. Y. K. Shirasawa, and H. Takato, "Corrosion of the Glass and Formation of Lead Compounds in the Metallization by High Temperature and High Humidity Test of Crystalline Silicon PV Module," in *2018 IEEE 7th World Conference on Photovoltaic Energy Conversion, WCPEC 2018 - A Joint Conference of 45th IEEE PVSC, 28th PVSEC and 34th EU PVSEC*, 2018, pp. 1333–1335.

[69] M. Benghanem, A. Almohammedi, … M. K.-I. J. P. E. & D., and undefined 2018, "Effect of Dust Accumulation on the Performance of Photovoltaic Panels in Desert Countries: A Case Study for Madinah, Saudi Arabia," *Researchgate.Net*.

[70] D. A. Quansah and M. S. Adaramola, "Comparative study of performance degradation in poly- and mono-crystalline-Si solar PV modules deployed in different applications," *Int. J. Hydrogen Energy*, vol. 43, no. 6, pp. 3092–3109, 2018.

[71] A. Ziane *et al.*, "Experimental investigation of observed defects in crystalline silicon PV modules under outdoor hot dry climatic conditions in Algeria," *Sol. Energy*, 2017.

[72] J. Ramanujam and U. P. Singh, "Copper indium gallium selenide based solar cells - A review," *Energy Environ. Sci.*, vol. 10, no. 6, pp. 1306–1319, 2017.

[73] D. H. W. Li, T. N. T. Lam, W. W. H. Chan, and A. H. L. Mak, “Energy and cost analysis of semi-transparent photovoltaic in office buildings,” *Appl. Energy*, vol. 86, no. 5, pp. 722–729, 2009.

[74] M. Ordenes, D. L. Marinoski, P. Braun, and R. Rüther, “The impact of building-integrated photovoltaics on the energy demand of multi-family dwellings in Brazil,” *Energy Build.*, vol. 39, no. 6, pp. 629–642, 2007.

[75] T. Miyazaki, A. Akisawa, and T. Kashiwagi, “Energy savings of office buildings by the use of semi-transparent solar cells for windows,” *Renew. Energy*, vol. 30, no. 3, pp. 281–304, Mar. 2005.

[76] L. Olivieri, F. Frontini, C. Polo-López, D. Pahud, and E. Caamaño-Martín, “G-value indoor characterization of semi-transparent photovoltaic elements for building integration: New equipment and methodology,” *Energy Build.*, vol. 101, pp. 84–94, Aug. 2015.

[77] A. Ghahremani and A. E. Fathy, “High efficiency thin-film amorphous silicon solar cells,” *Energy Sci. Eng.*, vol. 4, no. 5, pp. 334–343, Oct. 2016.

[78] A. Bosio, N. Romeo, S. Mazzamuto, and V. Canevari, “Polycrystalline CdTe thin films for photovoltaic applications,” *Prog. Cryst. Growth Charact. Mater.*, vol. 52, no. 4, pp. 247–279, 2006.

[79] M. J. Sorgato, K. Schneider, and R. Rüther, “Technical and economic evaluation of thin-film CdTe building-integrated photovoltaics (BIPV) replacing façade and rooftop materials in office buildings in a warm and sunny climate,” *Renew. Energy*, vol. 118, pp. 84–98, 2018.

[80] S. Barman, A. Chowdhury, S. Mathur, and J. Mathur, “Assessment of the efficiency of window integrated CdTe based semi-transparent photovoltaic module,” *Sustain. Cities Soc.*, vol. 37, pp. 250–262, Feb. 2018.

[81] R. H. Crawford *et al.*, “Energy Evaluation and Optimal Design of Semi-transparent Photovoltaic Faç ade for Office Buildings in Central China,” *Dimens. (Jurnal Tek. Arsitektur)*, vol. 6, no. 1, pp. 964–973, 2014.

[82] K. A. Aris *et al.*, “A comparative study on thermally and laser annealed copper and silver doped CdTe thin film solar cells,” *Sol. Energy*, vol. 173, pp. 1–6, 2018.

[83] P. A. B. James, M. F. Jentsch, and A. S. Bahaj, “Quantifying the added value of BiPV as a shading solution in atria,” *Sol. Energy*, vol. 83, no. 2, pp. 220–231, 2009.

[84] J. Han, L. Lu, and H. Yang, “Numerical evaluation of the mixed convective heat transfer in a double-pane window integrated with see-through a-Si PV cells with low-e coatings,” *Appl. Energy*, vol. 87, no. 11, pp. 3431–3437, 2010.

[85] E. Leite Didoné and A. Wagner, “Semi-transparent PV windows: A study for office buildings in Brazil,” *Energy Build.*, vol. 67, pp. 136–142, 2013.

[86] M. Wang *et al.*, “Comparison of energy performance between PV double skin facades and PV insulating glass units,” *Appl. Energy*, vol. 194, pp. 148–160, May 2017.

[87] Y. T. Chae, J. Kim, H. Park, and B. Shin, “Building energy performance evaluation of building integrated photovoltaic (BIPV) window with semi-transparent solar cells,” *Appl. Energy*, vol. 129, pp. 217–227, 2014.

[88] K. Kapsis, V. Dermardiros, and A. K. Athienitis, “Daylight performance of perimeter office façades utilizing semi-transparent photovoltaic windows: A simulation study,” *Energy Procedia*, vol. 78, pp. 334–339, 2015.

[89] A. Ghosh, B. Norton, and A. Duffy, “Measured thermal & daylight performance of an evacuated glazing using an outdoor test cell,” *Appl. Energy*, vol. 177, pp. 196–203, 2016.

[90] H. A, N. B, and D. A, “Measured thermal performance of a combined suspended particle switchable device evacuated glazing,” *Appl. Energy*, vol. 169, no. 169, p. 469–480., 2016.

[91] N. Aste, L. C. Tagliabue, P. Palladino, and D. Testa, “Integration of a luminescent solar concentrator: Effects on daylight, correlated color temperature, illuminance level and color rendering index,” *Sol. Energy*, vol. 114, pp. 174–182, 2015.

[92] N. Lynn, L. Mohanty, and S. Wittkopf, “Color rendering properties of semi-transparent thin-film PV modules,” *Build. Environ.*, vol. 54, pp. 148–158, 2012.

[93] J. Wook, G. Kim, M. Shin, and S. Jin, “Solar Energy Materials & Solar Cells Colored a-Si : H transparent solar cells employing ultrathin transparent multi-layered electrodes,” *Sol. Energy Mater. Sol. Cells*, vol. 163, no. January, pp. 164–169, 2017.

[94] S. L. Do, M. Shin, J. C. Baltazar, and J. Kim, “Energy benefits from semi-transparent BIPV window and daylight-dimming systems for IECC code-compliance residential buildings in hot and humid climates,” *Sol. Energy*, vol. 155, pp. 291–303, 2017.

[95] Y. Fang, P. C. Eames, B. Norton, and T. J. Hyde, “Experimental validation of a numerical model for heat transfer in vacuum glazing,” *Sol. Energy*, vol. 80, no. 5, pp. 564–577, May 2006.

[96] A. Ghosh, S. Ghosh, and S. Neogi, “Performance evaluation of a guarded hot box U-value measurement facility under different software based temperature control strategies,” *Energy Procedia*, vol. 54, pp. 448–454, 2014.

[97] T. T. Chow, G. Pei, L. S. Chan, Z. Lin, and K. F. Fong, “A Comparative Study of PV Glazing Performance in Warm Climate,” *Indoor Built Environ.*, vol. 18, no. 1, pp. 32–40, Feb. 2009.

[98] D. P. Grimmer, R. D. McFarland, and J. D. Balcomb, “Initial experimental tests on the use of small passive-solar test-boxes to model the thermal performance of passively solar-heated building designs,” *Sol. Energy*, vol. 22, no. 4, pp. 351–354, Jan. 1979.

[99] P. Wouters, L. Vandaele, P. Voit, and N. Fisch, “The use of outdoor test cells for thermal and solar building research within the PASSYS project,” *Build. Environ.*, vol. 28, no. 2, pp. 107–113, Apr. 1993.

[100] U. G. Measurement, I. Windows, and E. T. H. Zurich, “gSKIN ® application note : U-value Glass Measurement,” 2014.

[101] P. Robinson and J. Littler, “Advanced glazing: Outdoor test room measurements, performance prediction and building thermal simulation,” *Build. Environ.*, vol. 28, no. 2, pp. 145–152, 1993.

[102] A. Ghosh, B. Norton, and A. Duffy, “Measured overall heat transfer coefficient of a suspended particle device switchable glazing,” *Appl. Energy*, vol. 159, pp. 362–369, Dec. 2015.

[103] BSI, “ISO 9869-1:2014- Thermal insulation — Building elements — Insitu measurement of thermal resistance and thermal transmittance; Part 1: Heat flow meter method,” 2014. [Online]. Available: https://www.iso.org/standard/59697.html. [Accessed: 24-Apr-2019].

[104] J. A. Duffie and W. A. Beckman, *Solar Engineering of Thermal Processes: Fourth Edition*. Hoboken, NJ, USA: John Wiley & Sons, Inc., 2013.

[105] American society of heating refrigerating and air conditioning engineers, *1997 ASHRAE Handbook: Fundamentals*. Atlanta GA: ASHRAE, 1997.

[106] H. Manz, P. Loutzenhiser, T. Frank, P. A. Strachan, R. Bundi, and G. Maxwell, "Series of experiments for empirical validation of solar gain modeling in building energy simulation codes-Experimental setup, test cell characterization, specifications and uncertainty analysis," *Build. Environ.*, vol. 41, no. 12, pp. 1784–1797, Dec. 2006.

[107] K. J. Lomas and T. Kane, "Summertime temperatures and thermal comfort in UK homes," *Build. Res. Inf.*, vol. 41, no. 3, pp. 259–280, Jun. 2013.

[108] O. Seppanen, W. J. Fisk, and Q. H. Lei, "Effect of Temperature on Task Performance," *Lawrence Berkeley Natl. Lab.*, 2006.

[109] J. Peng, D. C. Curcija, L. Lu, S. E. Selkowitz, H. Yang, and W. Zhang, "Numerical investigation of the energy saving potential of a semi-transparent photovoltaic double-skin facade in a cool-summer Mediterranean climate," *Appl. Energy*, vol. 165, pp. 345–356, Mar. 2016.

[110] CIBSE, *CIBSE Guide A: Environmental Design*, vol. 30. 2015.

[111] D. Jenkins and M. Newborough, "An approach for estimating the carbon emissions associated with office lighting with a daylight contribution," *Appl. Energy*, vol. 84, no. 6, pp. 608–622, Jun. 2007.

[112] M. B. C. Aries, J. A. Veitch, and G. R. Newsham, "Windows, view, and office characteristics predict physical and psychological discomfort," *J. Environ. Psychol.*, vol. 30, no. 4, pp. 533–541, Dec. 2010.

[113] L. Bellia and F. Fragliasso, "Automated daylight-linked control systems performance with illuminance sensors for side-lit offices in the Mediterranean area," *Autom. Constr.*, vol. 100, no. July 2018, pp. 145–162, 2019.

[114] E. Vine, E. Lee, R. Clear, D. DiBartolomeo, and S. Selkowitz, "Office worker response to an automated Venetian blind and electric lighting system: a pilot study," *Energy Build.*, vol. 28, no. 2, pp. 205–218, Oct. 1998.

[115] L. Roche, "Summertime performance of an automated lighting and blinds control system," *Light. Res. Technol.*, vol. 34, no. 1, pp. 11–25, Mar. 2002.

[116] L. Roche, E. Dewey, and P. Littlefair, "Occupant reactions to daylight in offices," *Light. Res. Technol.*, vol. 32, no. 3, pp. 119–126, Jan. 2000.

[117] O. Walkenhorst, J. Luther, C. Reinhart, and J. Timmer, "Dynamic annual daylight simulations based on one-hour and one-minute means of irradiance data," *Sol. Energy*, vol. 72, no. 5, pp. 385–395, May 2002.

[118] A. Nabil and J. Mardaljevic, "Useful daylight illuminances: A replacement for daylight factors," *Energy Build.*, vol. 38, no. 7, pp. 905–913, Jul. 2006.

[119] U. Berardi and H. K. Anaraki, "Analysis of the Impacts of Light Shelves on the Useful Daylight Illuminance in Office Buildings in Toronto," *Energy Procedia*, vol. 78, pp. 1793–1798, Nov. 2015.

[120] U. Berardi and H. K. Anaraki, "Analysis of the impacts of light shelves on the useful daylight illuminance in office buildings in Toronto," *Energy Procedia*, vol. 78, pp. 1793–1798, 2015.

[121] P. Petherbridge and R. G. Hopkinson, "Discomfort Glare and the Lighting of Buildings," *Light. Res. Technol.*, vol. 15, no. 2 IEStrans, pp. 39–79, Feb. 2015.

[122] R. G. Hopkinson, "Glare from daylighting in buildings," *Appl. Ergon.*, vol. 3, no. 4, pp. 206–215,

Dec. 1972.

[123] H. D. Einhorn, “Discomfort glare: A formula to bridge differences,” *Light. Res. Technol.*, vol. 11, no. 2, pp. 90–94, Jun. 1979.

[124] P. Chauvel, J. B. Collins, R. Dogniaux, and J. Longmore, “Glare from windows: Current views of the problem,” *Light. Res. Technol.*, vol. 14, no. 1, pp. 31–46, Mar. 1982.

[125] A. Nazzal, “A New Daylight Glare Evaluation Method: Introduction of The Monitoring Protocol and Calculation Method,” *Energy Build.*, vol. 33, no. 3, pp. 257–265, 2001.

[126] J. R. Howell and M. P. Mengüç, “Radiative transfer configuration factor catalog: A listing of relations for common geometries,” *J. Quant. Spectrosc. Radiat. Transf.*, vol. 112, no. 5, pp. 910–912, Mar. 2011.

[127] IWATA and T., “Subjective response on discomfort glare caused by windows,” in *Proc. CIE 22nd Session, 1991*, 1991.

[128] J. Wienold, “DYNAMIC DAYLIGHT GLARE EVALUATION.”

[129] N. Ibrahim and A. Zain-Ahmed, “Daylight availability in an office interior due to various fenestration options,” 2007.